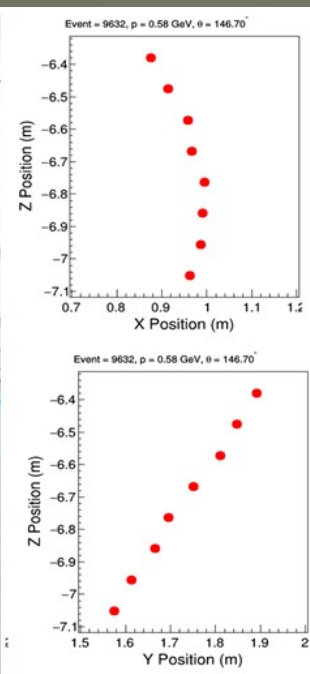
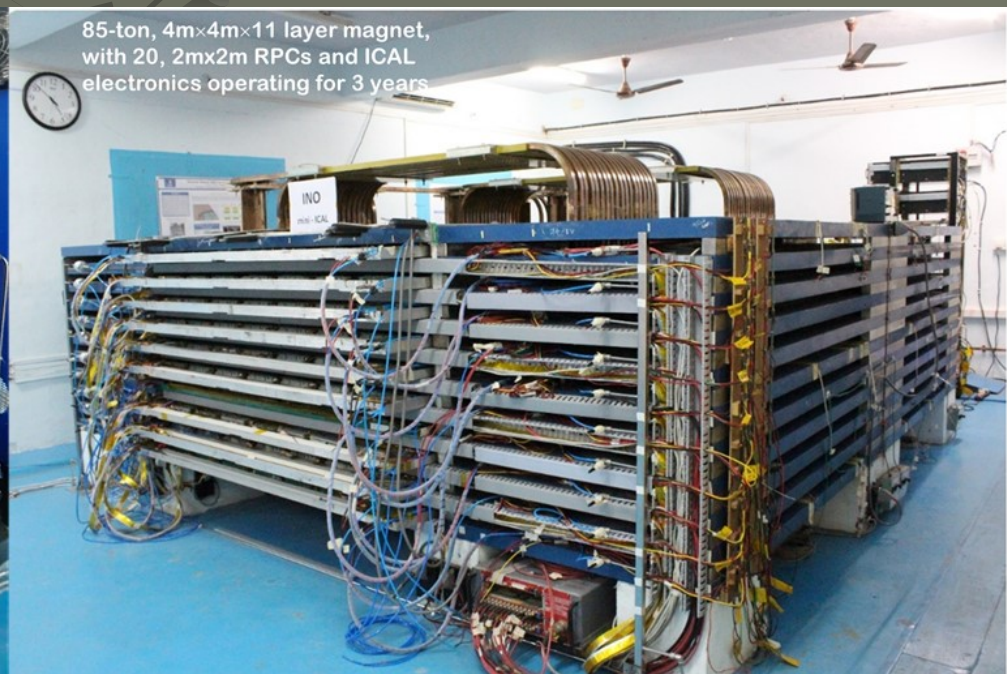
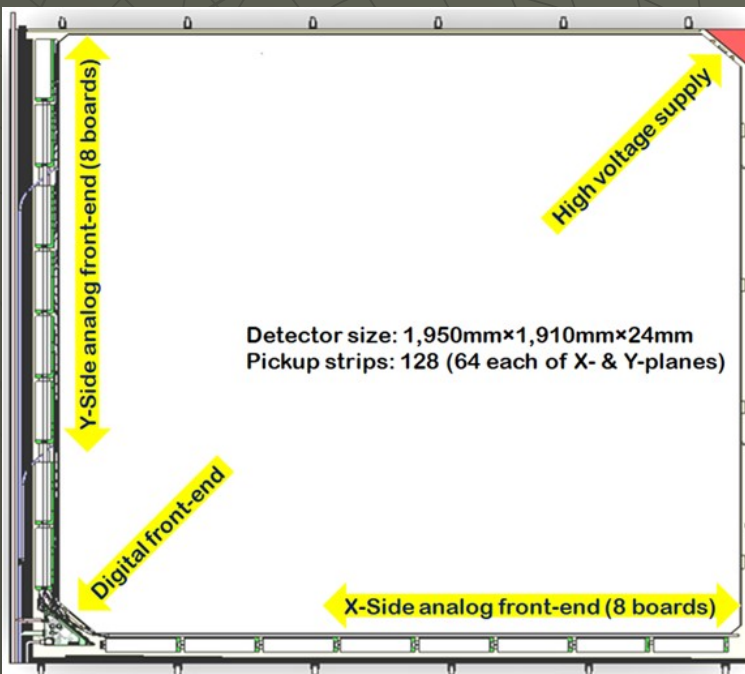


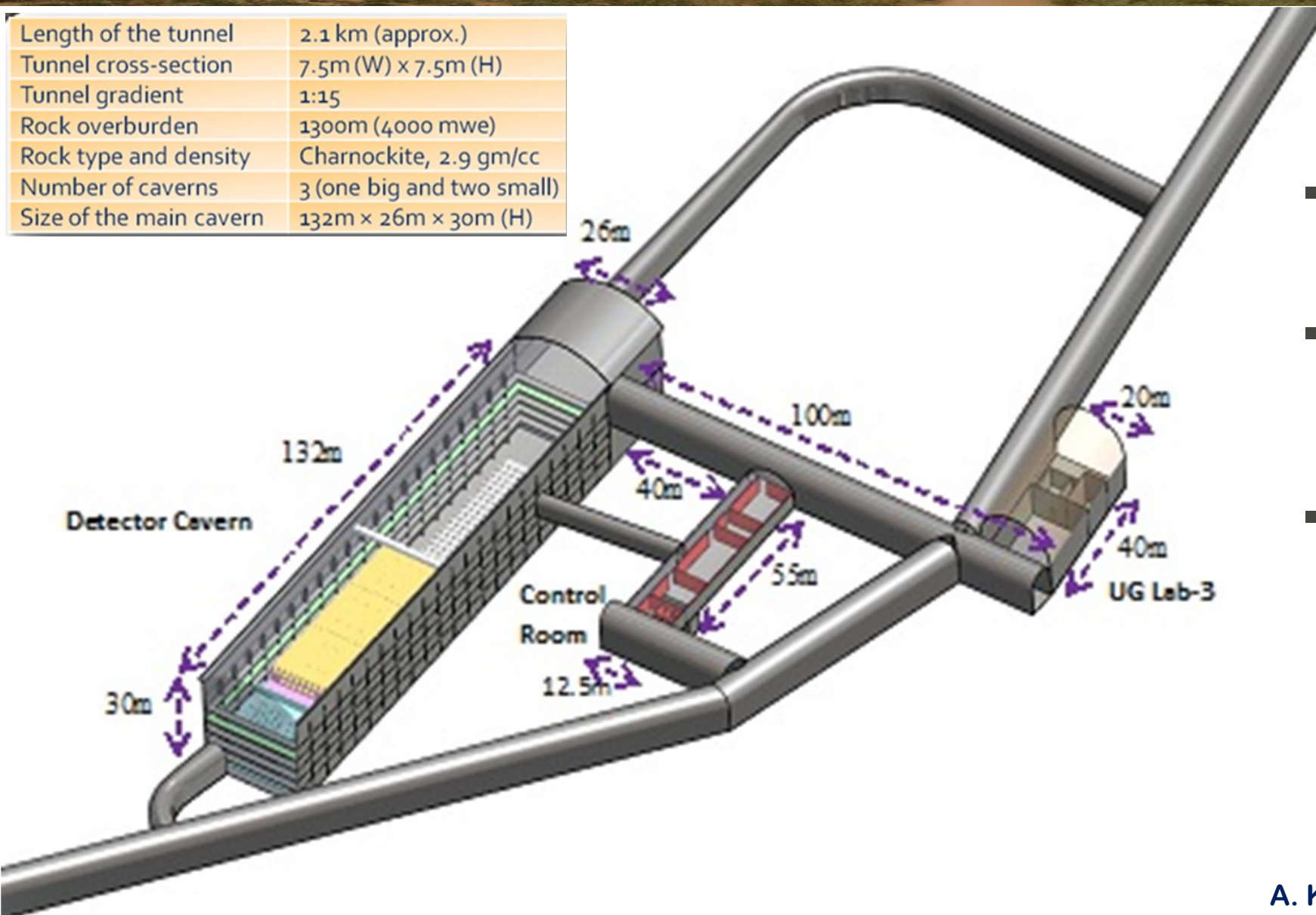
Indigenous development of RPC technologies and applications



Dr. B.Satyanarayana
Scientific Officer (H), Tata Institute of Fundamental Research, Mumbai
Coordinator, India-based Neutrino Observatory (INO) Project, Pottipuram
Visiting Faculty, Department of Applied Science, The American College, Madurai
AICTE-INAIE Distinguished Visiting Professor, Symbiosis Institute of Technology, Pune
T: 09987537702 ■ E: bsn@tifr.res.in ■ W: <http://www.tifr.res.in/~bsn> ■ F: bheesette

India-based Neutrino Observatory project

Length of the tunnel	2.1 km (approx.)
Tunnel cross-section	7.5m (W) x 7.5m (H)
Tunnel gradient	1:15
Rock overburden	1300m (4000 mwe)
Rock type and density	Charnockite, 2.9 gm/cc
Number of caverns	3 (one big and two small)
Size of the main cavern	132m x 26m x 30m (H)



What INO can do?

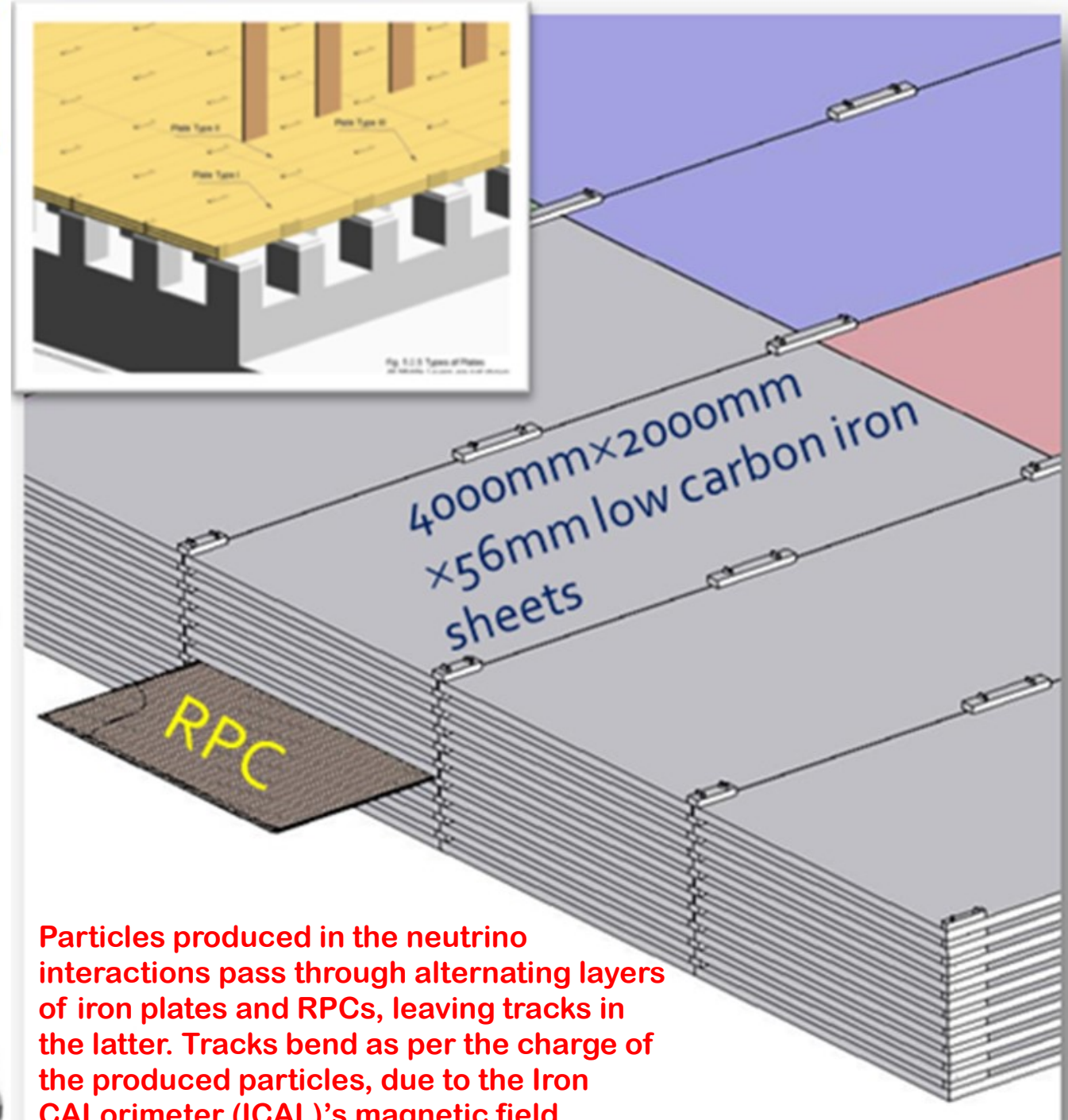
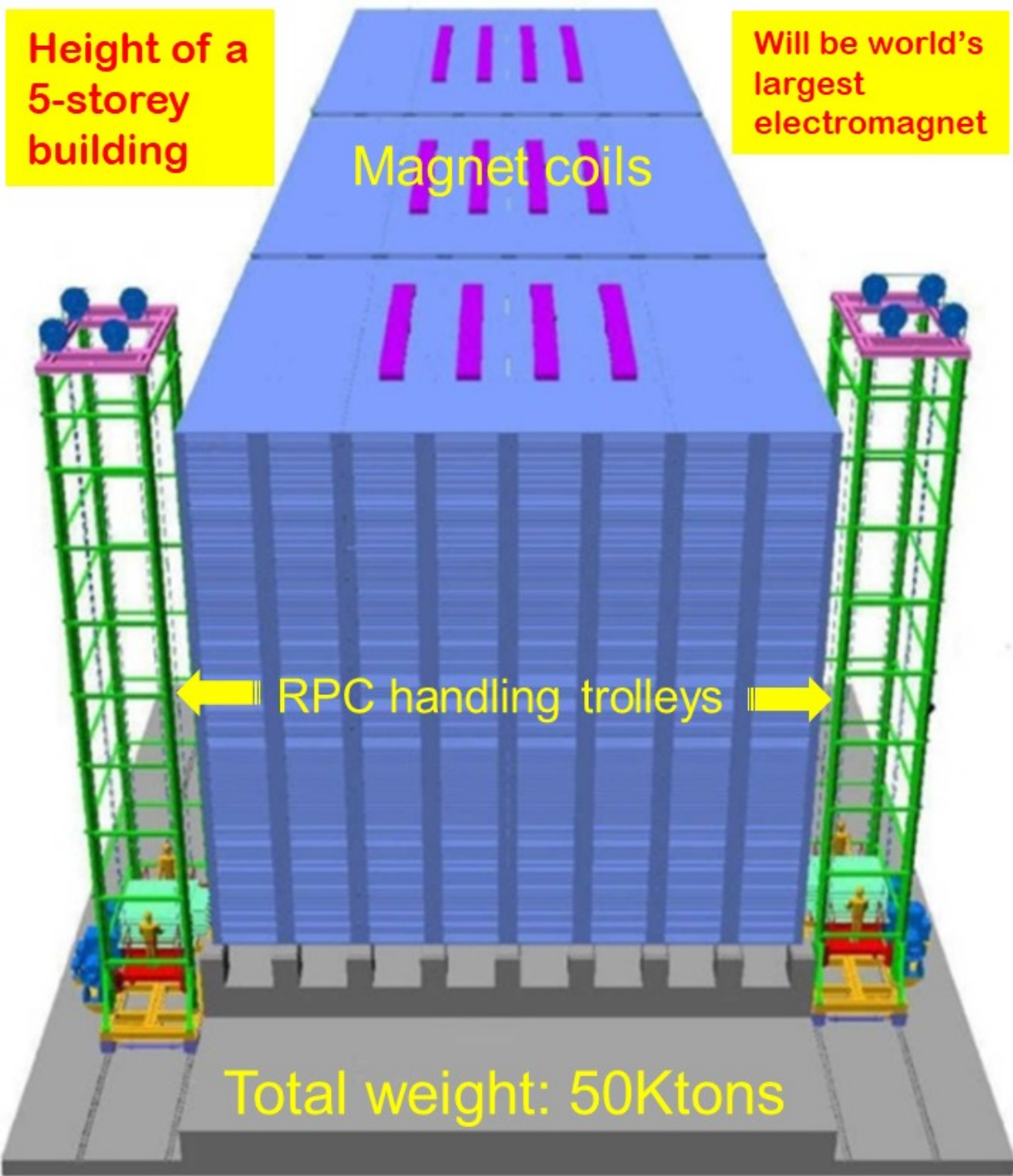
- Measure atmospheric muon neutrinos and antineutrinos, separately.
- Will target the open problem of ordering of the three tiny neutrino masses - Mass Hierarchy.
- Will help address CP violation in the neutrino sector, which could help in our understanding of why there is a preponderance of matter over anti-matter in the universe.

A. Kumar, *et al*, *Pramana – J. Phys.* (2017) 88:79

Bodi West Hills, Pottipuram, Theni: 9°58' North; 77°16' East, 110km West of Madurai (South India)

Choice of INO detector: Iron CALorimeter (ICAL)

- ◆ Use (magnetised) iron as target mass and Resistive Plate Chambers (RPCs) as active detector elements for tracking.
- ◆ Atmospheric neutrinos have large L and E range. So, ICAL has large target mass: 50kton in its current design.
- ◆ Nearly 4π coverage in solid angle (except near horizontal).
- ◆ Upto 20 GeV muons contained in fiducial volume; most interesting region for observing matter effects in 2–3 sector is 5–15 GeV.
- ◆ **Good tracking and energy resolution.**
- ◆ **ns time resolution for up/down discrimination; good directionality.**
- ◆ Good charge resolution; magnetic field ~ 1.3 Tesla.
- ◆ **Ease of construction (modular; 3 modules of 17 kTons each).**
- ◆ ICAL is sensitive to muons only, very little sensitivity to electrons; Electrons leave few traces (radiation length 1.8 (11) cm in iron (glass)).



Facts and Figures of ICAL detectors

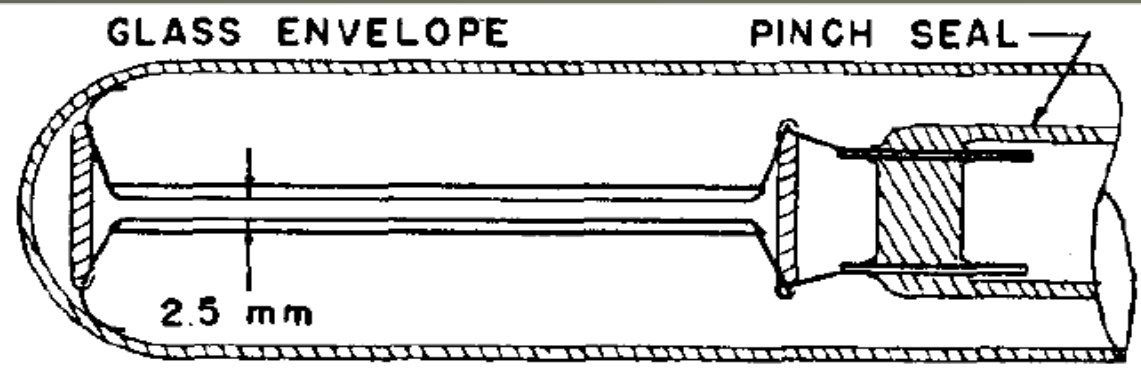
Parameter	ICAL	e-ICAL	m-ICAL
No. of modules	3	1	1
Module dimensions	16.2m×16m×14.5m	8m×8m×2.3m (90:1)	4m×4m×1m (720:1)
Detector dimensions	49m×16m×14.5m	8m×8m×2.3m	4m×4m×1m
No. of active layers	150	22	10
Iron plate thickness	56mm	56mm	56mm
Gap for RPC trays	40mm	40mm	45mm
Magnetic field	1.3Tesla	1.3Tesla	1.3Tesla
RPC dimensions	1,950mm×1,910mm×24mm	1,950mm×1,910mm×24mm	1,950mm×1,910mm×24mm
Readout strip pitch	30mm	30mm	30mm
No. of RPCs/Road/Layer	8	4	2
No. of Roads/Layer/Module	8	4	1
No. of RPC units/Layer	192	16	2
No. of RPC units	28,800 (107,266m ²)	352 (1,311m ²) (90:1)	20 (74.5m ²) (1440:1)
No. of readout strips	3,686,400	45,056 (90:1)	2,560 (1440:1)

RPC characteristics and merits

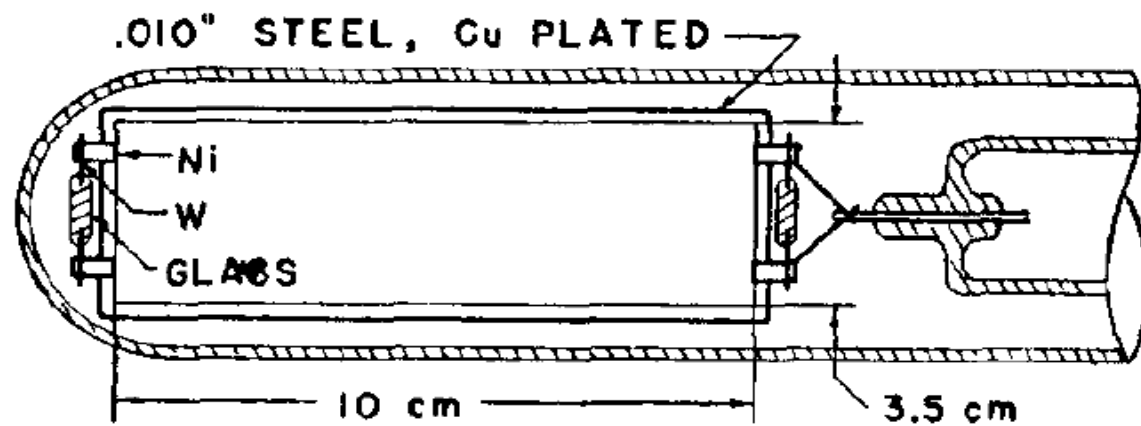
- ◆ Large detector area coverage, thin ($\sim 10\text{mm}$), small mass thickness
- ◆ Flexible detector and readout geometry designs
- ◆ Solution for tracking, calorimeter, muon detectors
- ◆ Trigger, timing and special purpose design versions
- ◆ Built from simple/common materials; low fabrication cost
- ◆ Ease of construction and operation
- ◆ Highly suitable for industrial production
- ◆ Detector bias and signal pickup isolation
- ◆ Simple signal pickup and front-end electronics; digital information acquisition
- ◆ High single particle efficiency ($>95\%$) and time resolution ($\sim 1\text{ns}$)
- ◆ Particle tracking capability; 2-dimensional readout from the same chamber
- ◆ Scalable rate capability (Low to very high); Cosmic ray to collider detectors
- ◆ Good reliability, long term stability
- ◆ Under laying Physics mostly understood!

Experiment	Area (m ²)	Electrodes	Gap(mm)	Gaps	Mode	Type
PHENIX	?	Bakelite	2	2	Avalanche	Trigger
NeuLAND	4	Glass	0.6	8	Avalanche	Timing
FOPI	6	Glass	0.3	4	Avalanche	Timing
HADES	8	Glass	0.3	4	Avalanche	Timing
HARP	10	Glass	0.3	4	Avalanche	Timing
COVER-PLASTEX	16	Bakelite	2	1	Streamer	Timing
EAS-TOP	40	Bakelite	2	1	Streamer	Trigger
STAR	50	Glass	0.22	6	Avalanche	Timing
CBM TOF	120	Glass	0.25	10	Avalanche	Timing
ALICE Muon	140	Bakelite	2	1	Streamer	Trigger
ALICE TOF	150	Glass	0.25	10	Avalanche	Timing
L3	300	Bakelite	2	2	Streamer	Trigger
BESIII	1200	Bakelite	2	1	Streamer	Trigger
BaBar	2000	Bakelite	2	1	Streamer	Trigger
Belle	2200	Glass	2	2	Streamer	Trigger
CMS	2953	Bakelite	2	2	Avalanche	Trigger
OPERA	3200	Bakelite	2	1	Streamer	Trigger
YBJ-ARGO	5630	Bakelite	2	1	Streamer	Trigger
ATLAS	6550	Bakelite	2	1	Avalanche	Trigger
ICAL	97,505	Both	2	1	Avalanche	Trigger

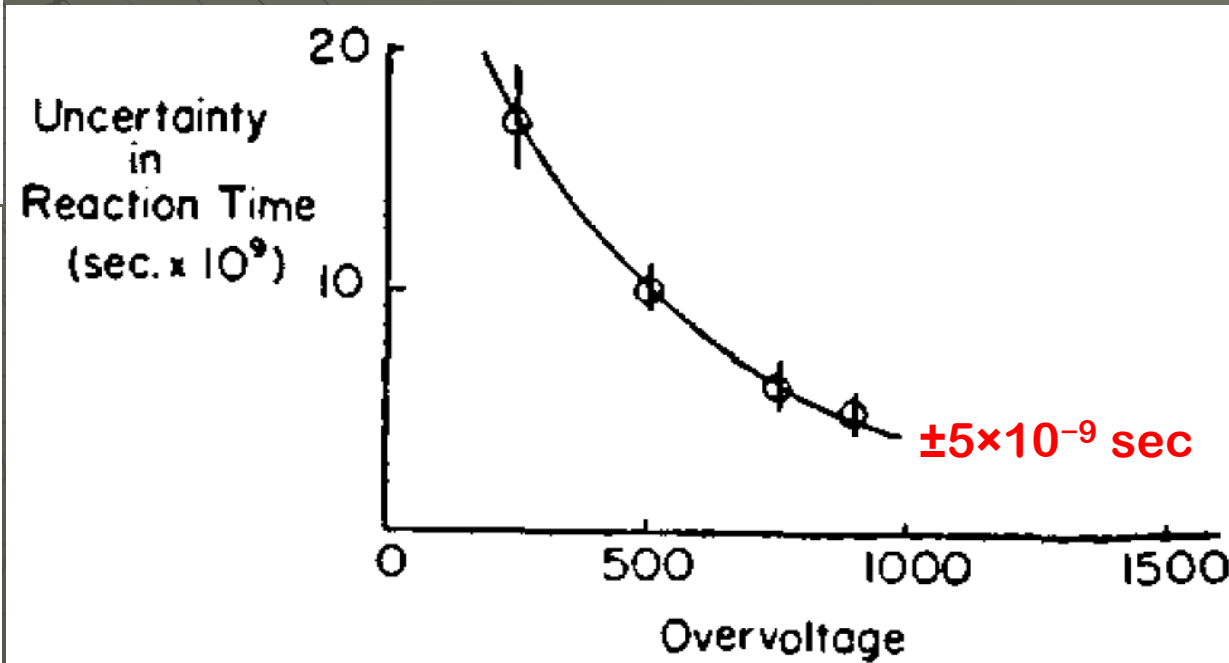
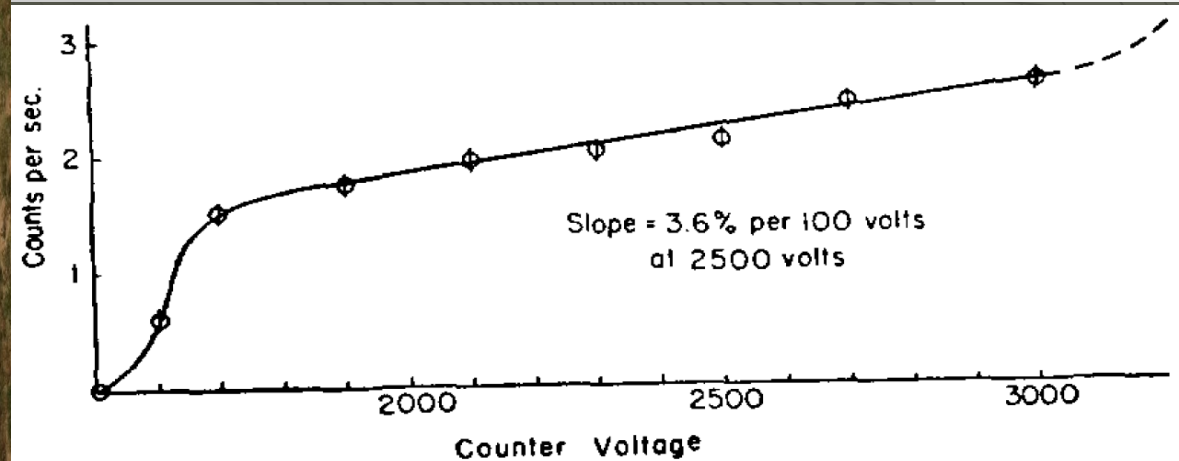
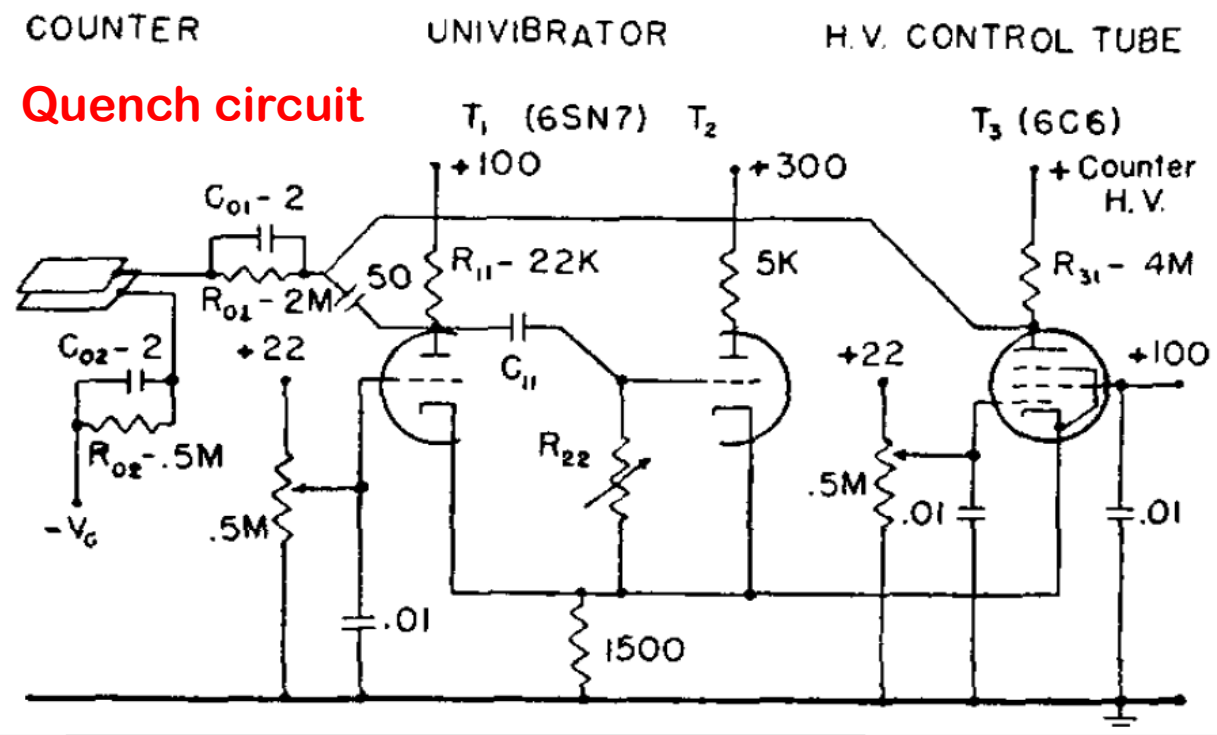
Keuffel's Parallel Plate Counters



Argon-Xylene mixture TO GROUND JOINT →



ALL METAL JOINTS SPOT-WELDED



Keuffel, J.W.;

Parallel-Plate Counters

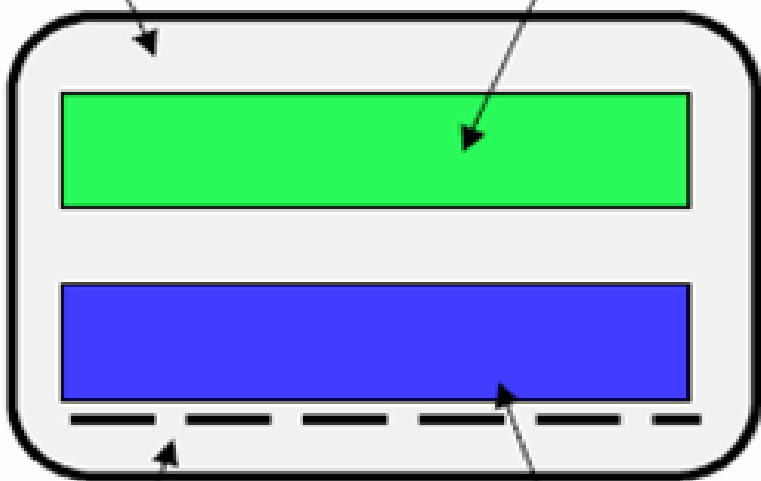
Rev. Sci. Inst. 20 (1949) 202

THIN GAP (100 μm) AND HIGH PRESSURES (~10 bar)
HIGH RESISTIVITY ELECTRODE
(PESTOV GLASS, 10⁹ Ω cm)

Yu.N. Pestov & G.V. Fedotovich (1978)

HIGH-PRESSURE GAS VESSEL

METAL CATHODE



SEMI-CONDUCTING GLASS ANODE

SIGNAL PICK-UP STRIPS

DEVELOPMENT OF RESISTIVE PLATE COUNTERS

R. SANTONICO and R. CARDARELLI

Istituto di Fisica dell'Università di Roma, Roma, Italy; Istituto Nazionale di Fisica Nucleare, Sezione di Roma, Italy

Received 12 January 1981

A dc operated particle detector has been developed and tested, whose constituent elements are two parallel electrode bakelite plates between which, in a 1.5 mm gap, a gas mixture of argon and butane at ordinary pressure is circulated. The counter has 97% efficiency and ~1 ns time resolution at an operating voltage of about 10 kV. The output pulse needs no amplification, being typically 300 mV over 25 Ω.

The detector presented in this paper...

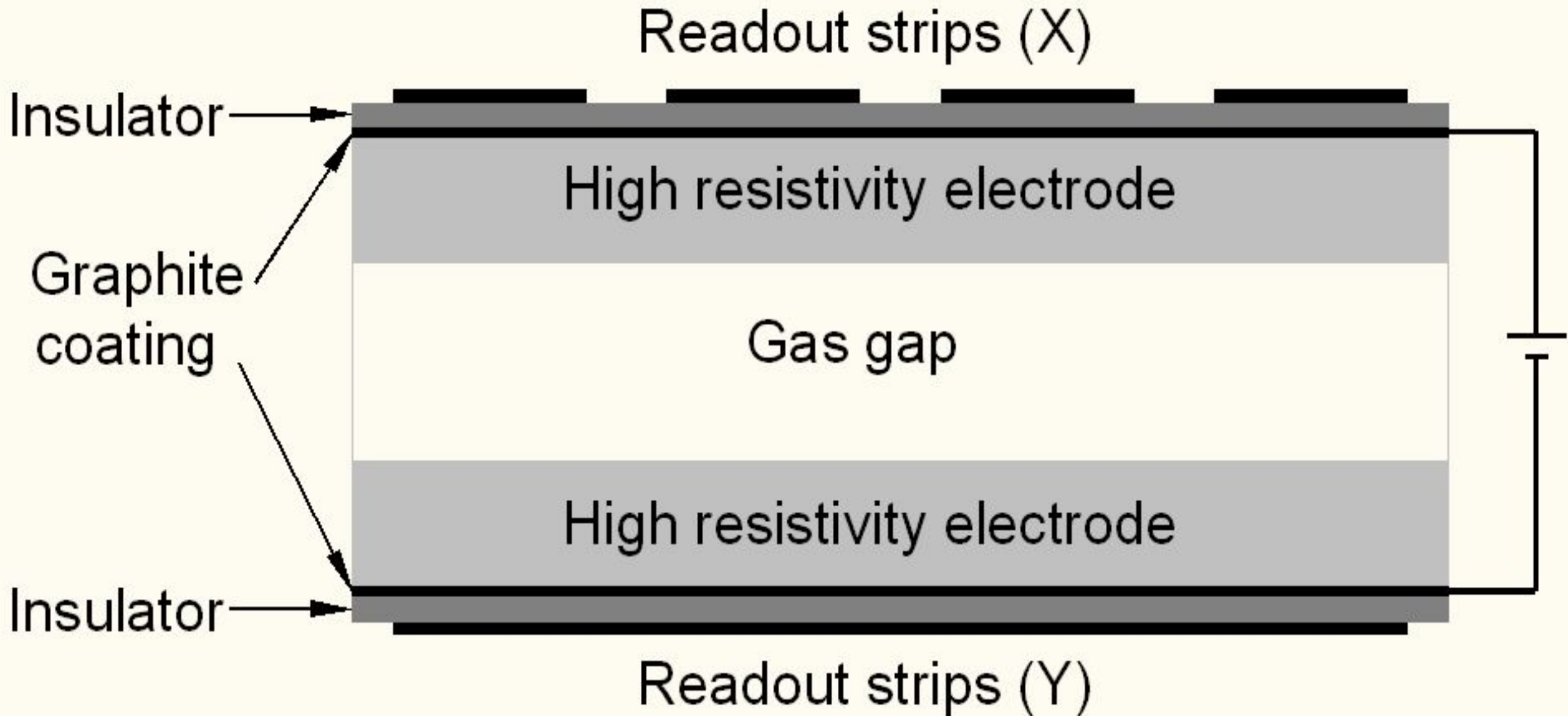
The detector presented in this paper, which will be called "Resistive Plate Counter" (RPC) is based on essentially the same principle as that recently developed by Pestov and Fedotovich [1]. Nevertheless the drastic simplifications introduced in its realization, such as the absence of high pressure gas, the low requirements of mechanical precision, and the use of plastic materials instead of glass, makes it of potential interest in a different and possibly wider range of applications. In particular it could replace with great economic advantages plastic scintillators, whenever large detecting areas are needed under not exceedingly high fluxes of particles.

... dimensions 103 X 22 X 0.2 cm³ on which a copper foil 50 μm thick is glued on the side not facing the gas*. The high voltage electrode is a... On the other hand, due to the ultra-violet absorbing component of the gas, the photons produced by the discharge are not allowed to propagate in the gas, thus avoiding the possibility to originate secondary discharges in other points of the detector.

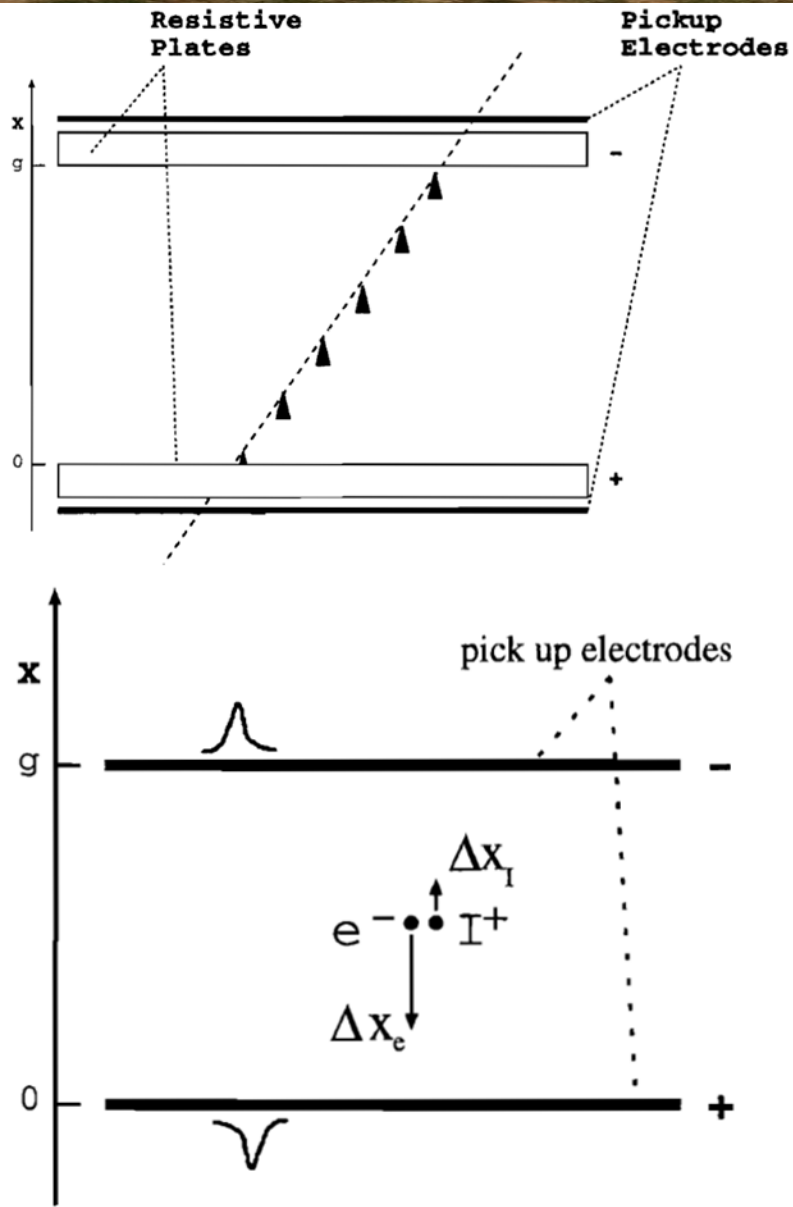
RPCs exhibit much better time resolution than

* The cement used here and in the following is epoxy resin which has been proven to guarantee a sufficient electrical contact between copper and bakelite. Its conductivity can be increased, if needed, by adding a small amount of graphite.

Resistive Plate Chamber (RPC)

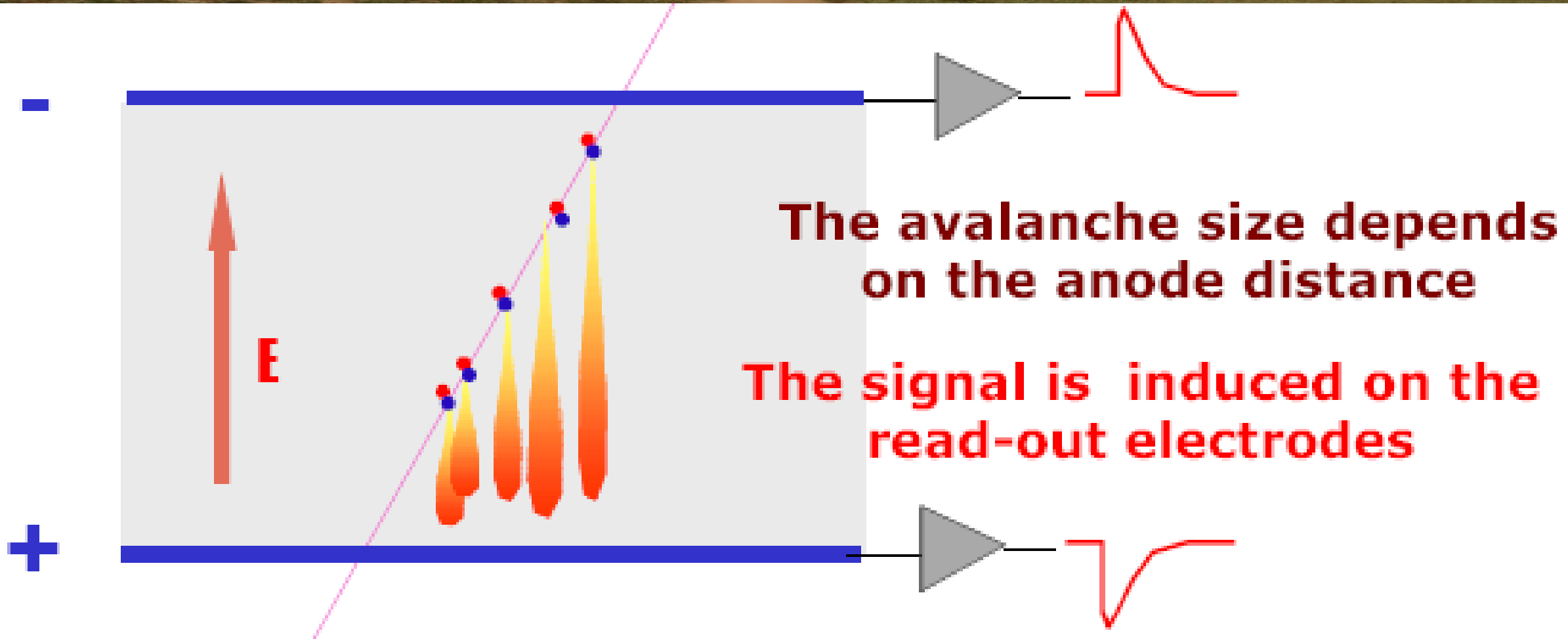


Principle of operation of RPC



- ◆ Electron-ion pairs produced in the ionisation process drift in the opposite directions.
- ◆ All primary electron clusters drift towards the anode plate with velocity v and simultaneously originate avalanches.
- ◆ A cluster is eliminated as soon as it reaches the anode plate.
- ◆ The charge induced on the pickup strips is $q = (-e\Delta x_e + e\Delta x_i)/g$.
- ◆ The induced current due to a single pair is $i = dq/dt = e(v + V)/g \approx ev/g$, $V \ll v$.
- ◆ Prompt charge in RPC is dominated by the electron drift.

Signal development in an RPC



- ❖ Each primary electron produced in the gas gap starts an avalanche until it hits the electrode.
- ❖ Avalanche development is characterized by two gas parameters, Townsend coefficient (α) and Attachment coefficient (η).
- ❖ Average number of electrons produced at a distance x , $n(x) = e^{(\alpha - \eta)x}$
- ❖ Current signal induced on the electrode, $i(t) = E_w \cdot v \cdot e_0 \cdot n(t) / V_w$, where $E_w / V_w = \epsilon_r / (2b + d\epsilon_r)$.

Shockley–Ramo theorem

The Shockley–Ramo theorem allows one to easily calculate the instantaneous electric current induced by a charge moving in the vicinity of an electrode. It is based on the concept that current induced in the electrode is due to the instantaneous change of electrostatic flux lines which end on the electrode, not the amount of charge received by the electrode per second.

The Shockley–Ramo theorem states that the instantaneous current, i induced on a given electrode due to the motion of a charge is given by:

$$i = E_v q v$$

q is the charge of the particle;
 v is its instantaneous velocity; and
 E_v is the component of the electric field in the direction of v at the charge's instantaneous position, under the following conditions: charge removed, given electrode raised to unit potential, and all other conductors grounded.

Signal induction process

The movement of the charges in the detector induces a current signal on the read out electrodes. Because of their small drift velocity, the current signal induced by the drifting ions is much smaller than the current induced by the electrons. The induced current signal of $N(t)$ charge carriers in a cluster that is moving with the velocity $\vec{v}_D(t) = \dot{\vec{x}}(t)$ at time t is given by

$$i(t) = \vec{E}_w(\vec{x}(t)) \cdot \vec{v}_D(t) e_0 N(t) ,$$

where e_0 is the unit charge and \vec{E}_w is the electric field in the gas gap if we put one RPC read out strip on 1 V and ground all other electrodes. The value \vec{E}_w is called the *weighting field*. It should not be confused with the actual electric field. A schematic plot of the weighting field and the signal induction process is given in Fig. 2.17. For n_{Cl} clusters moving in the gas gap of an RPC, the induced current signal is the sum over all clusters

$$i(t) = \sum_{j=1}^{n_{Cl}} \vec{E}_w(\vec{x}_j(t)) \cdot \vec{v}_{Dj}(t) e_0 N_j(t) .$$

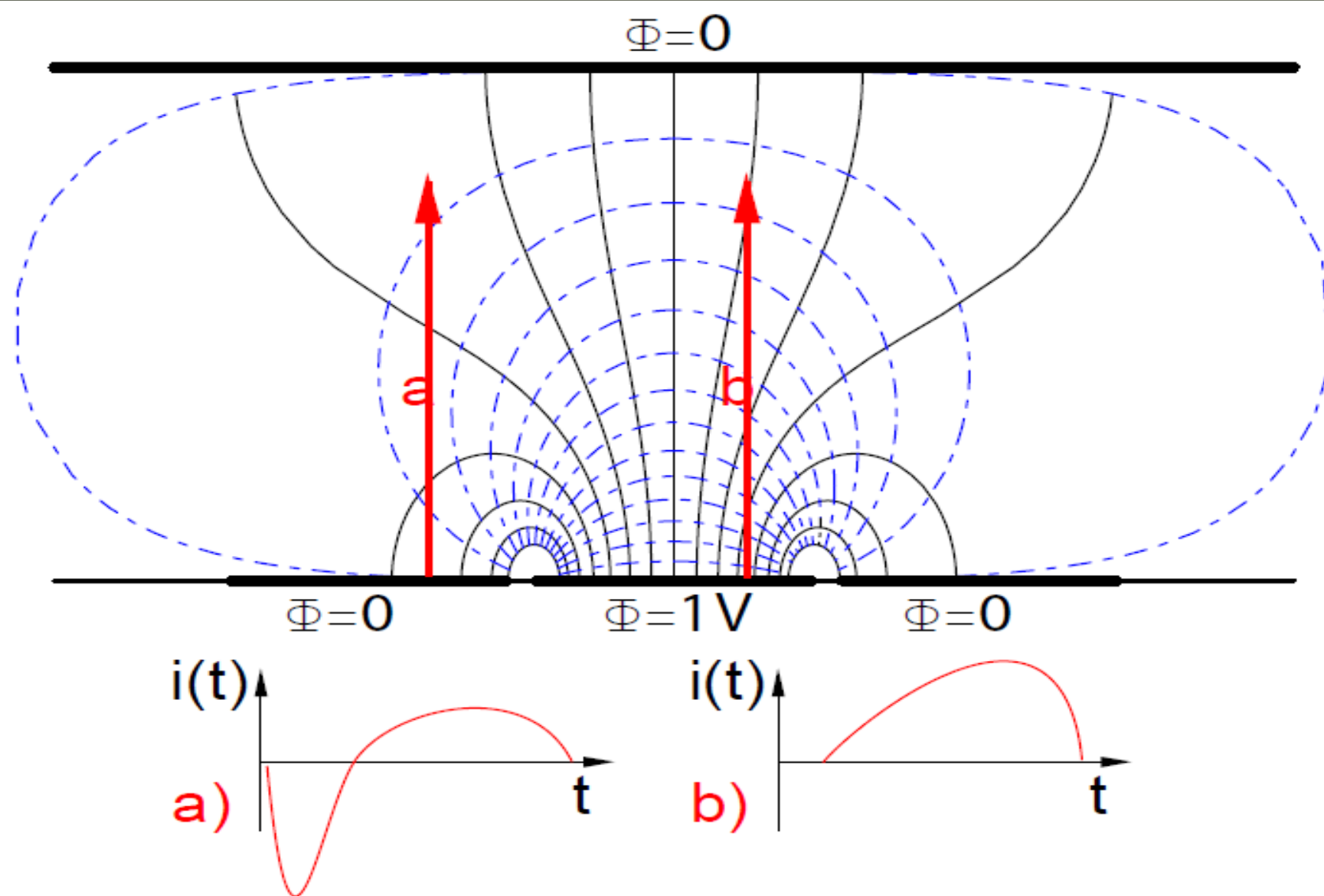
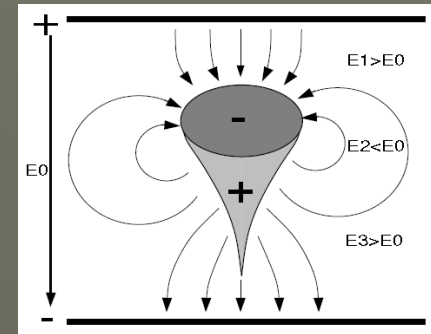


Figure 2.17: A schematic plot of the weighting field in a strip detector and the signal induction process in two examples. The induced current is calculated using the scalar product of the weighting field vector and the velocity vector(s) of the moving charge(s).

Control of avalanche process

- ◆ Role of RPC gases in avalanche control
 - R134a is the ionising gas (83 clusters/cm, compare with Argon's 30 clusters/cm used in the streamer mode).
 - R134a also captures free electrons and localise avalanches.
 - $e^- + X \rightarrow X^- + h\nu$ (Electron attachment)
 - $X^+ + e^- \rightarrow X + h\nu$ (Recombination)
 - Isobutane to stop photon induced streamers.
 - SF_6 for preventing streamer transitions.
- ◆ Growth of the avalanche is governed by $dN/dx = \alpha N$.
- ◆ The space charge produced by the avalanche, shields (at about $\alpha x = 20$) the applied field and avoids exponential divergence.
- ◆ Townsend equation should be $dN/dx = \alpha(E)N$.



The avalanche growth

- ◆ An ionising particle crossing the gas gap g produces ng free electrons, n being the average number per unit length.
- ◆ Number of drifting electrons at a time t after gas ionisation is $N(t) = n(g-vt)e^{\alpha t}$
- ◆ Current induced on the pickup electrodes is $i = eN(t)v/g = evn(1-vt/g)e^{\alpha t}$
- ◆ $q = \int i dt$ between 0 and $t_{\max} (= g/v)$ is the prompt charge, i.e. $q = le^{\alpha g}/(\alpha g)^2$, where $l = eng$. It is the electron charge delivered by the incoming particle.
- ◆ Total charge delivered in the gas is $Q = en \int l e^{\alpha x} dx = le^{\alpha g}/(\alpha g)$ (integrated between 0 and g)
- ◆ The ratio of prompt to total charge $q/Q = 1/\alpha g$ is $\ll 1$, as $\alpha g < 20$ (the limit of the avalanche to streamer transition).
- ◆ This is due to the fact that most free electrons are produced very near to the anode.

◆ RPC volume

- 2mm glass resistive plates
- 2mm gap

◆ Gas mixture

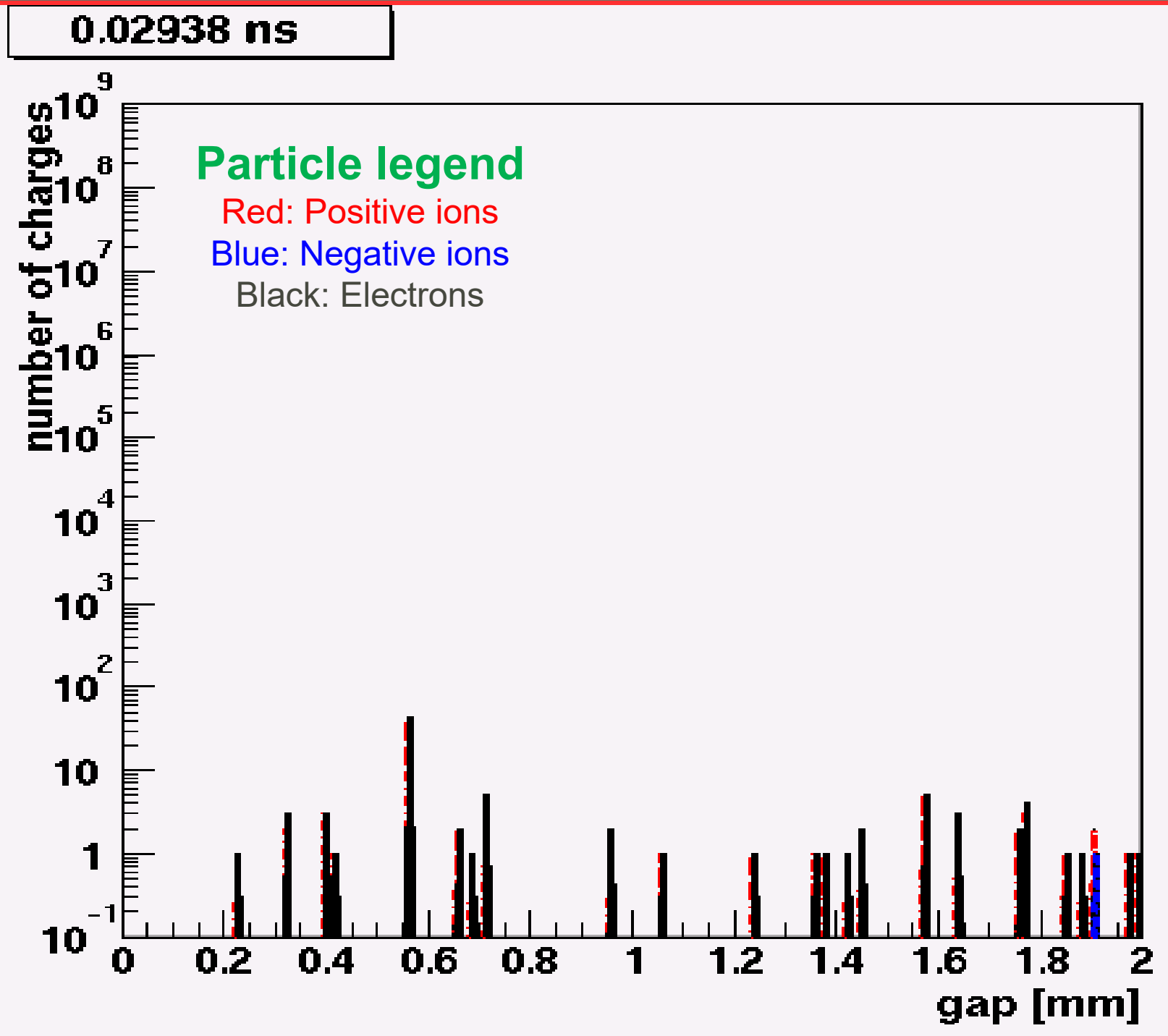
- C₂F₄H₂ (97%)
- iC₄H₁₀ (2.5%)
- SF₆ (0.5%)

◆ HV applied

- 10.0kV

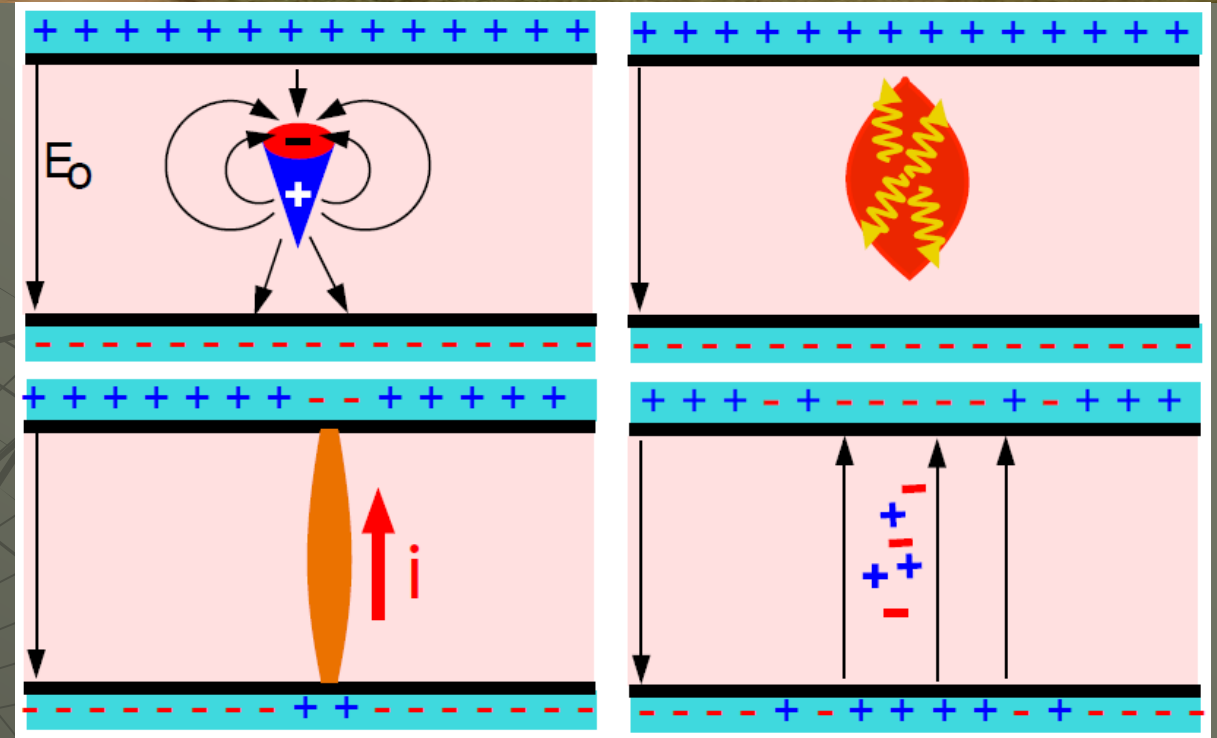
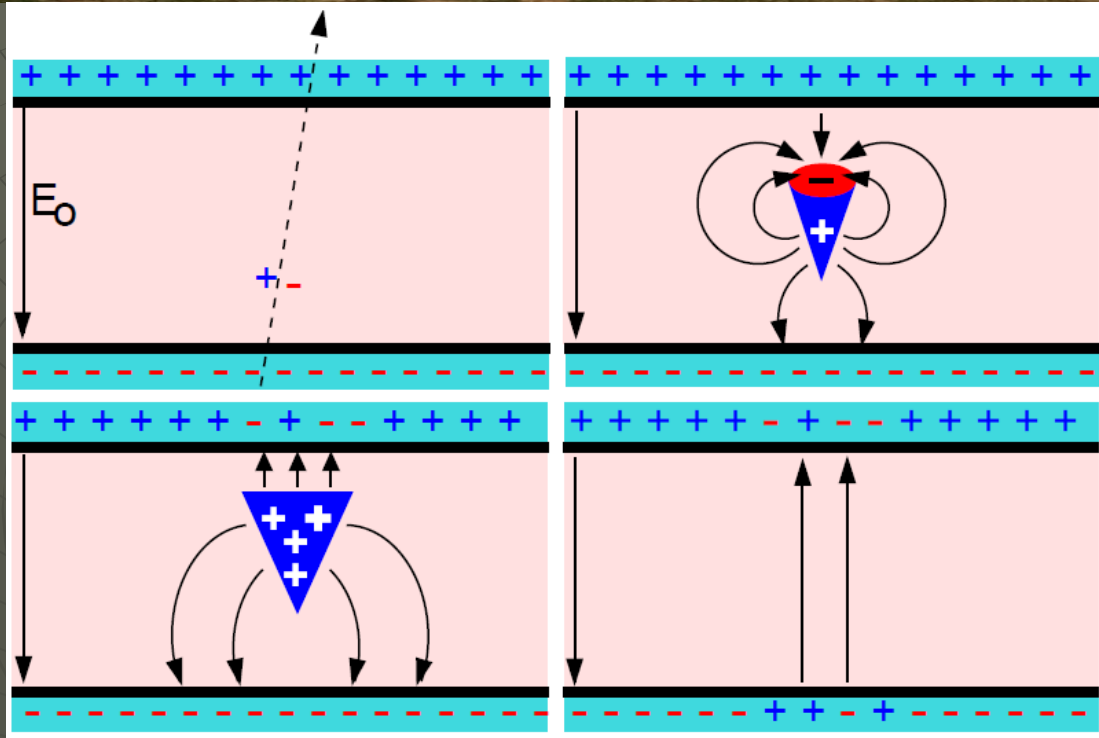
Credit:

Christian Lippmann



Two modes of RPC operation

Avalanche mode



Streamer mode

- Gain of the detector $\ll 10^8$
- Charge developed $\sim 1\text{pC}$
- Needs a preamplifier
- Longer detector life
- Typical gas mixture
R134a:iB:SF₆::94.5:4:0.5
- Moderate purity of gases is fine!
- Higher counting rate capability

- Gain of the detector $> 10^8$
- Charge developed $\sim 100\text{pC}$
- No need for a preamplifier
- Relatively shorter detector life
- Typical gas mixture
R134a:iB:Ar::62.8:30
- High purity of gases expected
- Low counting rate capability

Typical expected parameters

- ◆ No. of clusters in a distance g follows Poisson distribution with an average of $\bar{n} = g/\lambda$
 - ◆ Probability to have n clusters $p(n) = \frac{1}{n!} \left(\frac{g}{\lambda}\right)^n e^{-\frac{g}{\lambda}}$
 - ◆ Number of electrons reaching the anode $n = n_0 e^{(\alpha-\beta)x}$
 - ◆ Intrinsic efficiency $\epsilon_{\max} = 1 - e^{-\bar{n}}$
 - ◆ So ϵ_{\max} depends only on gas and gap
 - ◆ Intrinsic time resolution $\sigma_t = 1.28/(\alpha - \beta)v_D$
 - ◆ So σ_t doesn't depend on the threshold.
 - ◆ Area of signal pickup spot $S = Qd \div \epsilon V$ (\rightarrow counting rate capability)
-
- ❖ Gas: 96.7/3/0.3 (R134a/iB/SF₆)
 - ❖ Electrode thickness: 2mm
 - ❖ Gas gap: 2mm
 - ❖ HV: 10.0KV (E = 50KV/cm)
 - ❖ Relative permittivity (ϵ): 10
 - ❖ Mean free path (λ): 0.104mm
 - ❖ Avg. no. of electrons/cluster: 2.8
 - ❖ Drift velocity (V_D) = 130mm/ns
 - ❖ Townsend coefficient (α): 13.3/mm
 - ❖ Attachment coefficient (β): 3.5/mm
 - ❖ Total charge (q_{tot}): 200pC
 - ❖ Induced charge (q_{ind}): 6pC
 - ❖ Charge threshold: 0.1pC
 - ❖ Efficiency (ϵ_{\max}): 90%
 - ❖ Time resolution (σ_t): 950pS
 - ❖ Signal pickup spot (S) = 0.1mm²

RPC operating mode definitions

Let, n_0 = No. of electrons in a cluster
 α = Townsend coefficient (No. of ionisations/unit length)
 β = Attachment coefficient (No. of electrons captured by the gas/unit length)

Then, the no. of electrons reaching the anode,

$$n = n_0 e^{(\alpha - \beta)x}$$

Where x = Distance between anode and the point where the cluster is produced.

Gain of the detector, $M = n / n_0$

- A planar detector with resistive electrodes \approx Set of independent discharge cells
- Expression for the capacitance of a planar condenser \rightarrow Area of such cells is proportional to the total average charge, Q that is produced in the gas gap.

$$S = \frac{Qd}{\epsilon_0 V}$$

Where, d = gap thickness

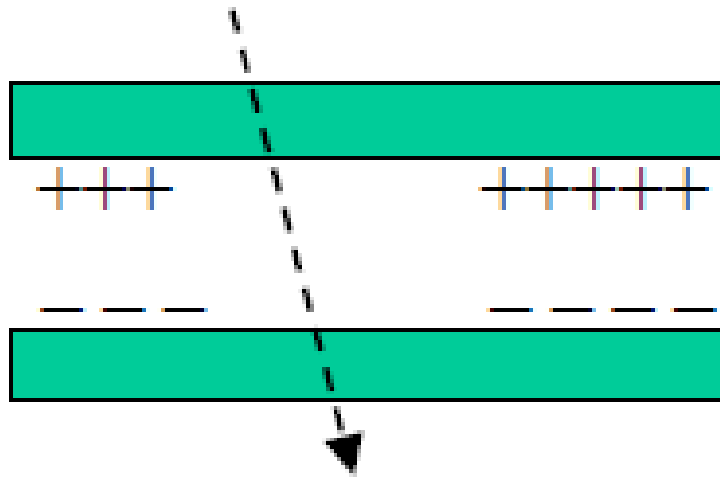
V = Applied voltage

ϵ_0 = Dielectric constant of the gas

- Lower the Q ; lower the area of the cell (that is 'dead' during a hit) and hence higher the rate handling capability of the RPC

Rate capability of a streamer RPC

As noted, each discharge locally deadens the RPC. The recovery time is approximately

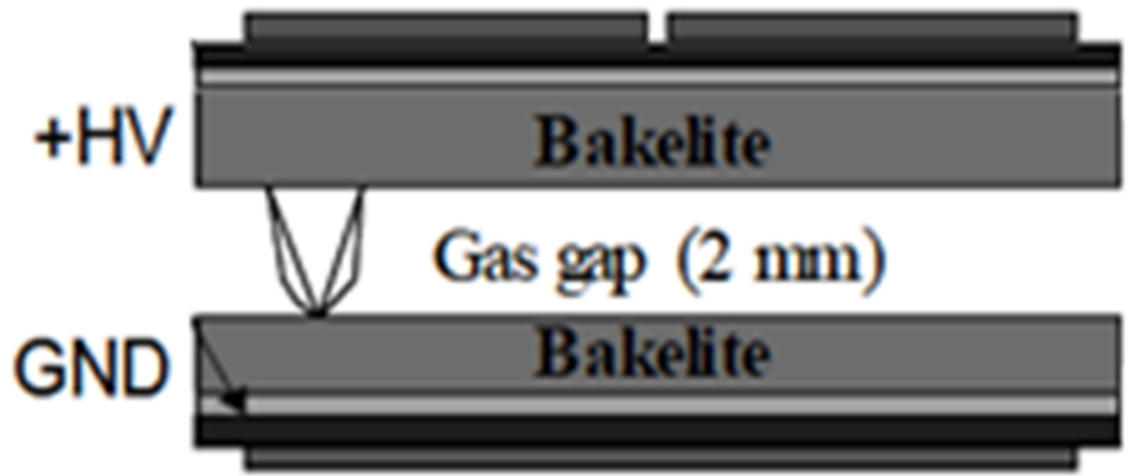


$$\tau = RC \cong \left(\frac{\rho l}{A} \right) \left(\frac{\kappa \epsilon_0 A}{l} \right) = \rho \kappa \epsilon_0$$

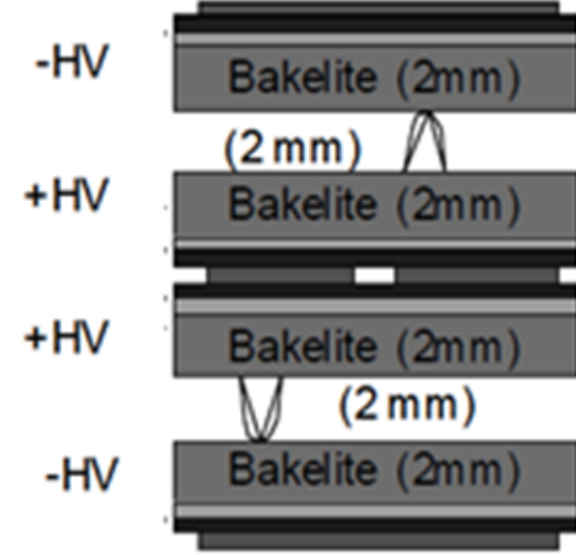
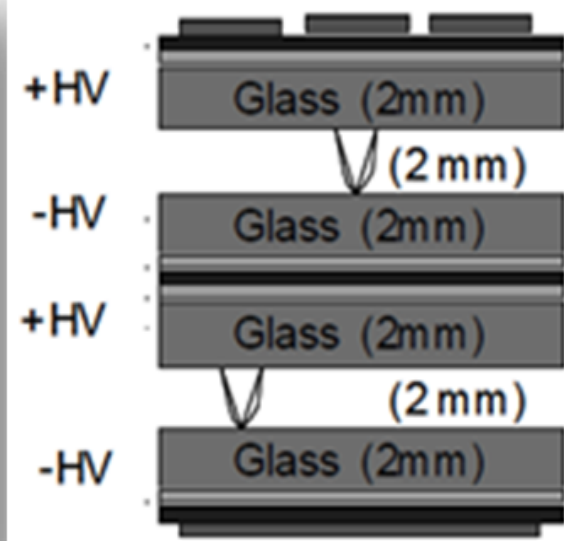
Numerically this is (MKS units)

$$\tau = (5 \times 10^{10}) \times 4 \times (8.85 \times 10^{-12}) = 2 \text{ s}$$

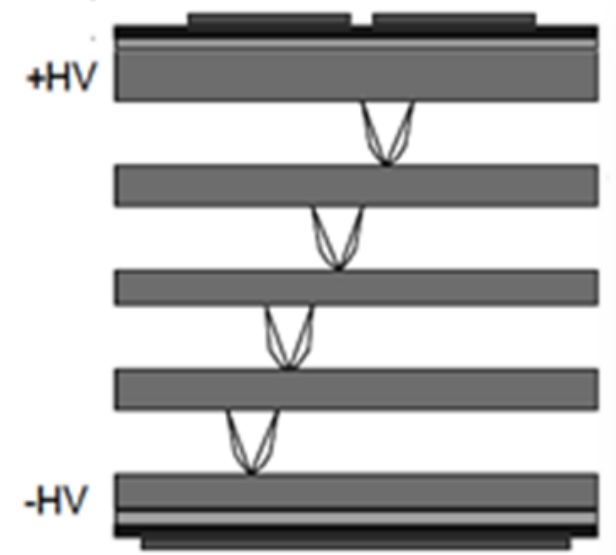
Assuming each discharge deadens an area of 0.1 cm^2 , rates of up to 500 Hz/m^2 can be handled with 1% deadtime or less. This is well below what is expected in our application.



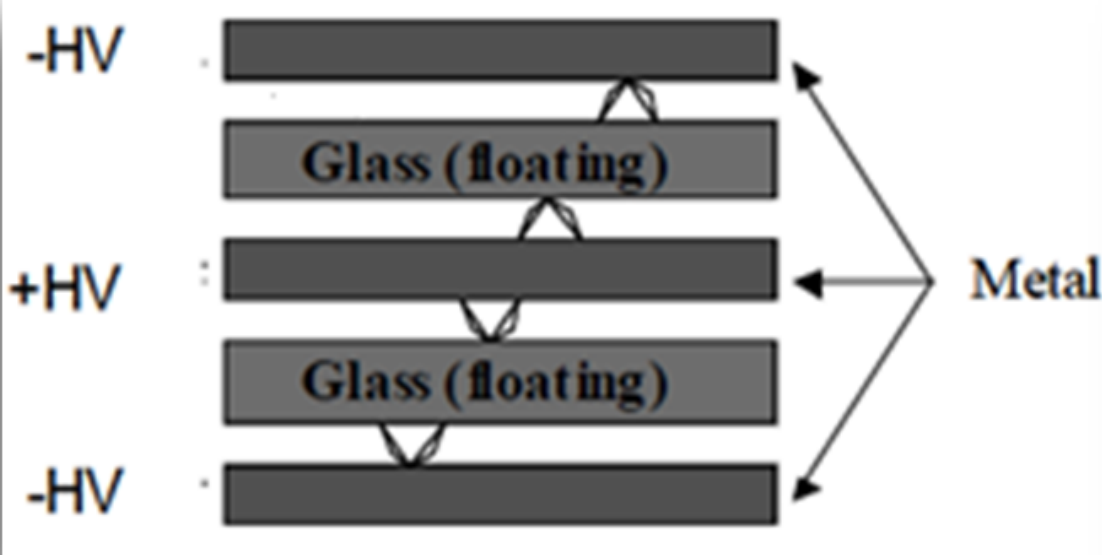
Single gap RPC



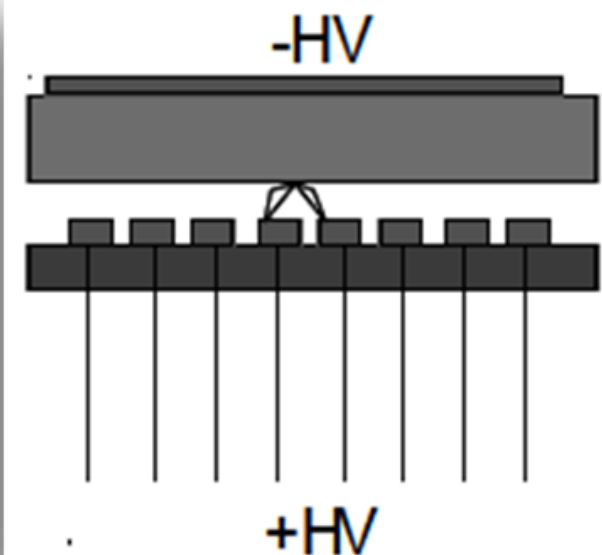
Double gap RPC



Multi gap RPC

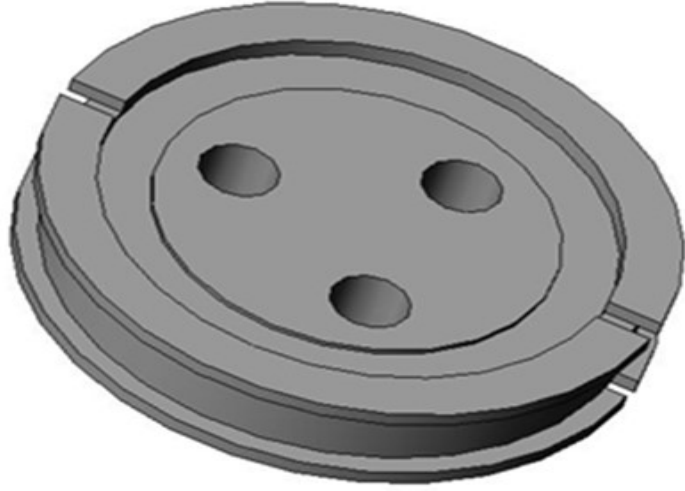


Hybrid RPC

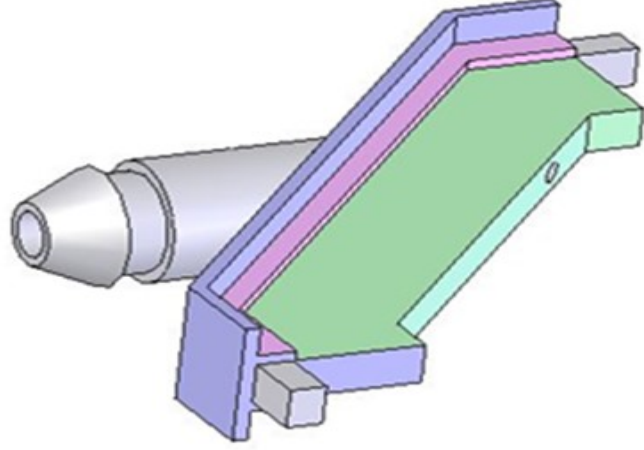


Micro RPC

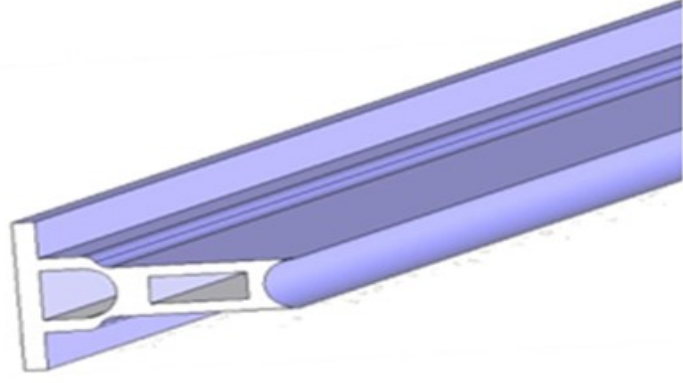
Materials for gas gap fabrication



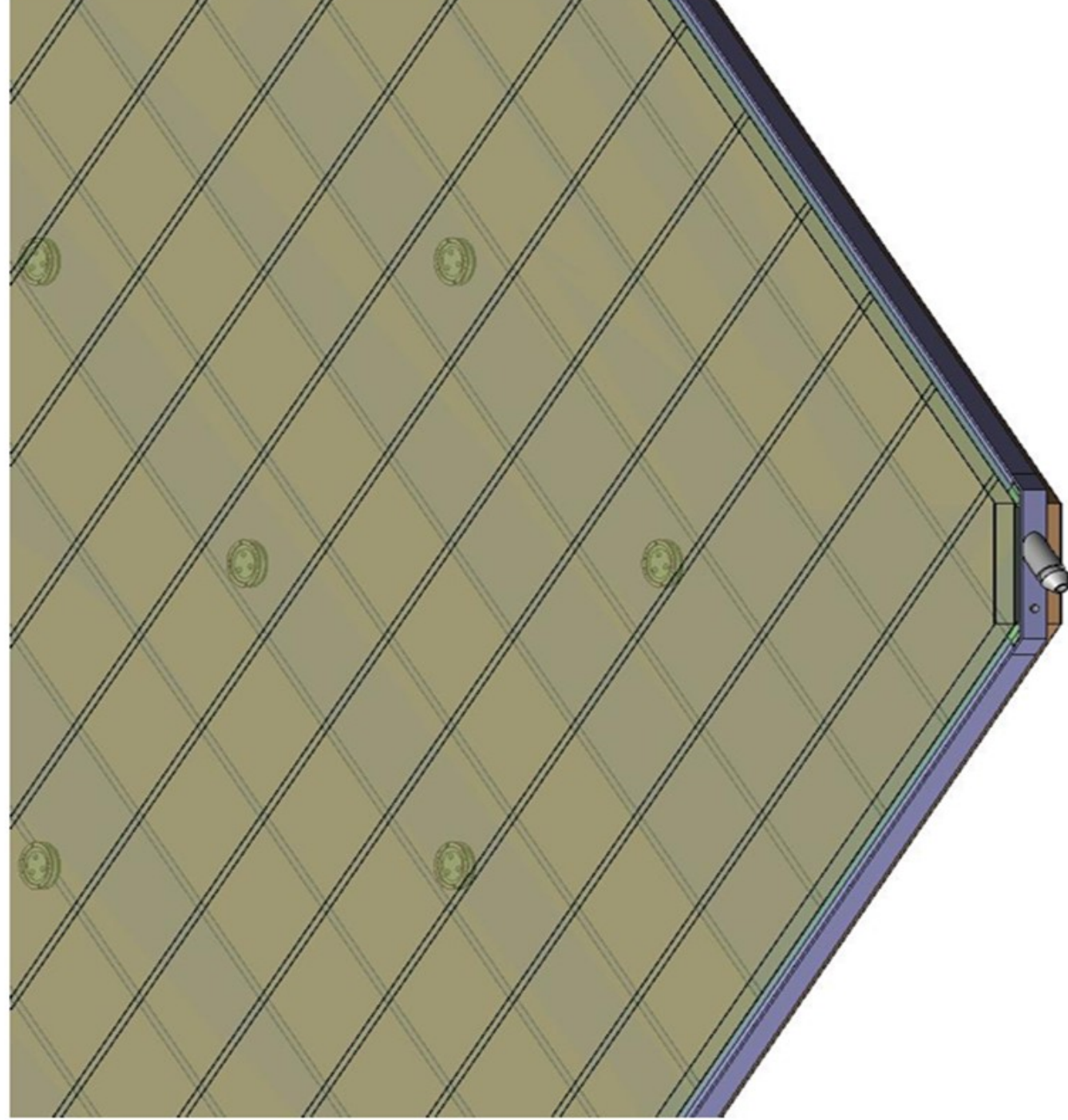
Glass spacer



Gas nozzle

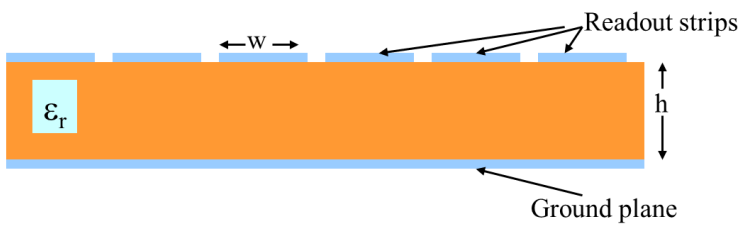


Edge spacer



Schematic of an assembled gas volume

Development of Pickup panels

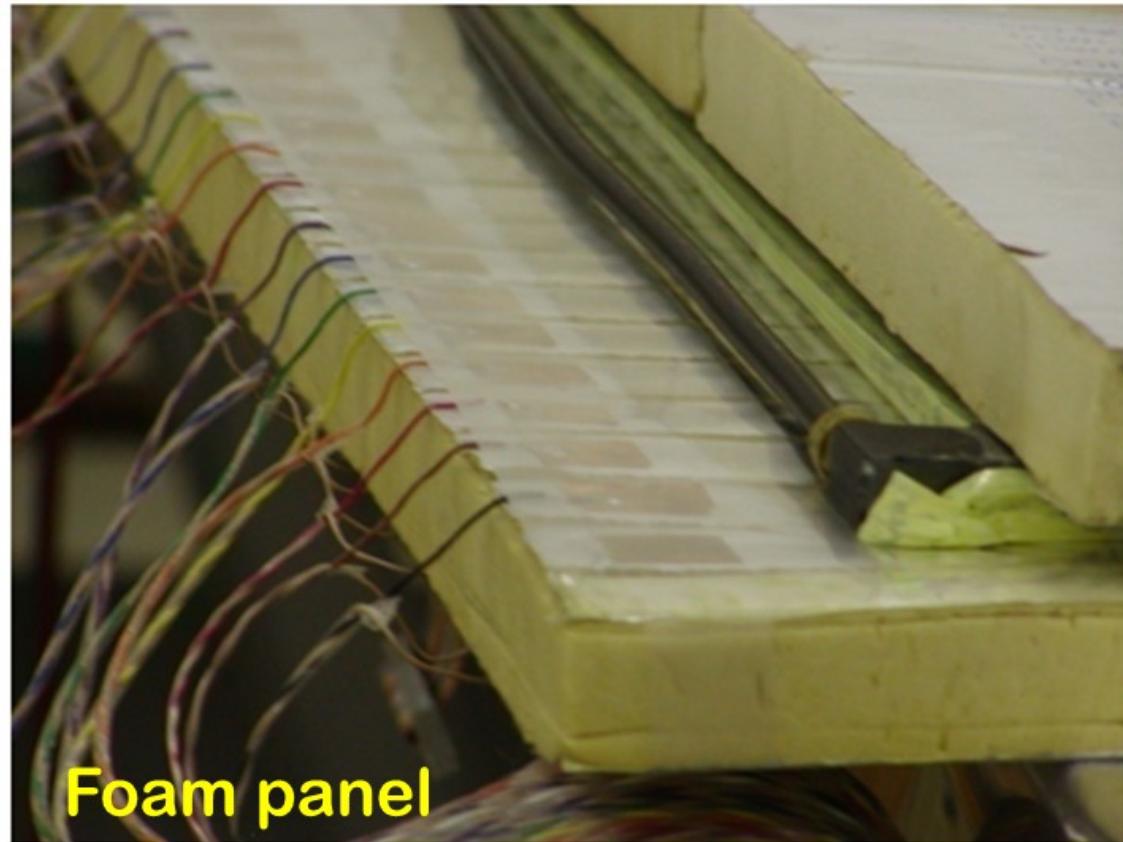


$$x \equiv w/h \quad \epsilon_r' = \frac{\epsilon_r + 1}{2} + \frac{\epsilon_r - 1}{2} (1 + 10x)^{-\frac{1}{2}}$$

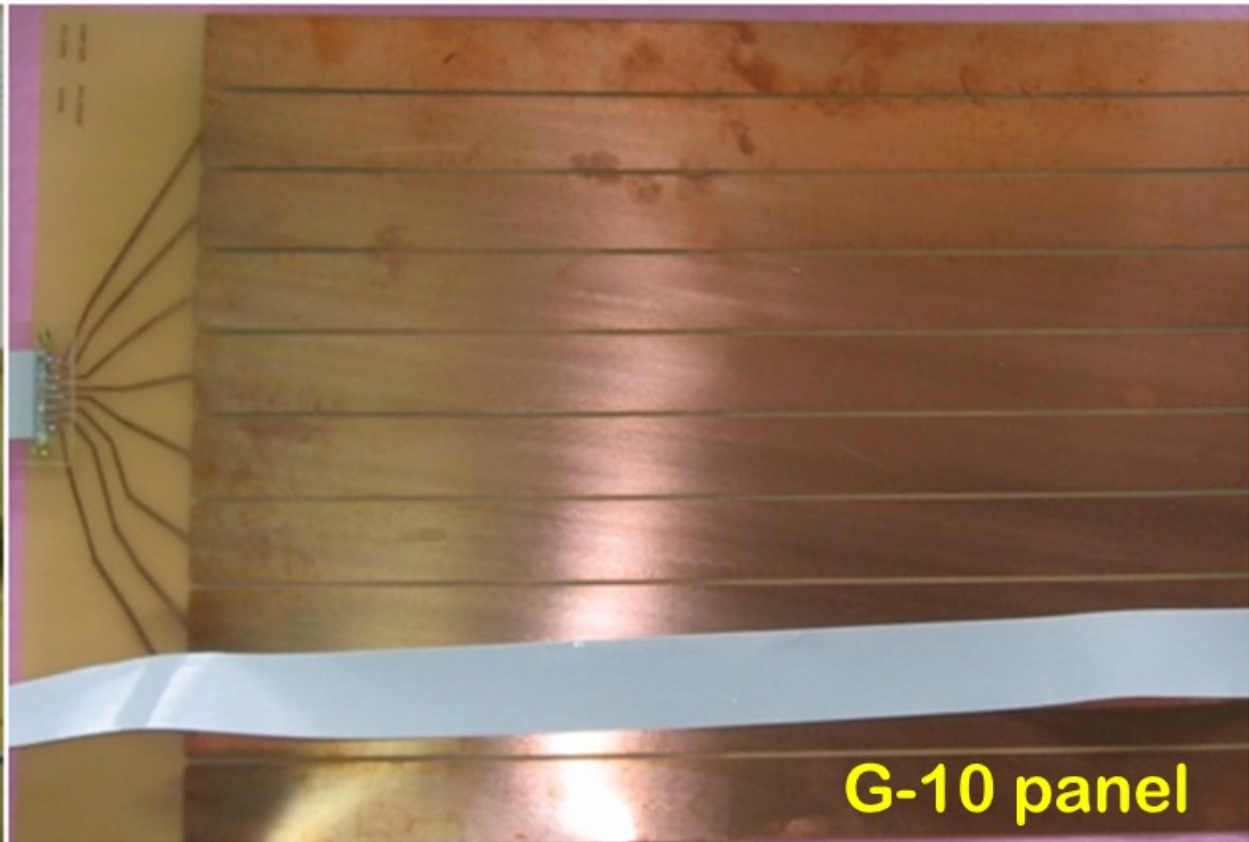
$$Z = \frac{377}{\sqrt{\epsilon_r'} (x + 1.393 + 0.667 \ln(x + 1.444))} : x \geq 1$$

Polypropylene as well as PVC panels are also developed.

Honeycomb panel

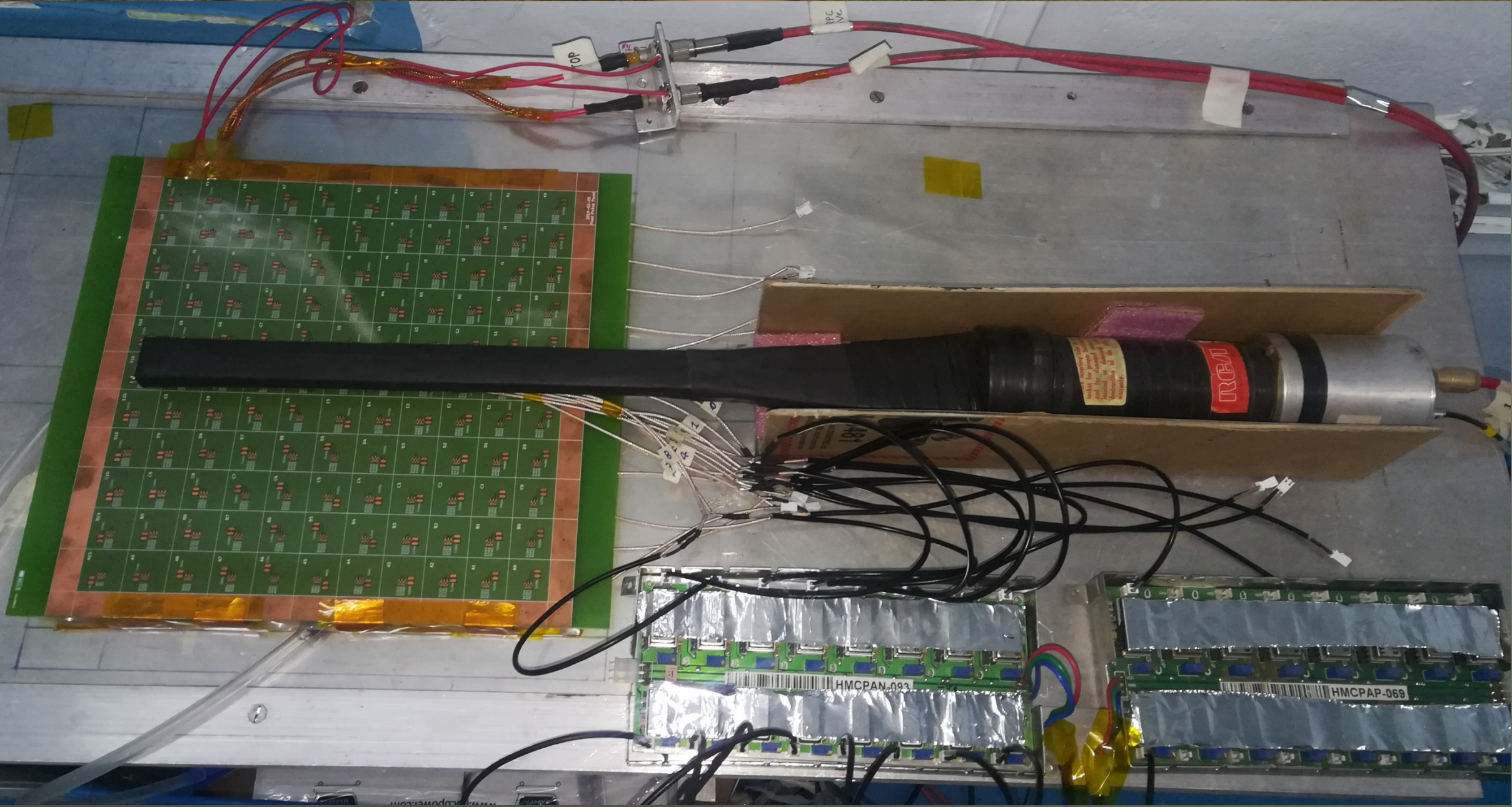


Foam panel



G-10 panel

Pad readout for digital readout



Regd office : Post Box No. 16322, Nerolac House, Ganpatrao Kadam Marg, Lower Parel, Mumbai – 400 013
 Tel. : 022-2493 4001 / 2492 8008 FAX : 022-493 5742 E-Mail : gnpnet @ bom3.vsnl.net.in

Product:-Conductive Coating Black for Glass
 Ref. No:-1019393/1026040
 Customer:-M/s. T. I. F. R. Mumbai.
 Date:-24.06.2013

PRODUCT DATA SHEET	REF. NO.	REVISION	DATE	PAGE
	1026040	00	31.01.2020	1/1
PRODUCT: CONDUCTIVE COATINGS BLACK FOR GLASS - A				

Application details of Glasscoat Conductive Black.

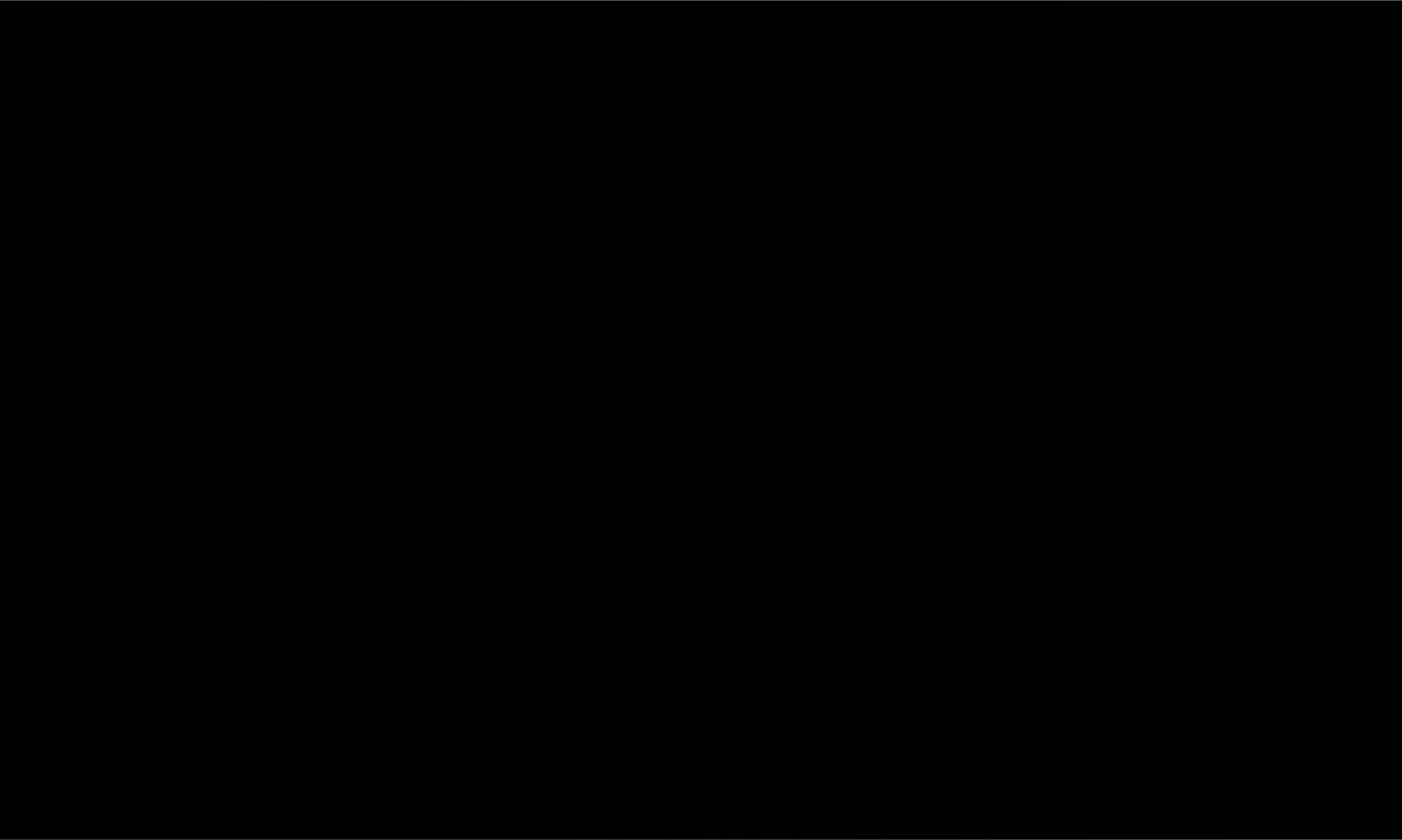
01	Supply Weight / 10 L	11.02 Kg ± 3 %
02	Supply Viscosity	25 ± 05 Sec by FCB4 @ 30°C
03	Total Solids by wt (Comp A)	40 ± 3 % by Kg
04	Recommended Thinner	1000052
05	Thinner Intake	15 ± 5 % By Wt.
06	Application Method	By spraying at 18±2 sec viscosity by F/C.B-4 @ 30°C
07	Recommended DFT	20 - 25 μ
08	Comp B – Hardener	Hardner for Conductive Coatings Black for Glass
09	Mixing Ratio	Comp. A : Comp. B = 100 : 05 By Wt.
10	Pot Life of Mixed Paint	3 - 4 Hrs at 30°C
11	Drying/Baking Schedule	Air Drying at 30-40°C for 72 Hrs. for full curing.
12	Color	Black
13	Dry Film Resistivity	1500- 3500 K Ohm at 20-25 μ DFT
14	Shelf Life	Six months from the date of manufacturing under normal storage conditions at 27-30°C when both the components are stored separately and away from contact of water and moisture. Thinner intake should not be more than the double of the original after six month of storage.



Note:-
 Dry Film Resistivity to be tested by using a TIFR - Jig made up of Glass Wool & Brass material.
 Recommended Thinner for application :- 1000052
 Air Pressure:- 4.0kg/cm²
 Application:-By conventional spraying.



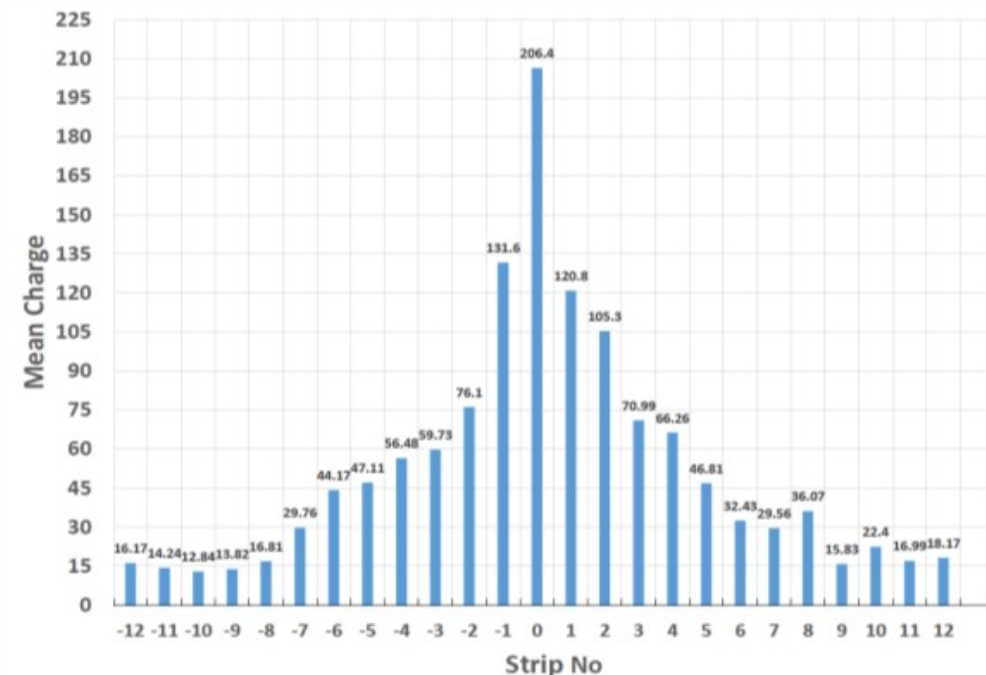
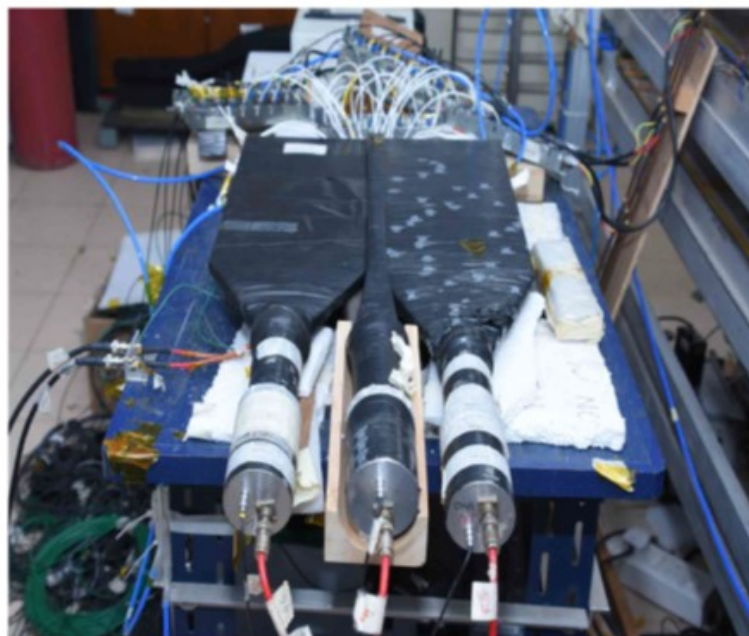
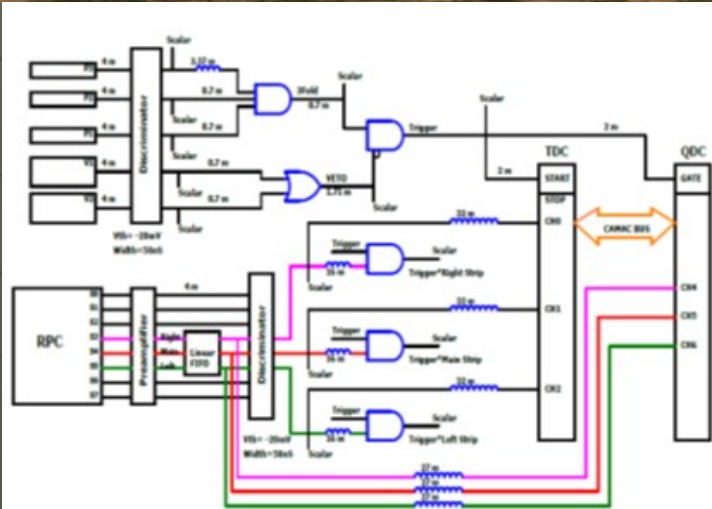
Spray printing on electrodes



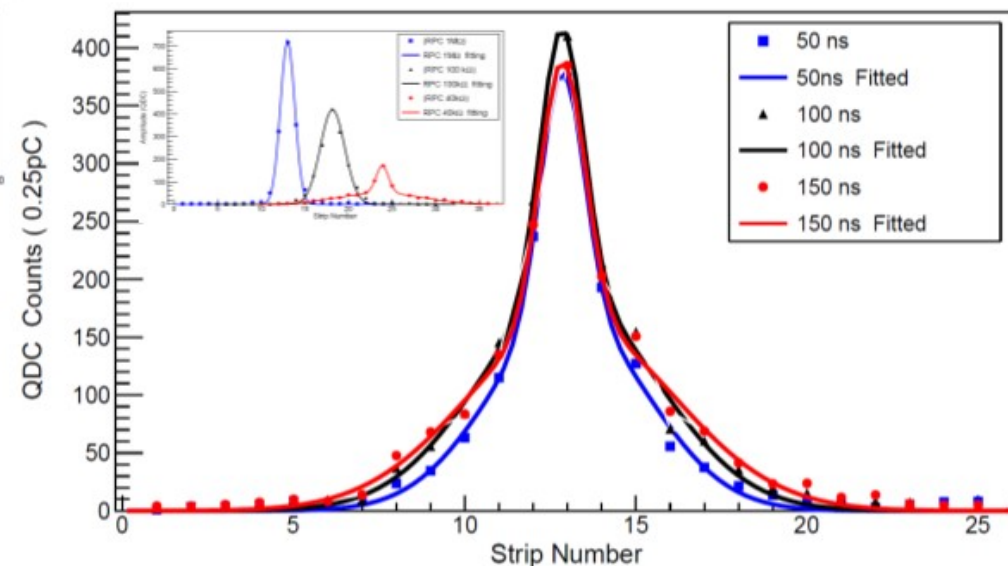
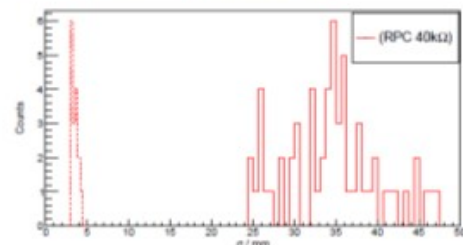
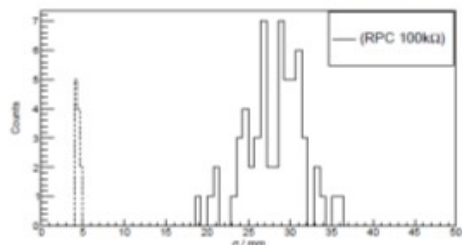
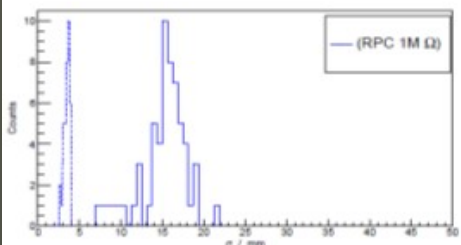
Screen printing on electrodes



Precision studies on coat resistance



Position resolution of (0.98 ± 0.11) mm with 5mm strips, (0.57 ± 0.21) mm with 3mm strips.



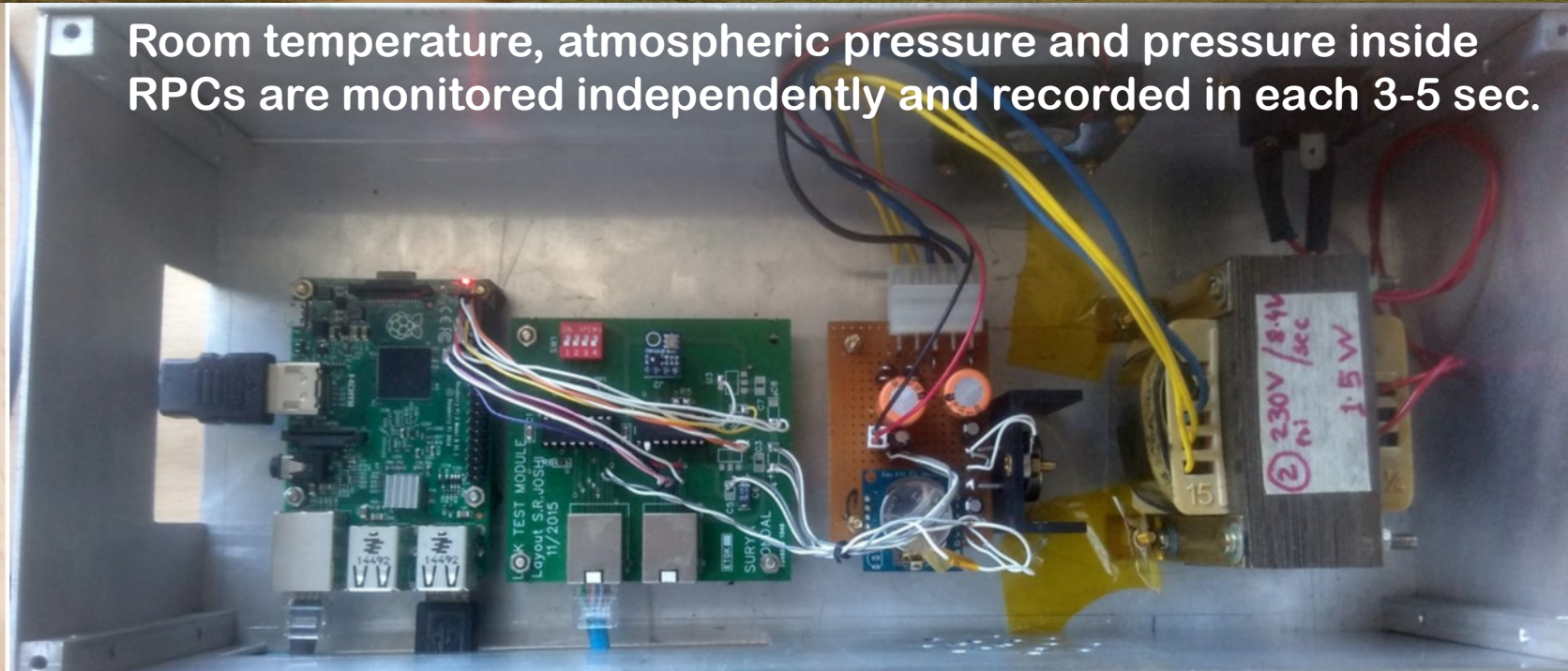
Experimental

Integration time	σ_1 (mm)	σ_2 (mm)
50ns	5.66 ± 0.12	37.28 ± 2.13
100ns	5.77 ± 0.13	43.94 ± 2.11
150ns	5.76 ± 0.12	51.23 ± 2.41

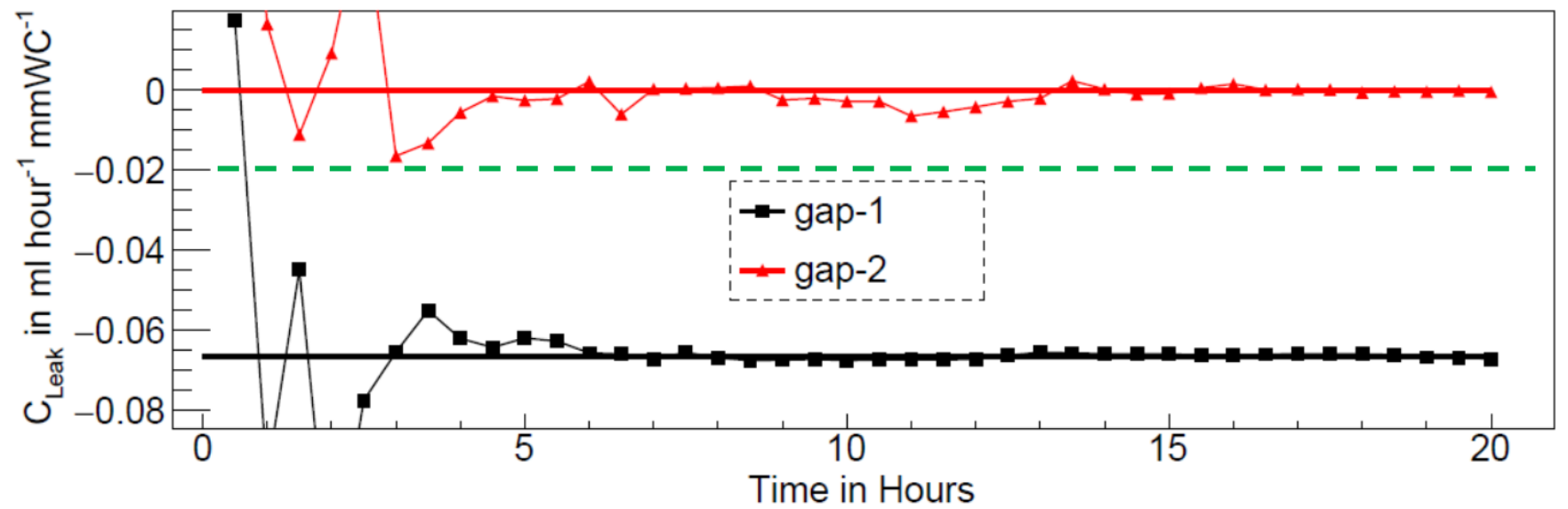
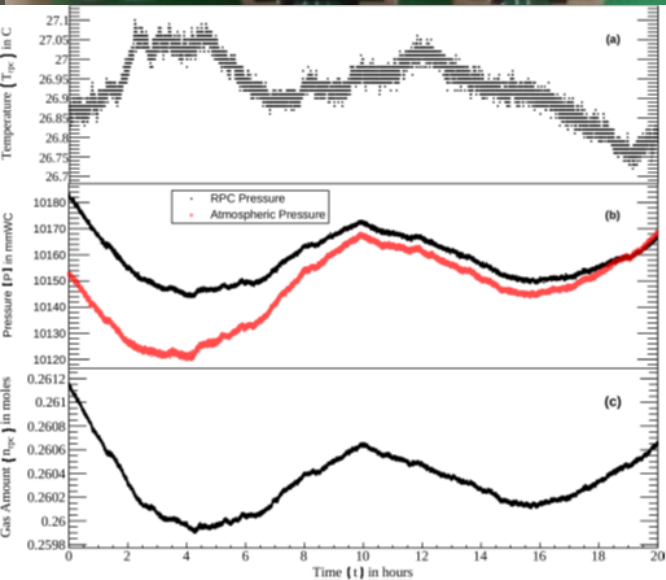
Automatic RPC gap making

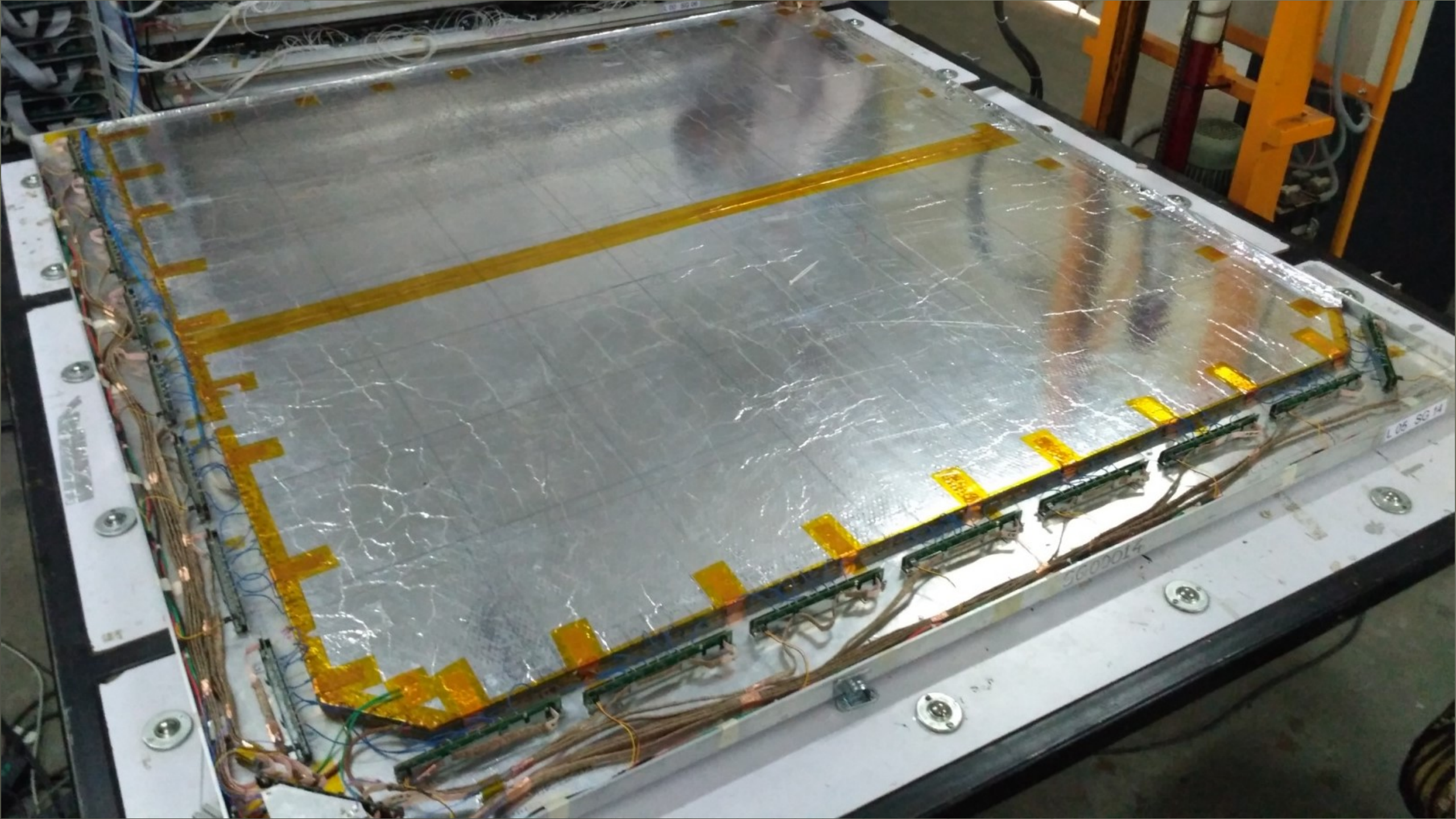
The background of the slide features a wide, flat landscape with a dirt road in the center that leads towards a range of low mountains in the distance. The sky is filled with soft, white clouds, and the overall scene is captured in a natural, outdoor setting.

Automated leak test system for RPC gaps

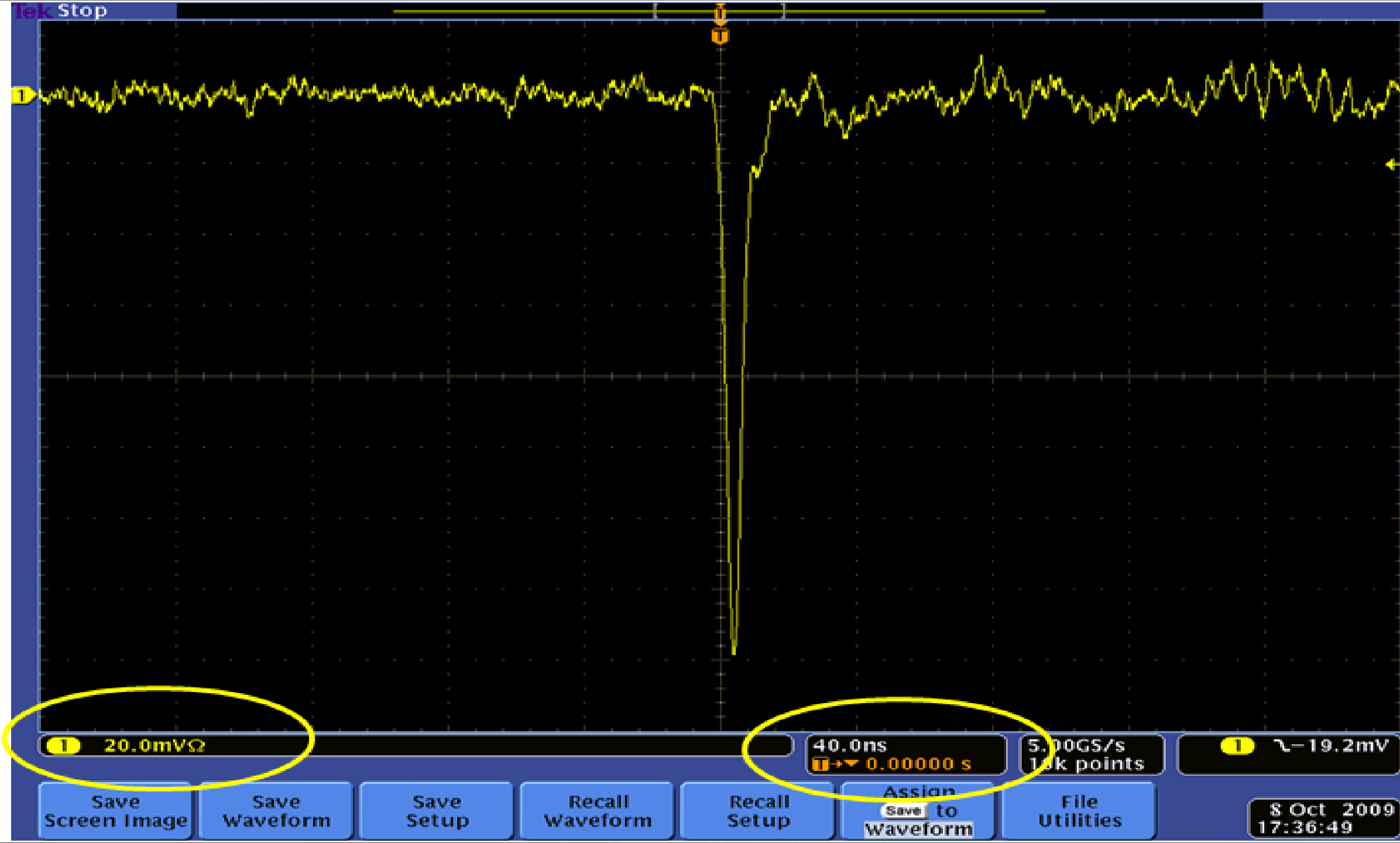


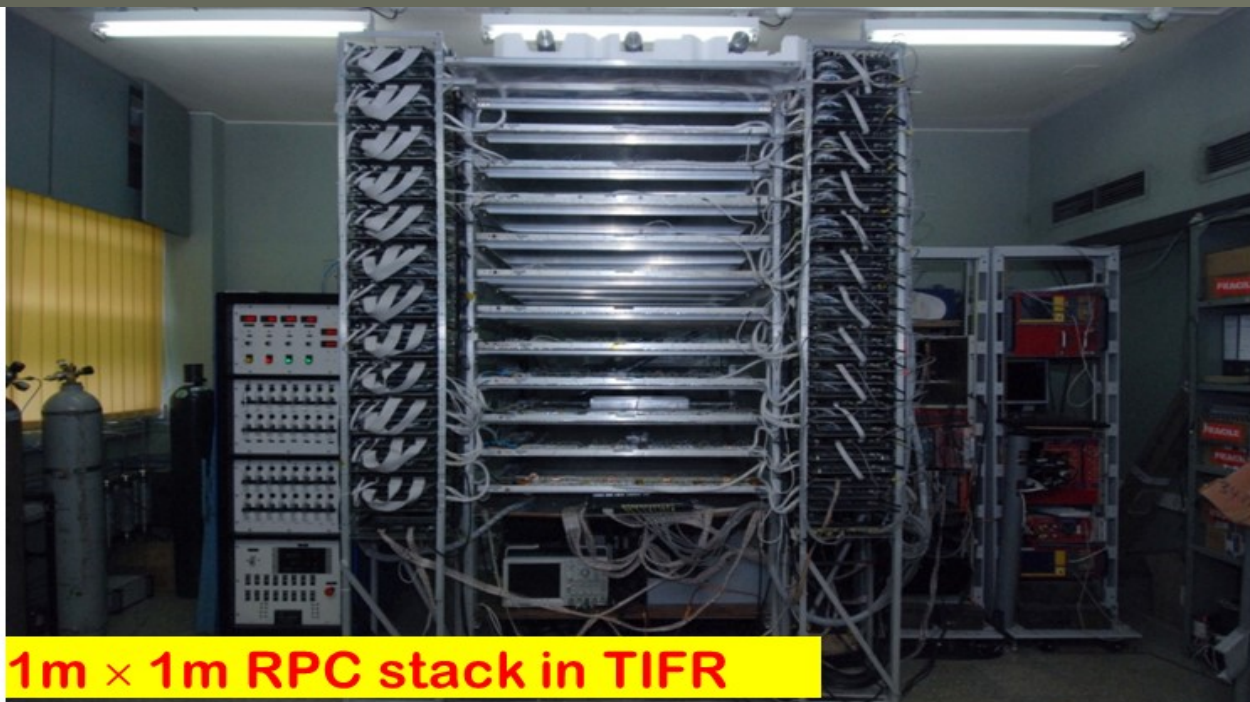
Room temperature, atmospheric pressure and pressure inside RPCs are monitored independently and recorded in each 3-5 sec.





Signal from an RPC strip

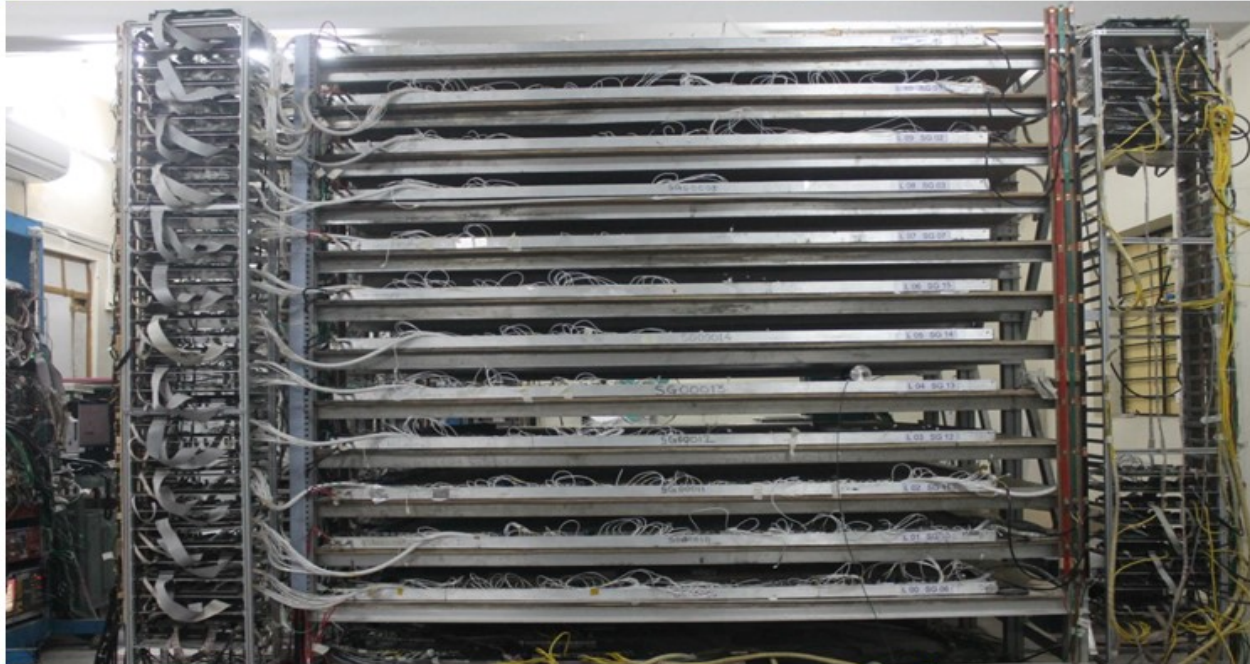




1m × 1m RPC stack in TIFR



2m × 2m RPC test stand in TIFR

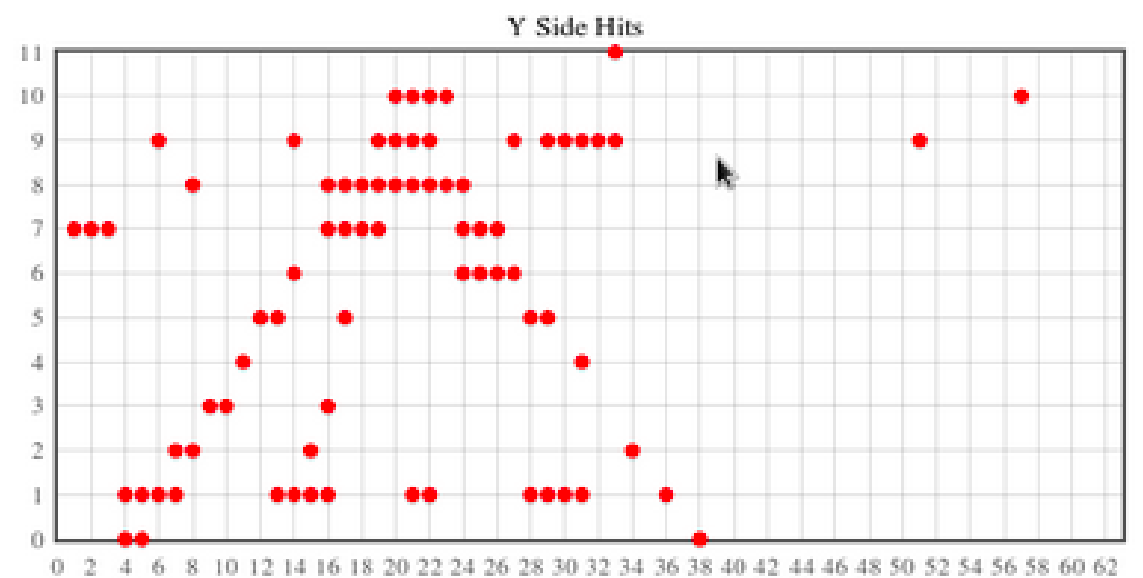
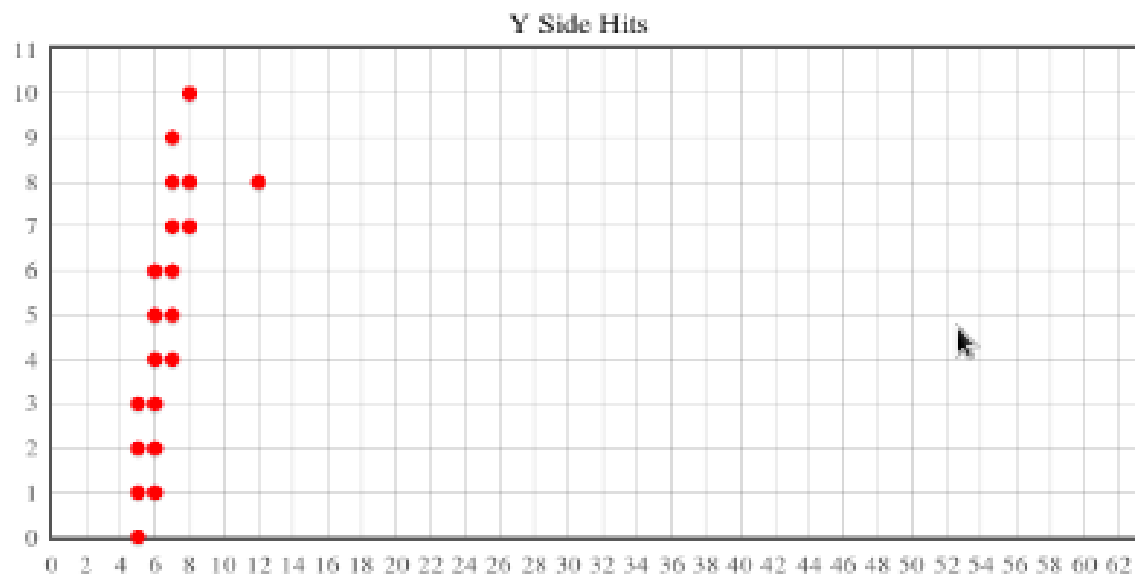
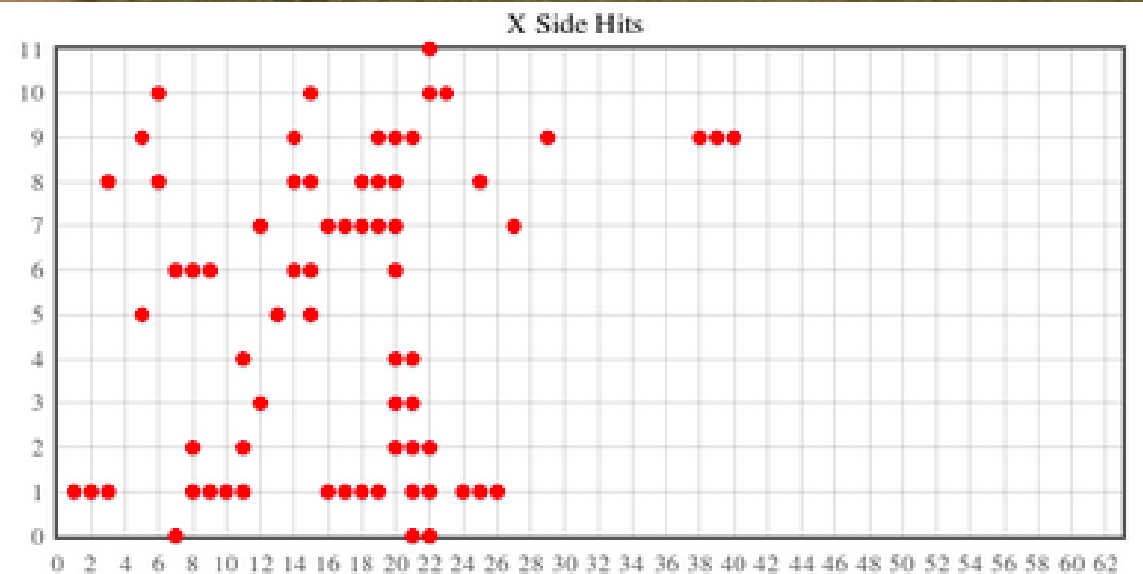
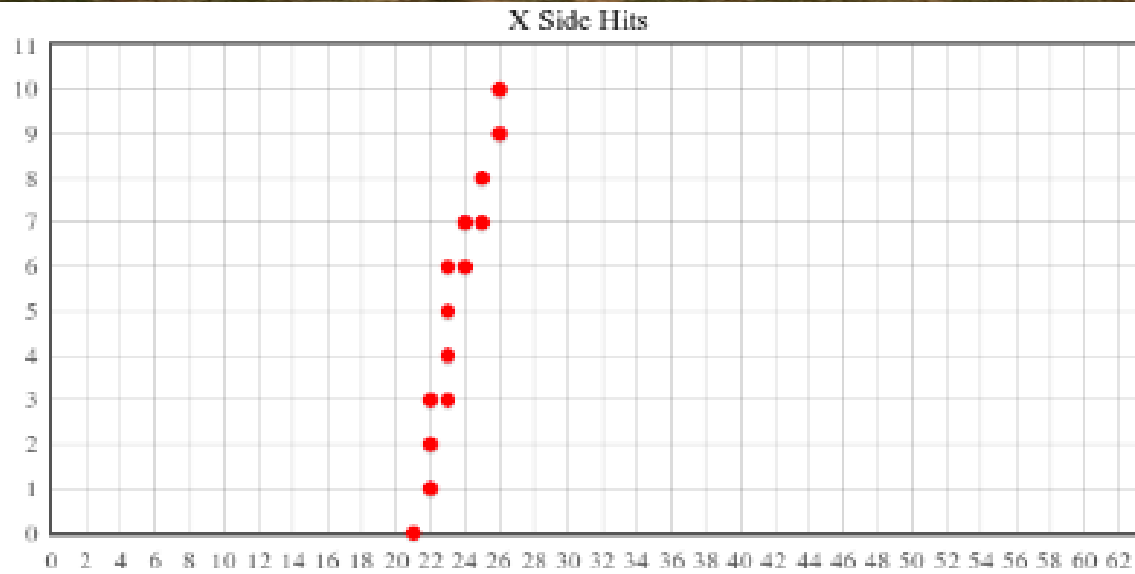


2m × 2m RPC stack in Madurai

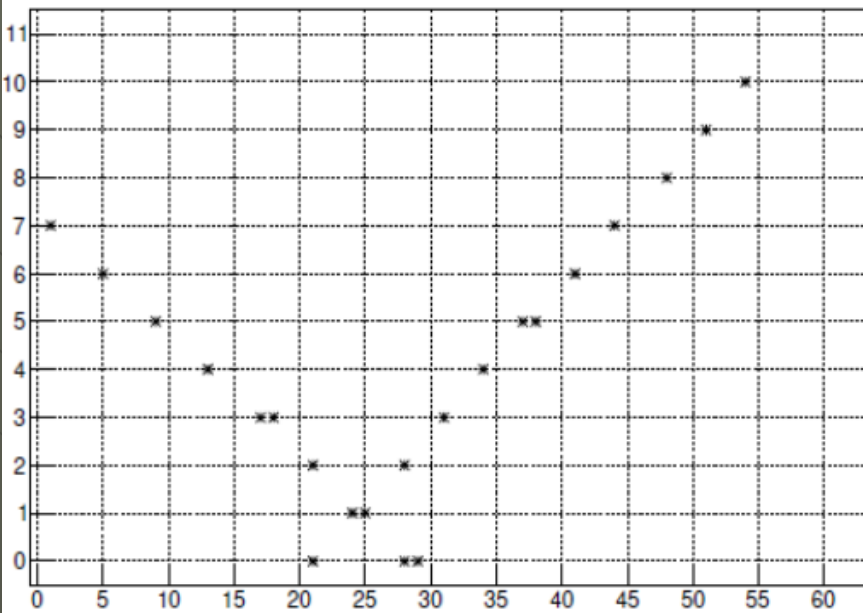


1m × 1m RPC stack in VECC

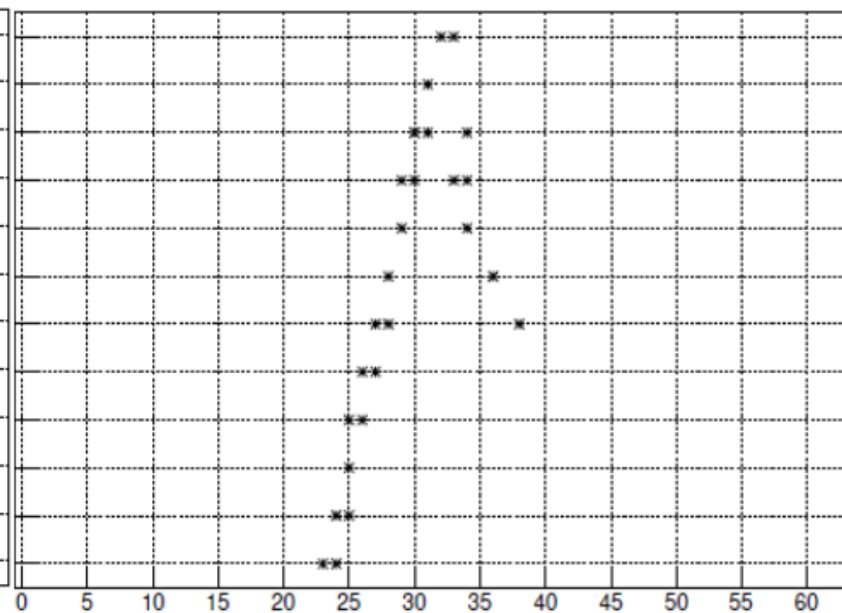
Muons and hadrons in the RPC stack



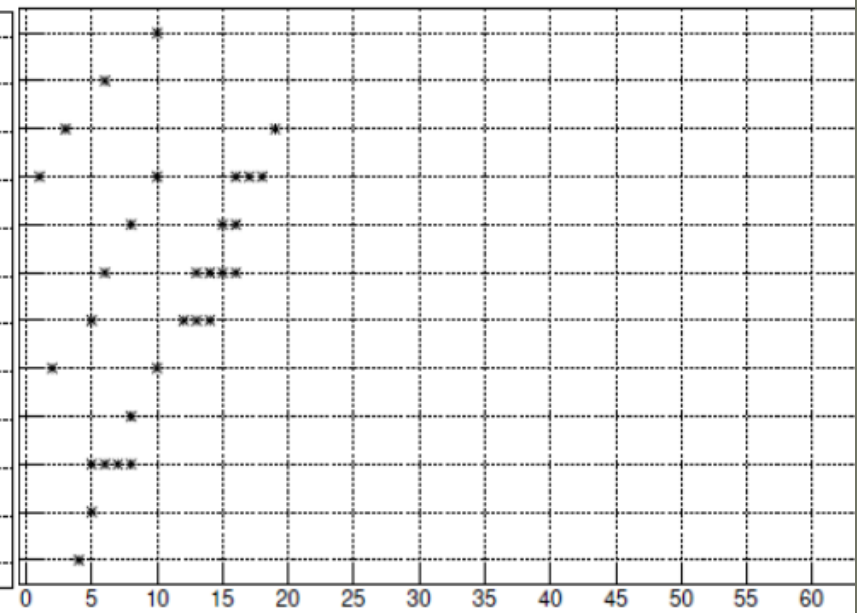
Multi_Event_x_0057_029933_m2



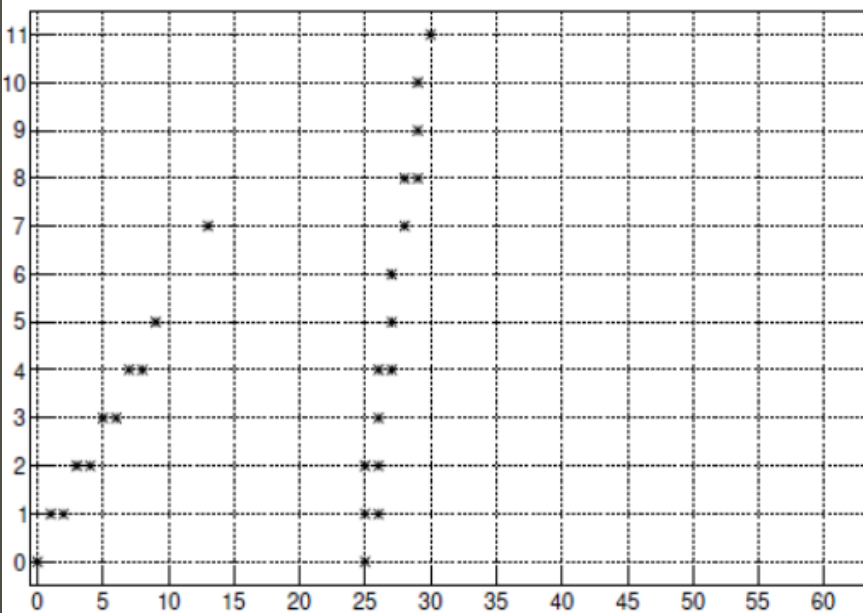
Multi_Event_x_0057_025969_m2



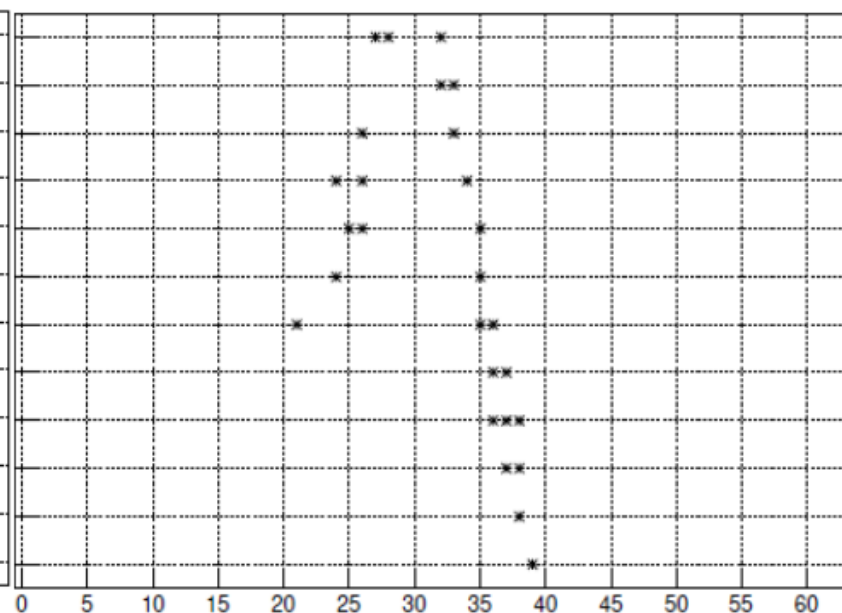
Multi_Event_x_0057_009718_m2



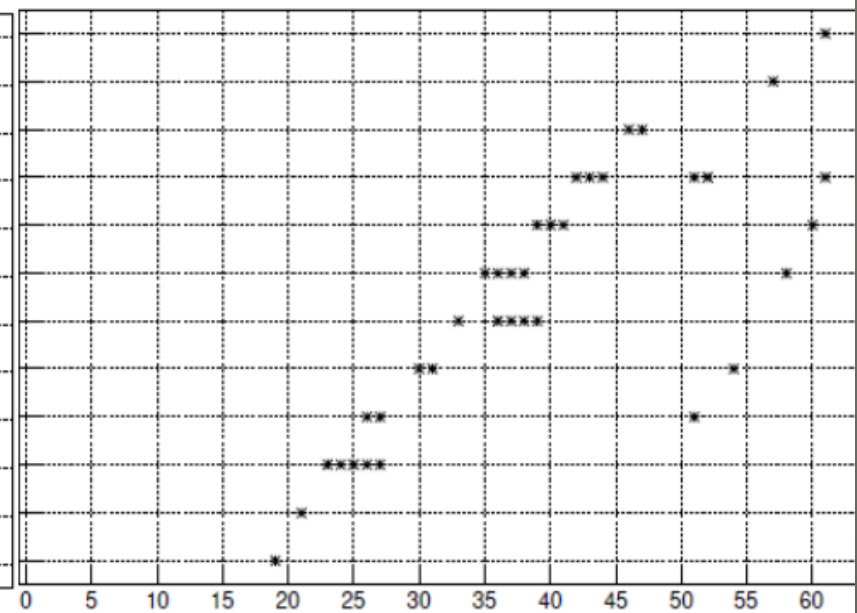
Multi_Event_y_0057_029933_m2

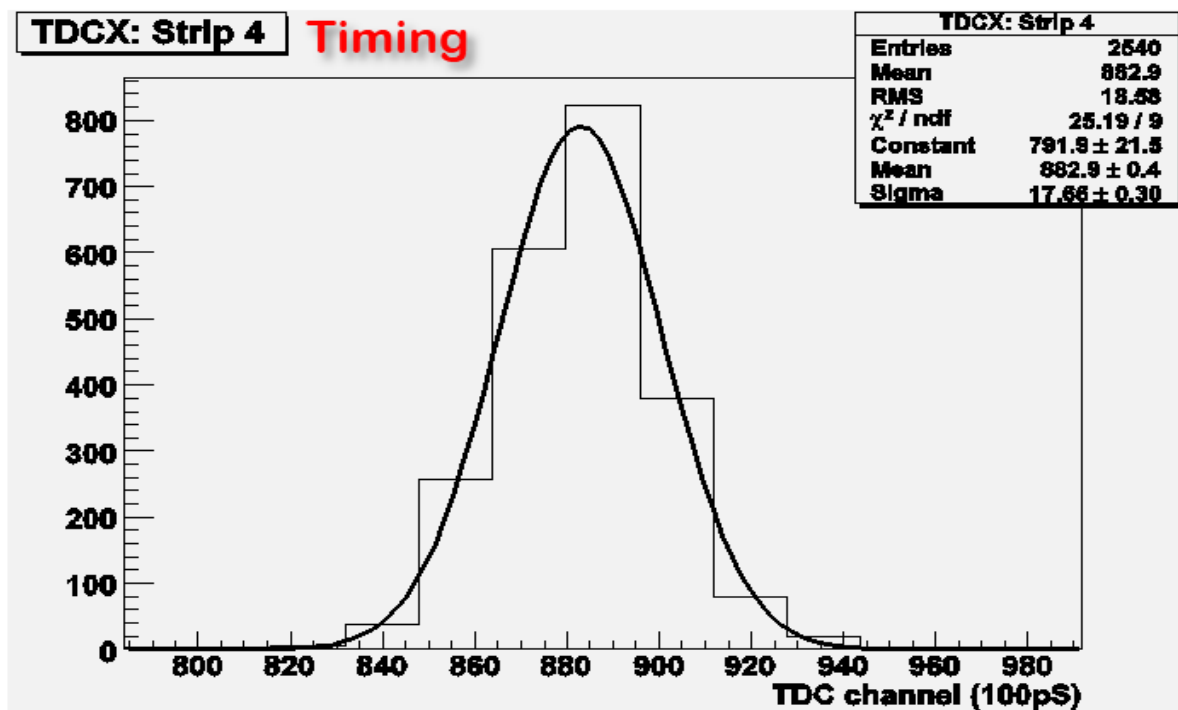
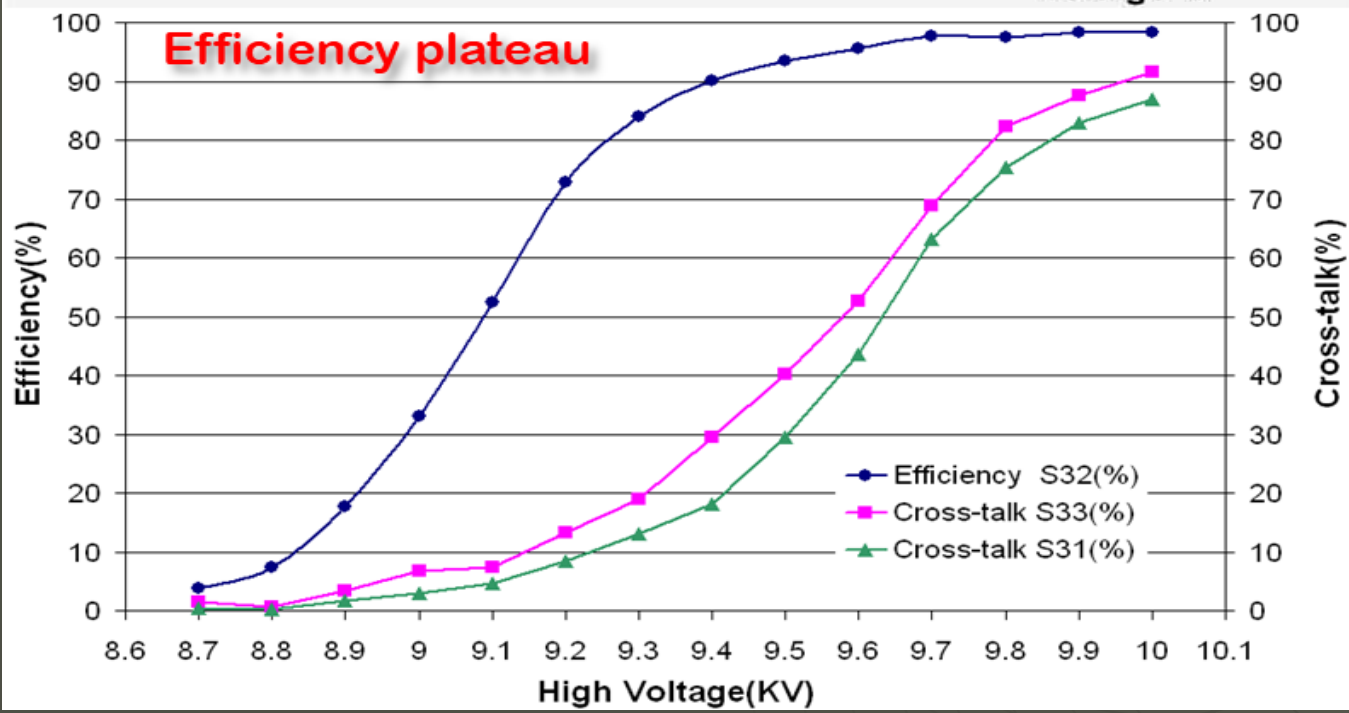
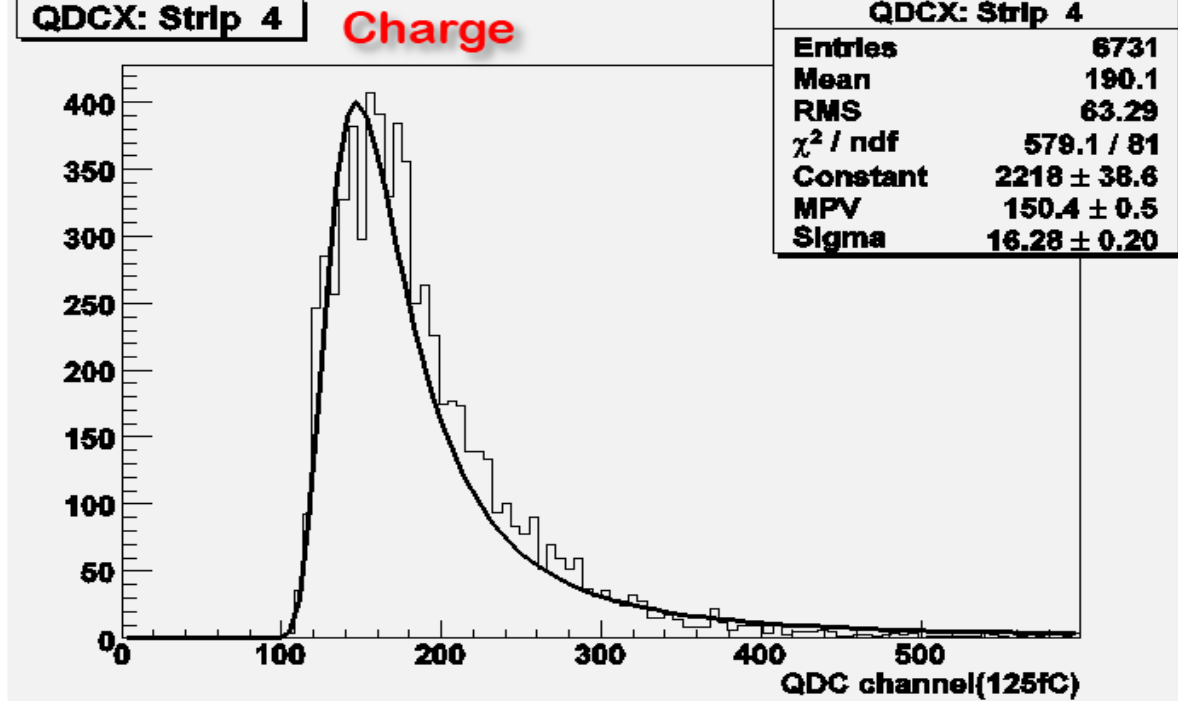
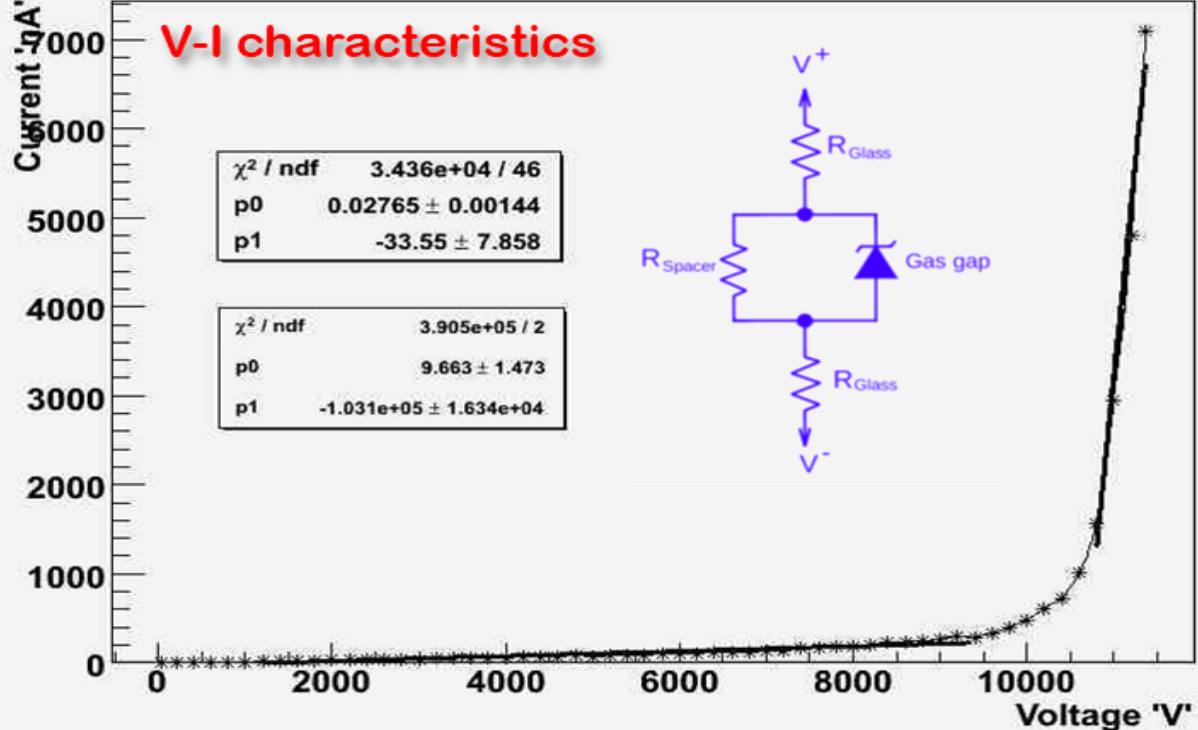


Multi_Event_y_0057_025969_m2

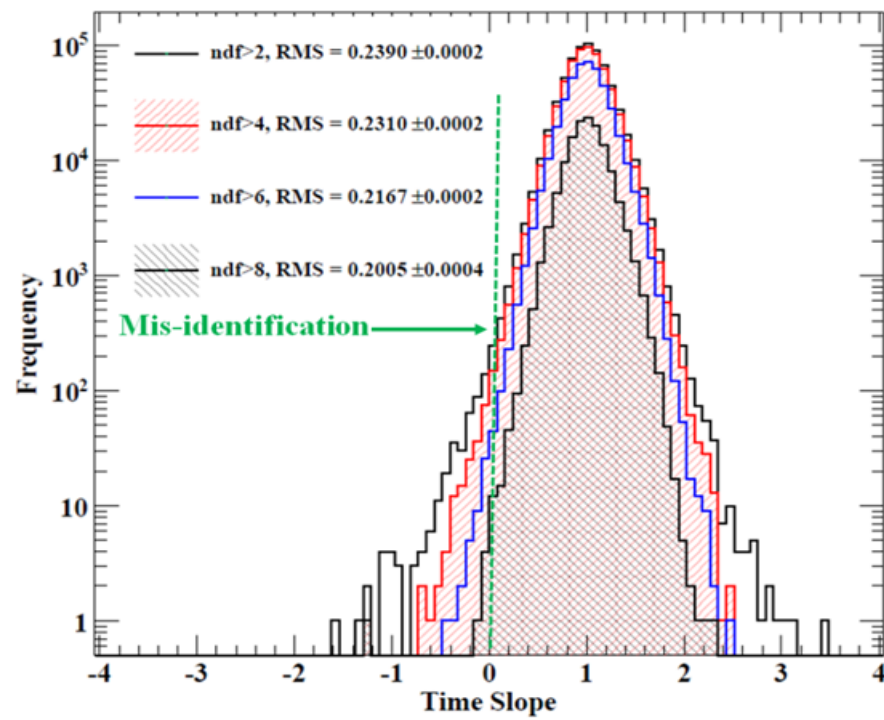
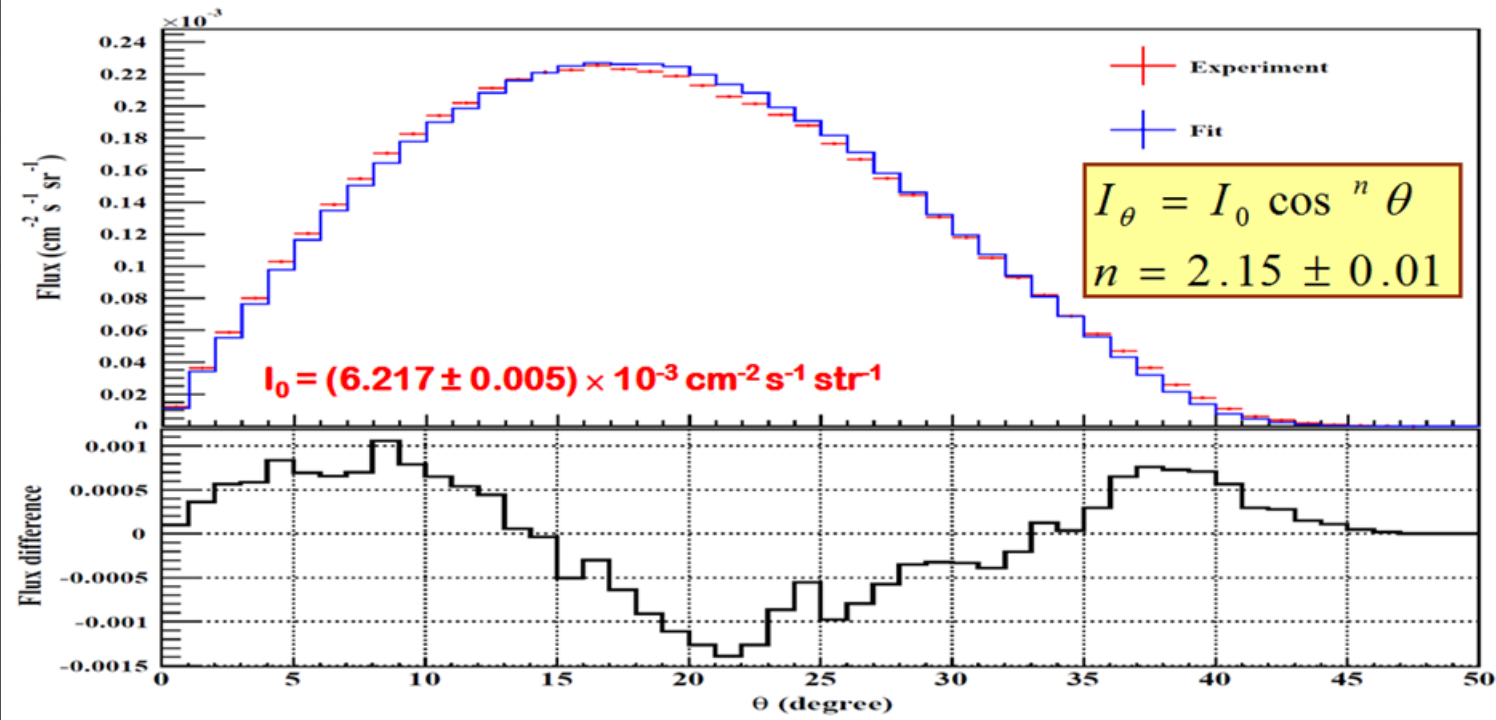
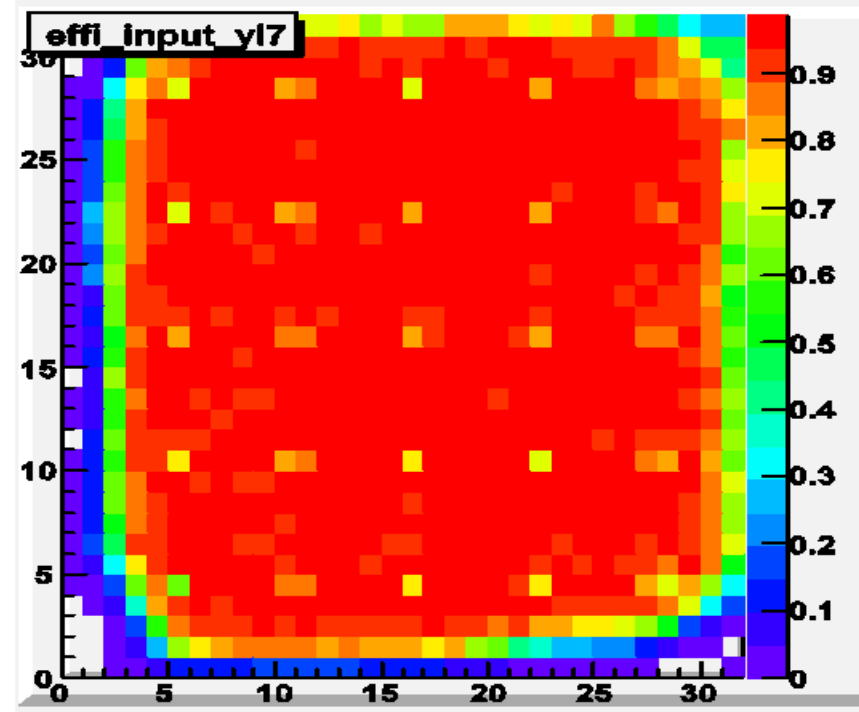
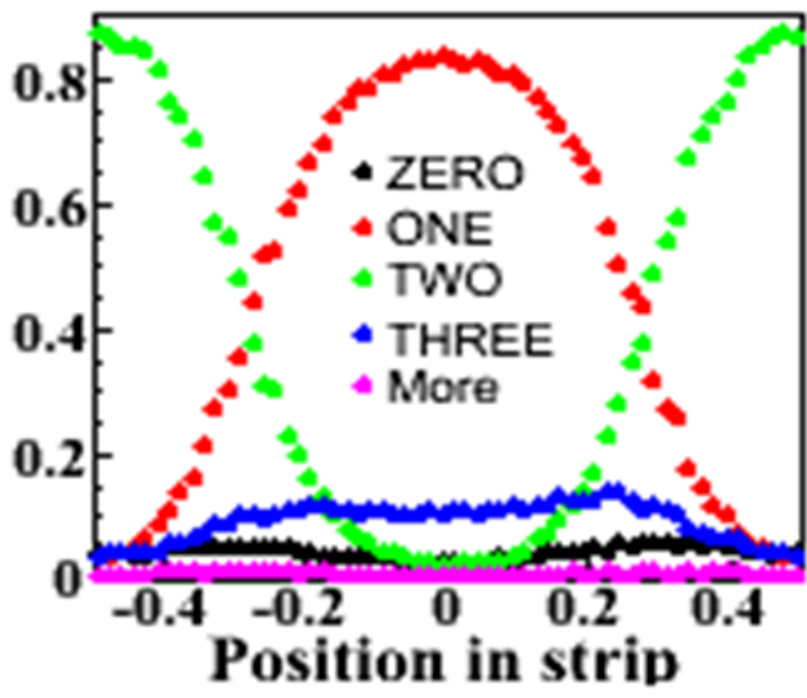
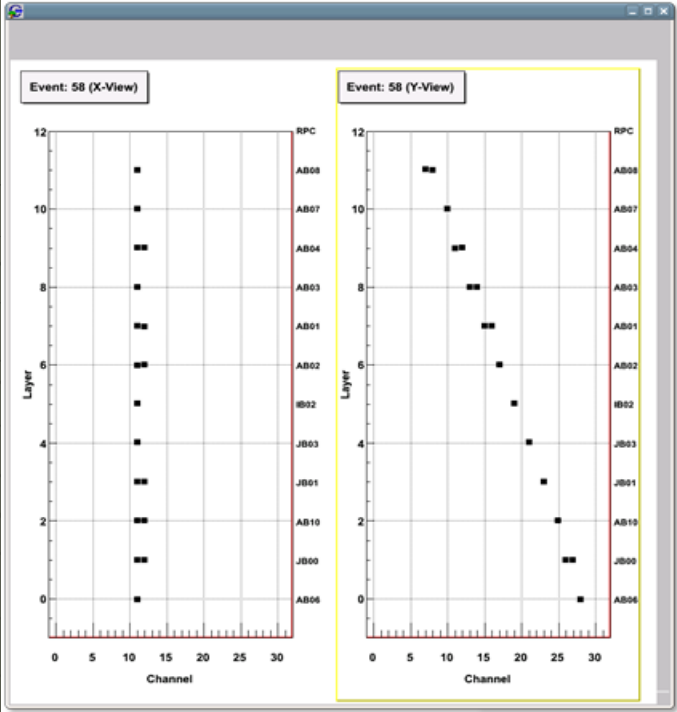


Multi_Event_y_0057_009718_m2

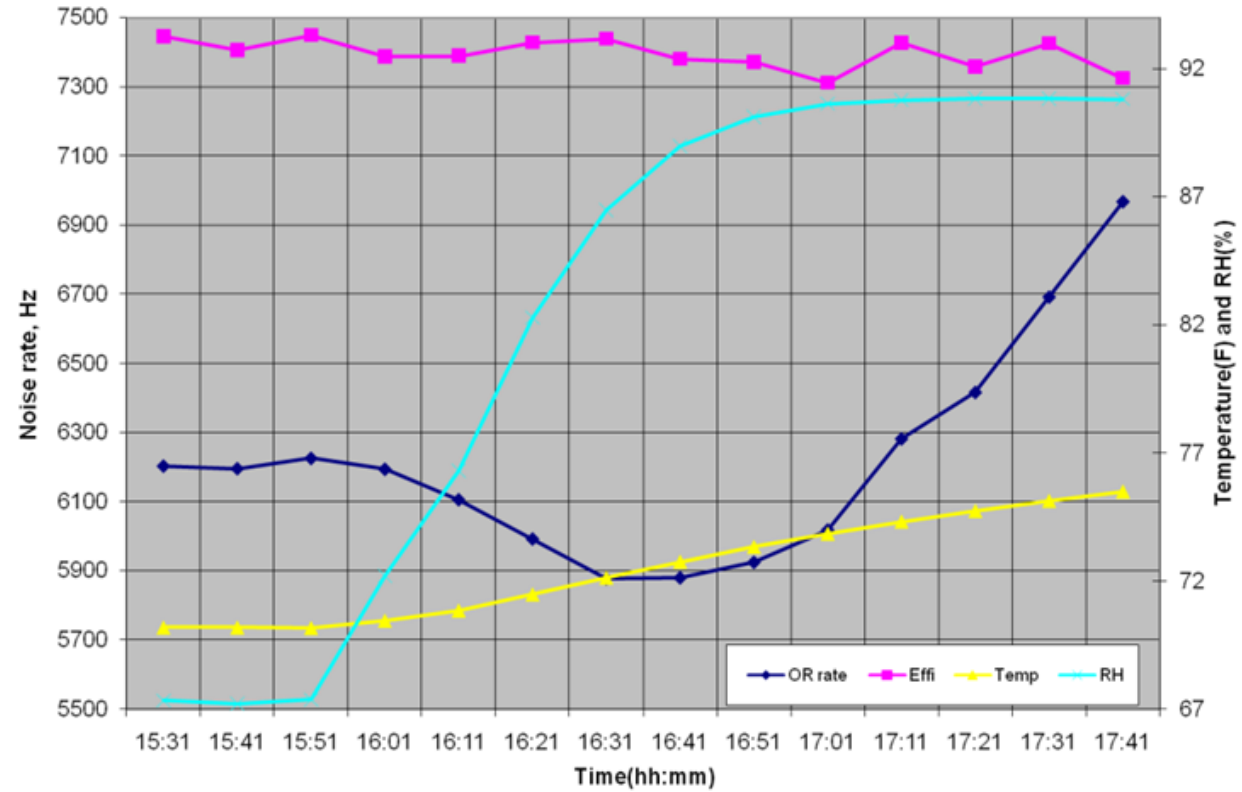
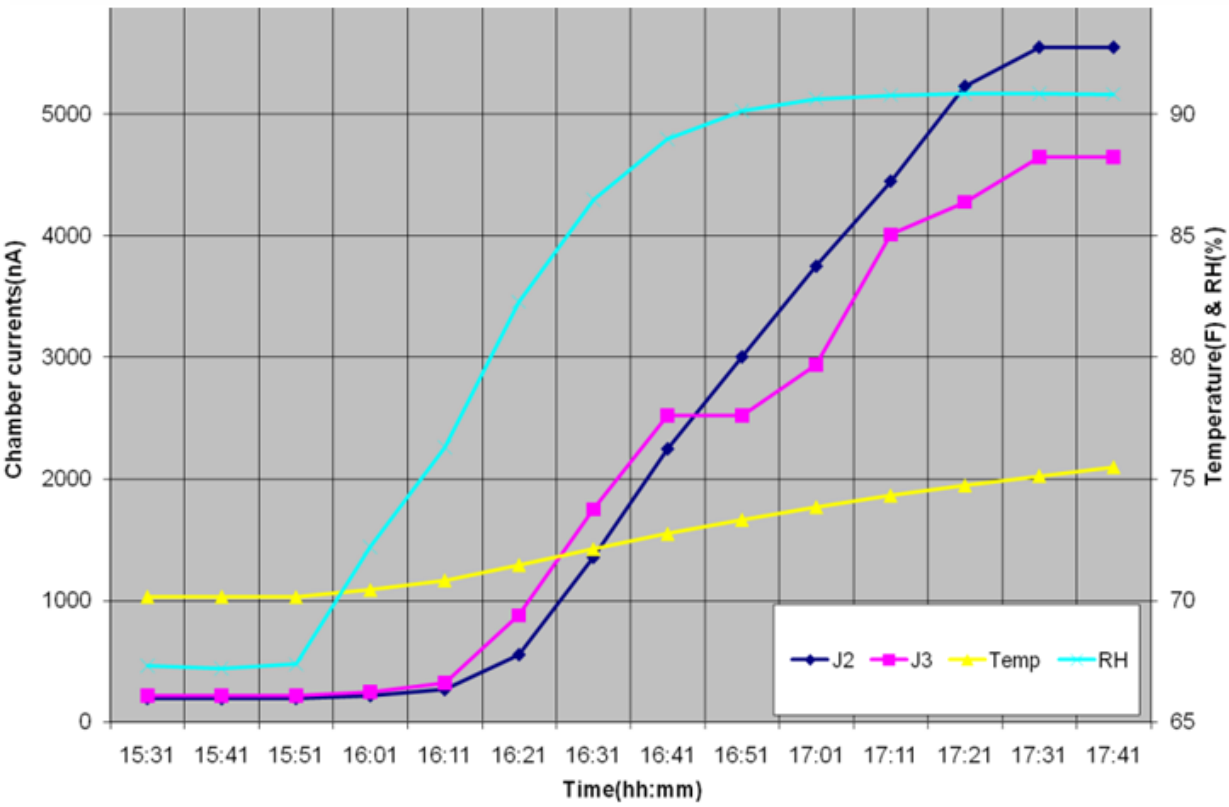
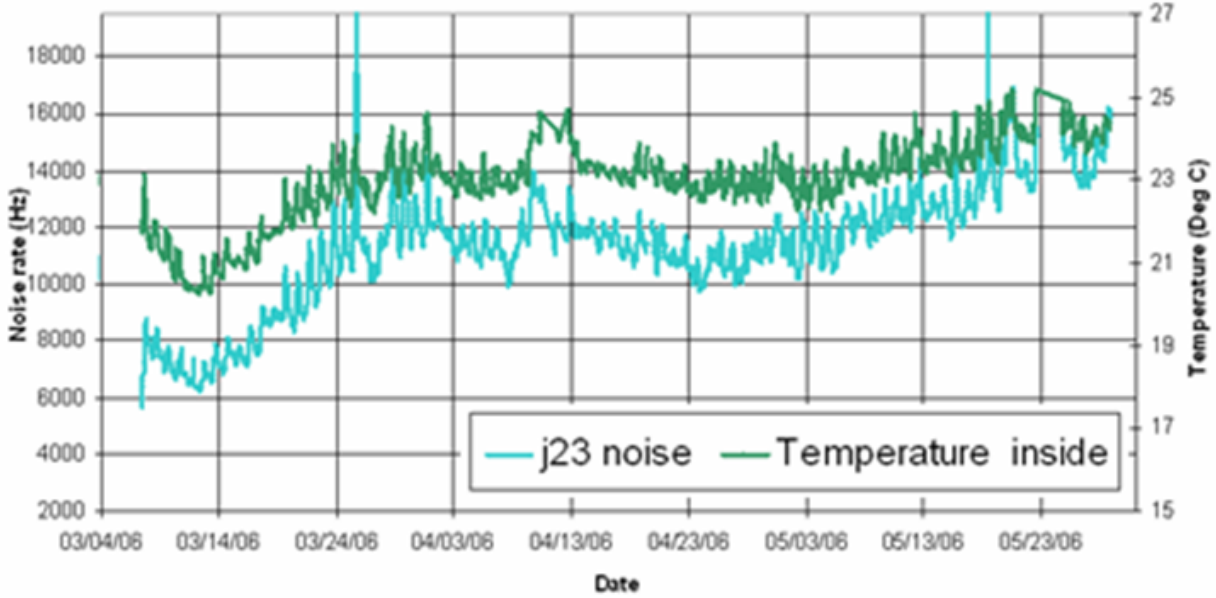


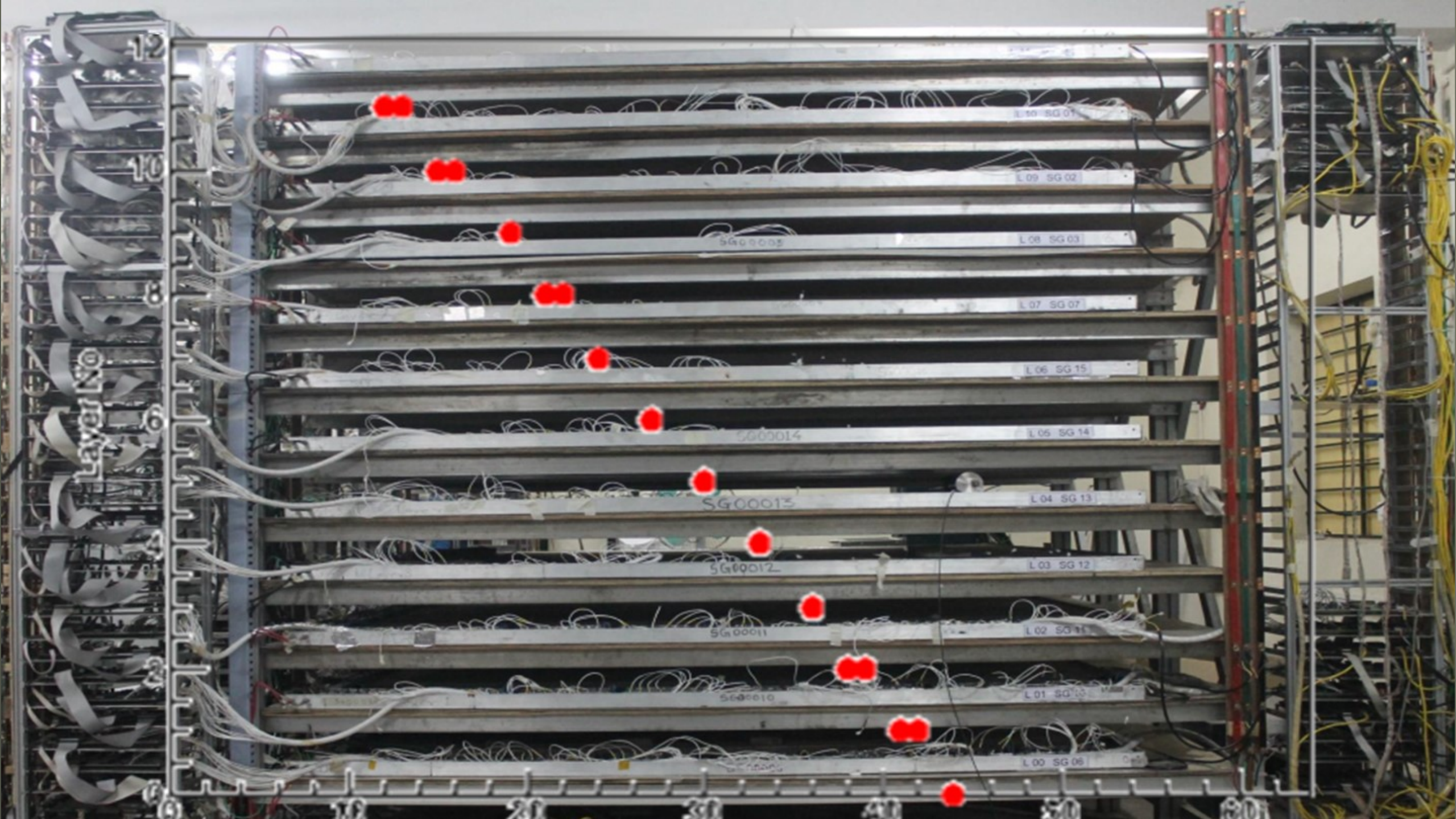


Results from prototype stacks

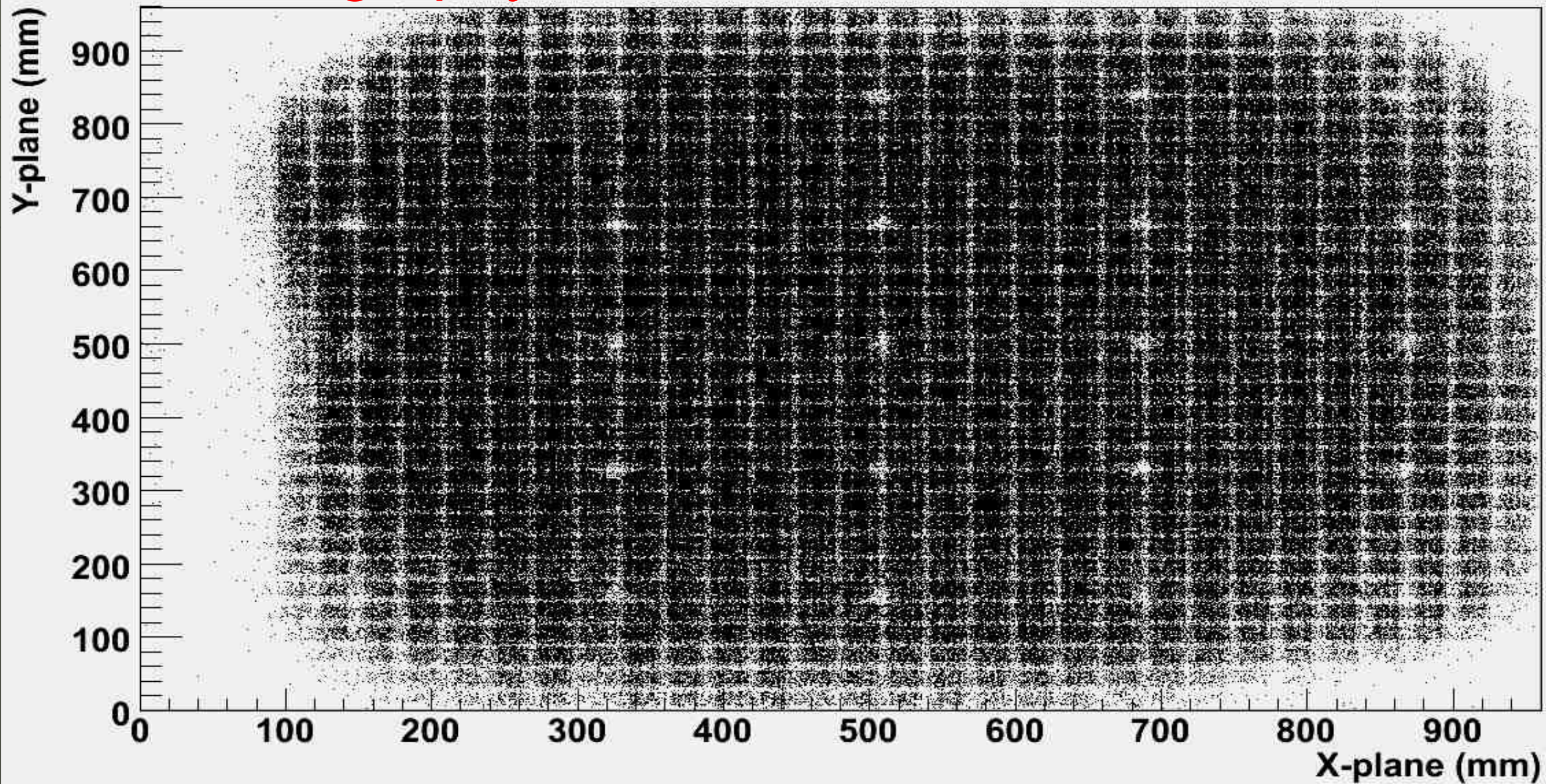


If the applied voltage at room temperature T_0 and barometric pressure P_0 is V_0 , then the voltage V to be applied at any temperature T and pressure $P = V_0 \times \left(\frac{T_0}{T}\right) \times \left(\frac{P}{P_0}\right)$
 Or what is the effective applied voltage?
 N.B: This accounts for gas behaviour only.

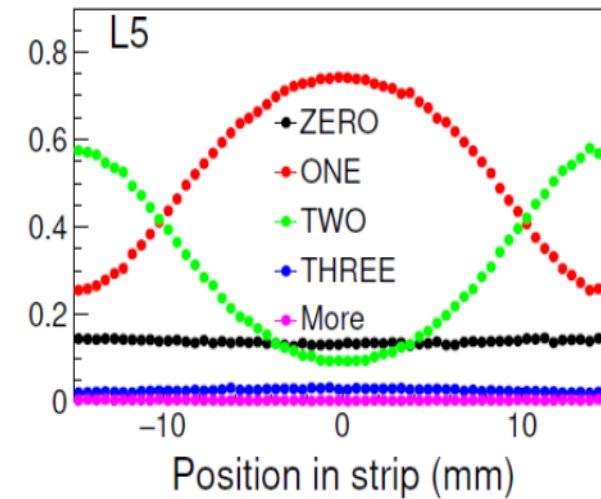
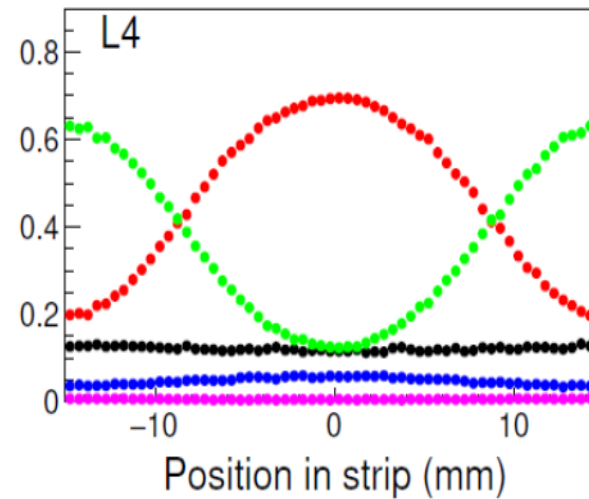
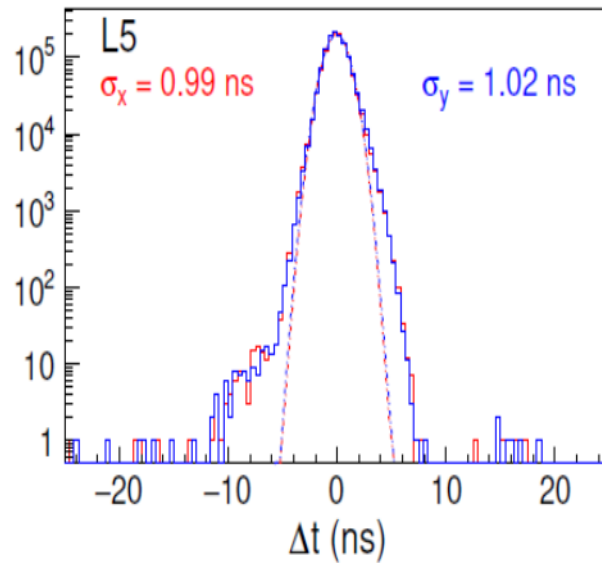
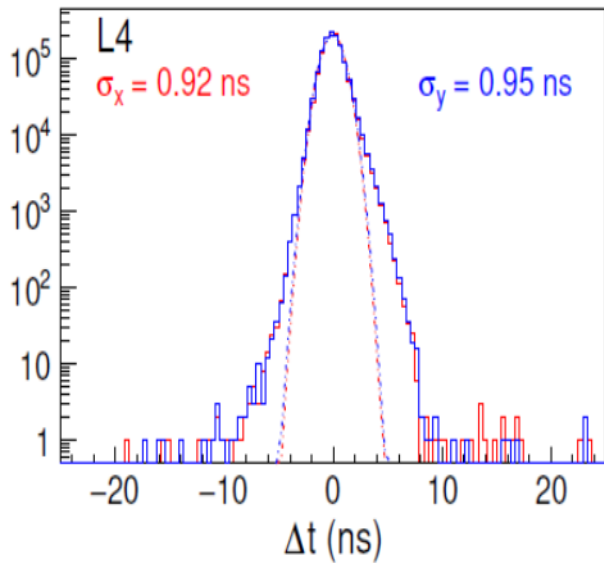
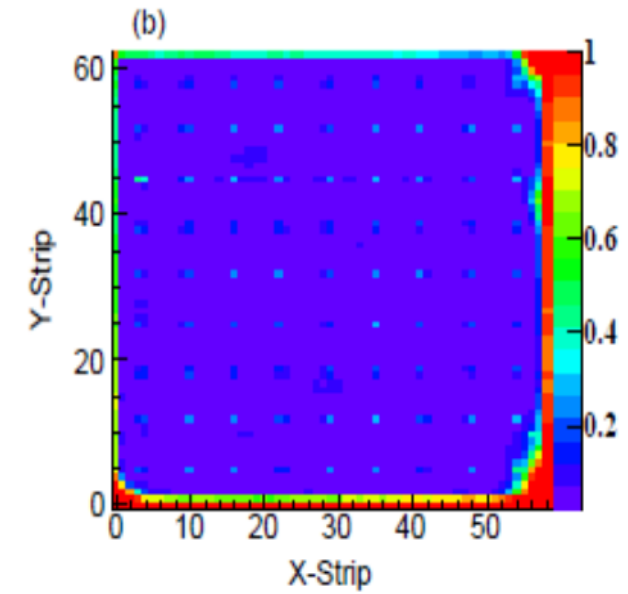
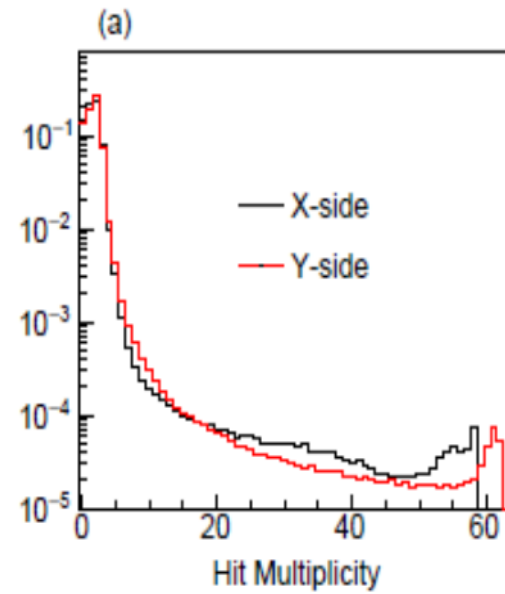
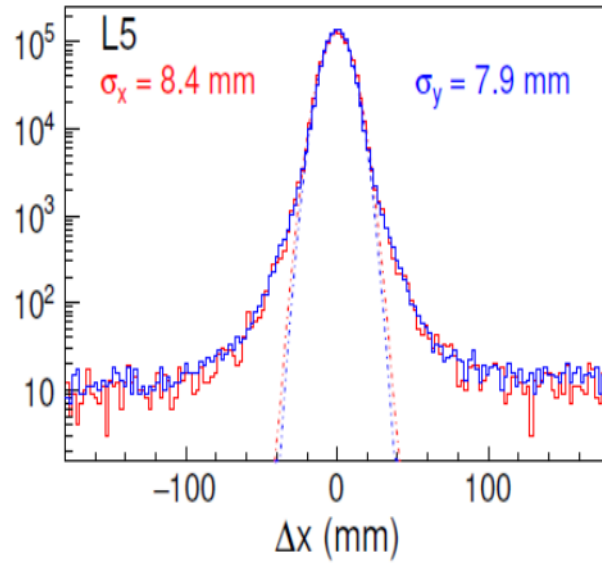
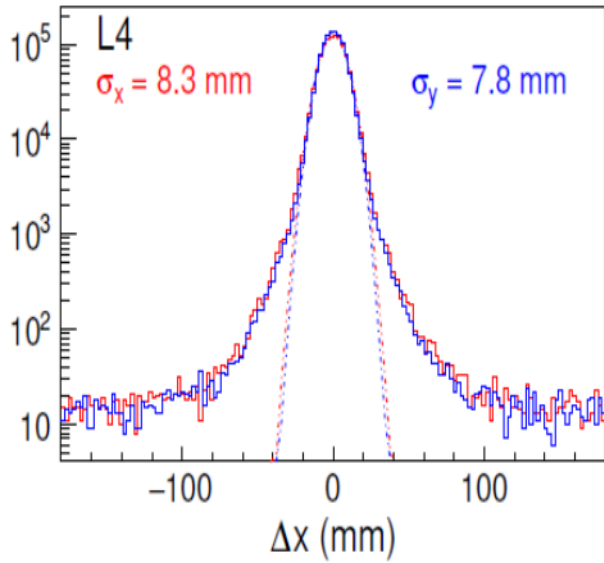




Selfie tomography of an RPC detector!



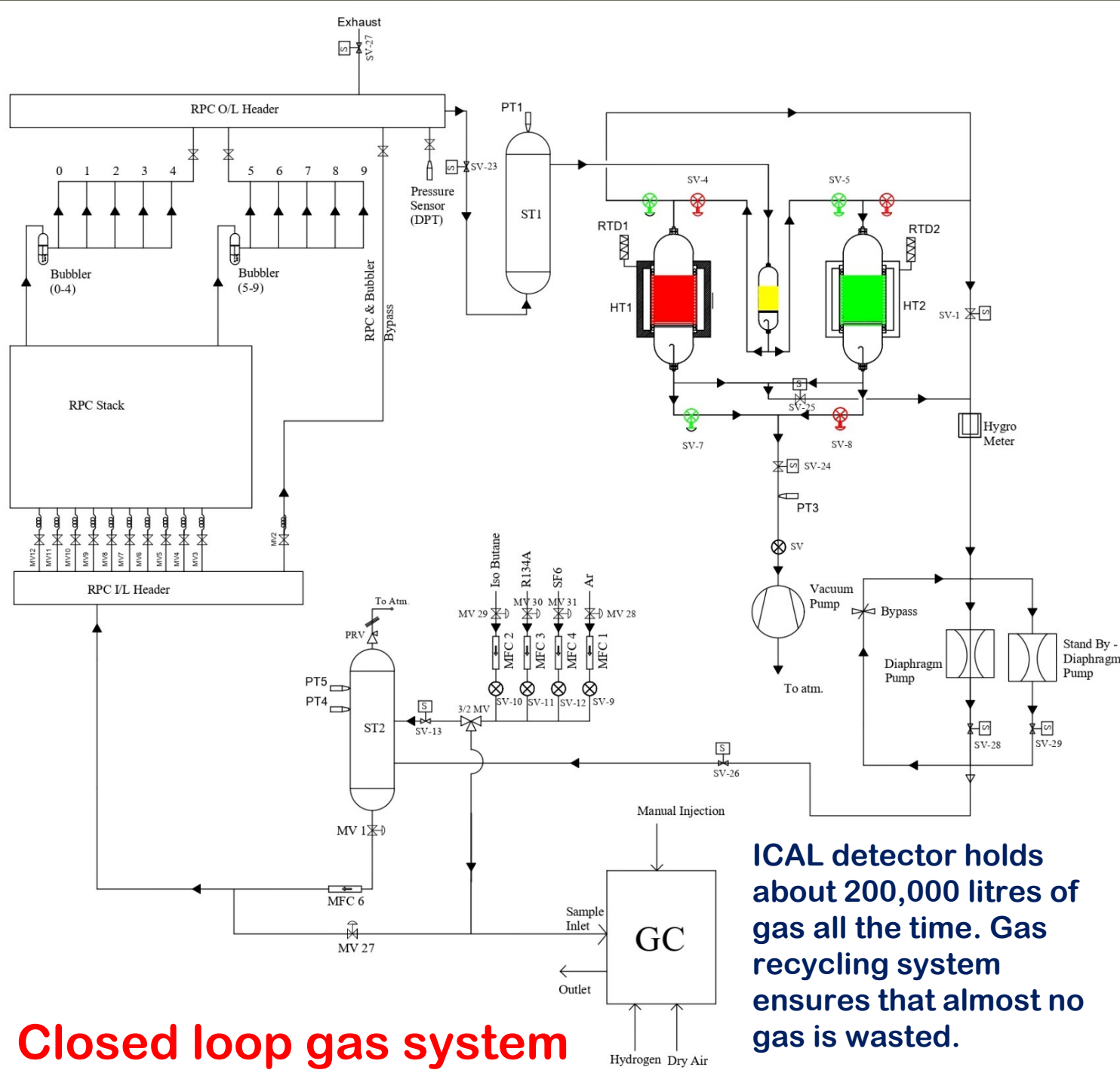
Characterisation studies of RPCs



Development of Gas systems



ICAL detector holds about 200,000 litres of gas all the time. Gas recycling system ensures that almost no gas is wasted.

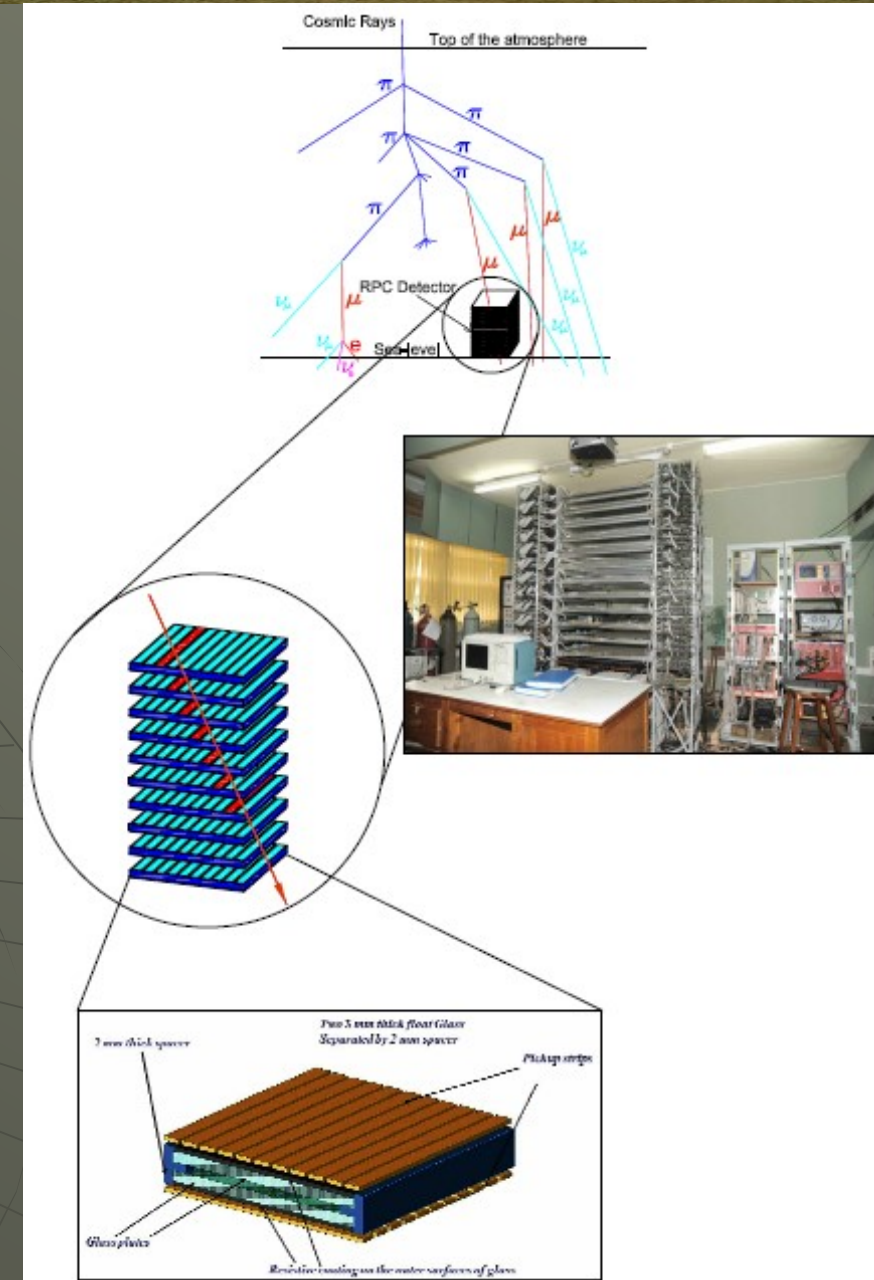


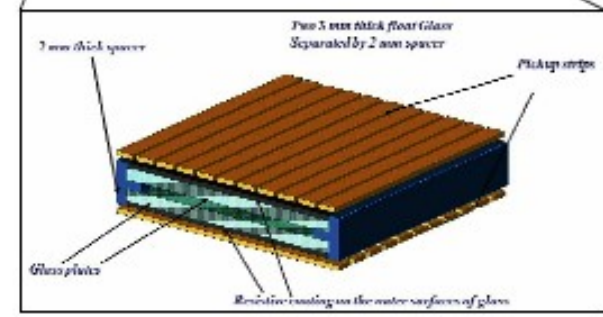
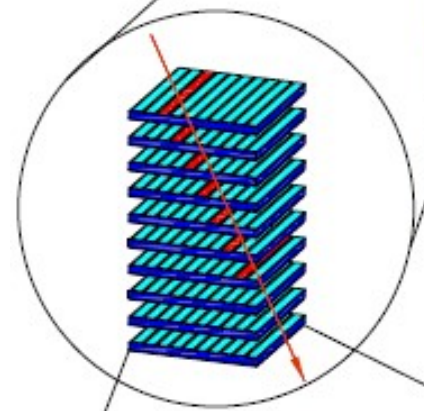
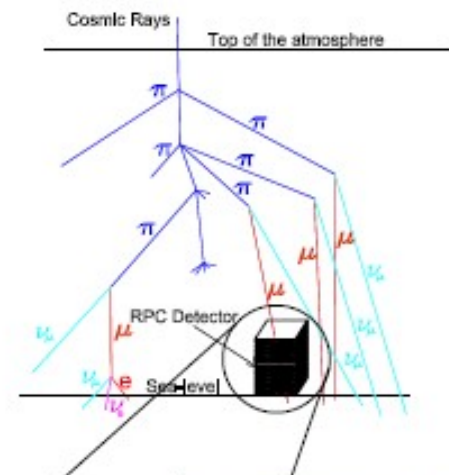
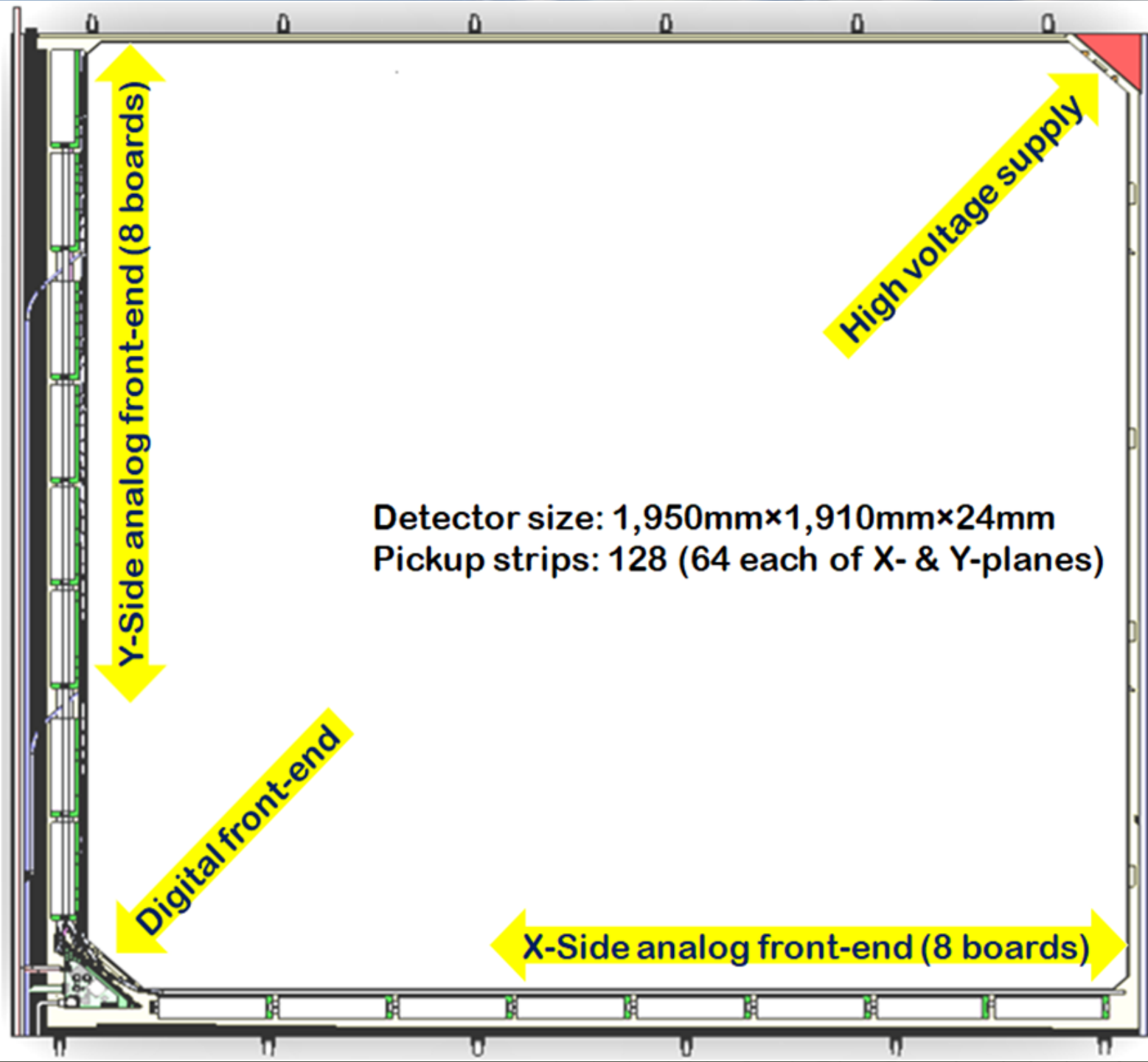
ICAL detector holds about 200,000 litres of gas all the time. Gas recycling system ensures that almost no gas is wasted.

Closed loop gas system

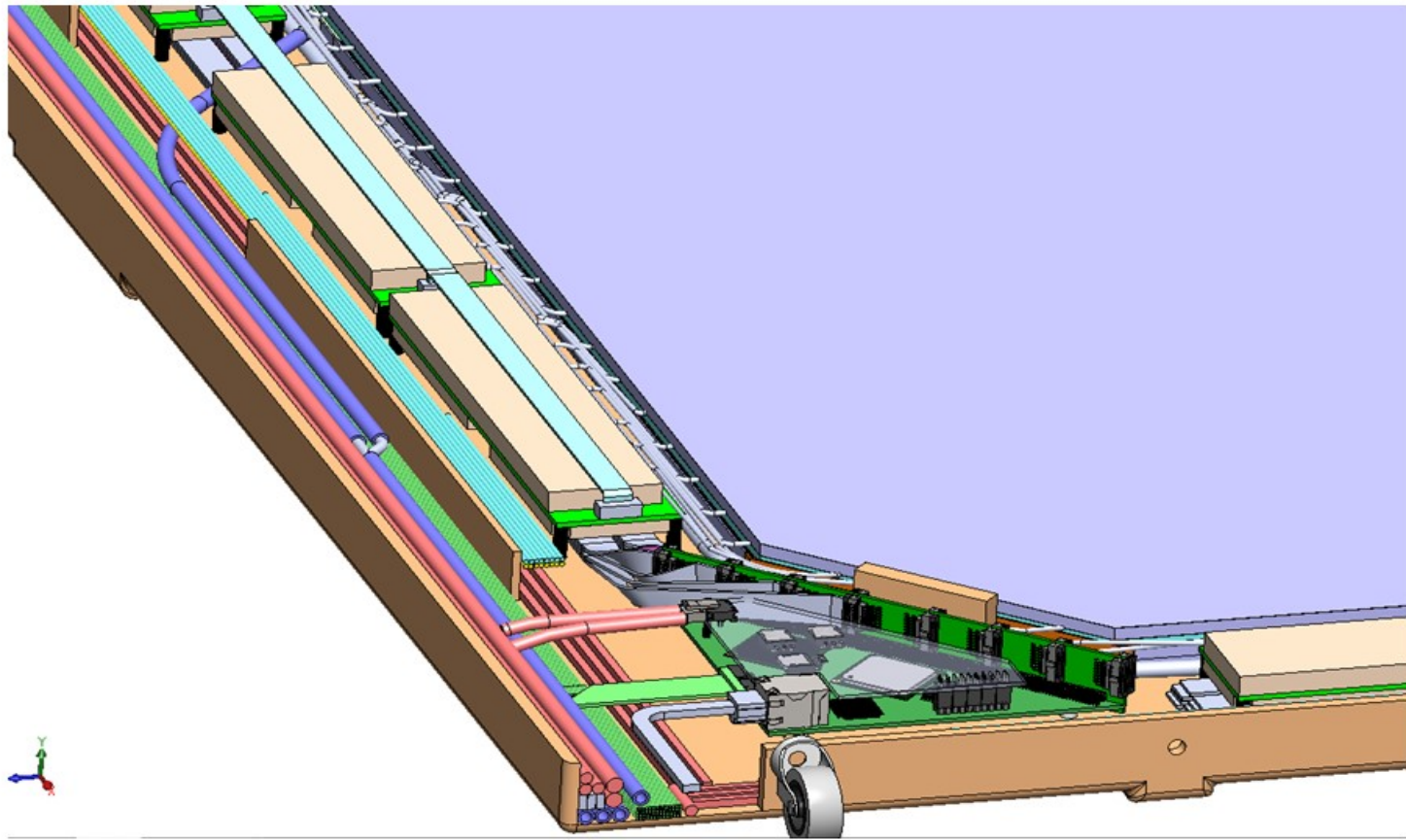
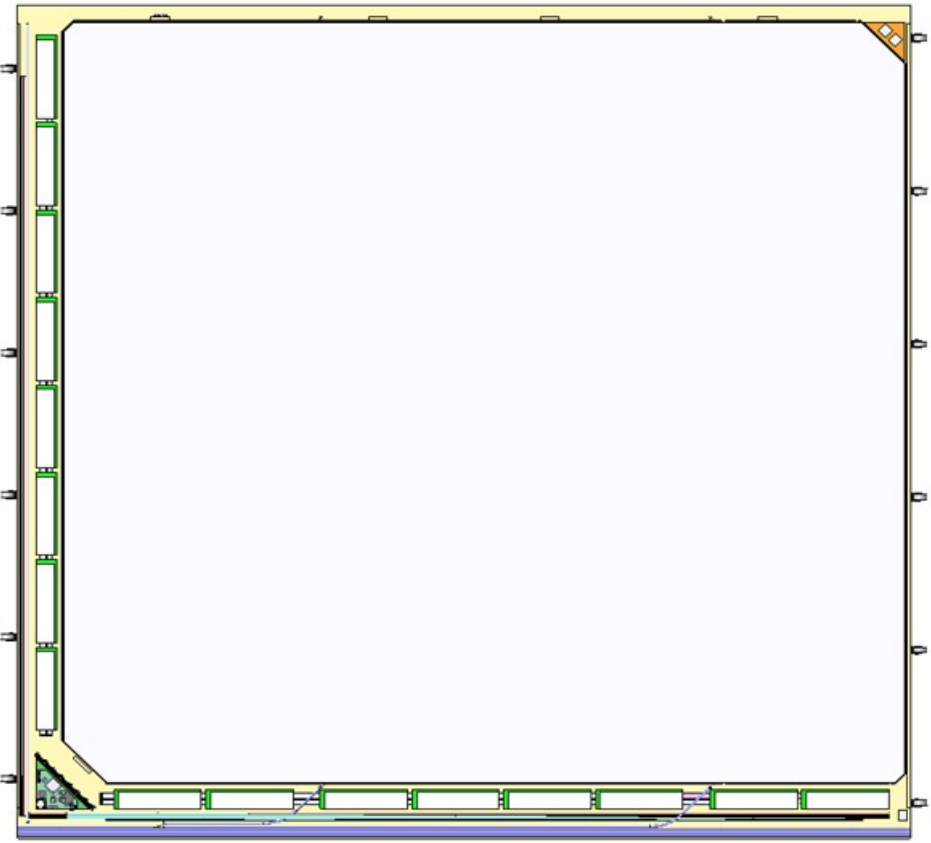
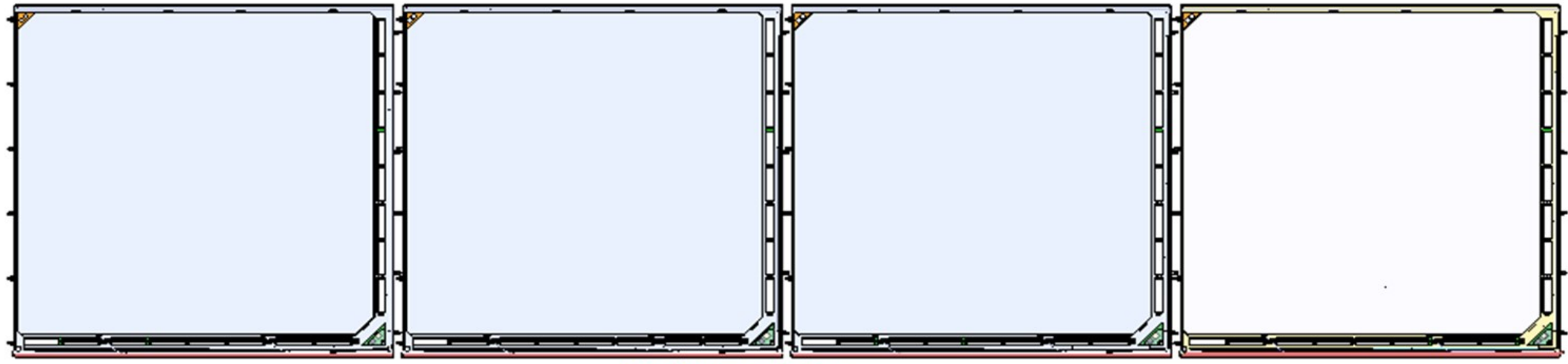
Functions of ICAL electronics

- ◆ Signal pickup and analog front-end
- ◆ **Strip hit latch (1-bit ADC)**
- ◆ Pulse shapers, timing units
- ◆ **Background noise rate monitor**
- ◆ Digital front-end and controller
- ◆ **Data network interface and architecture**
- ◆ Multilevel trigger system
- ◆ **Backend data concentrators**
- ◆ Event building, data storage systems
- ◆ **On-line data quality monitors**
- ◆ Slow control and monitoring
 - Gas system, magnet, power supplies
 - Ambient parameters (T, P and H)
 - Safety and interlocks
- ◆ Remote access to detector sub-systems and data



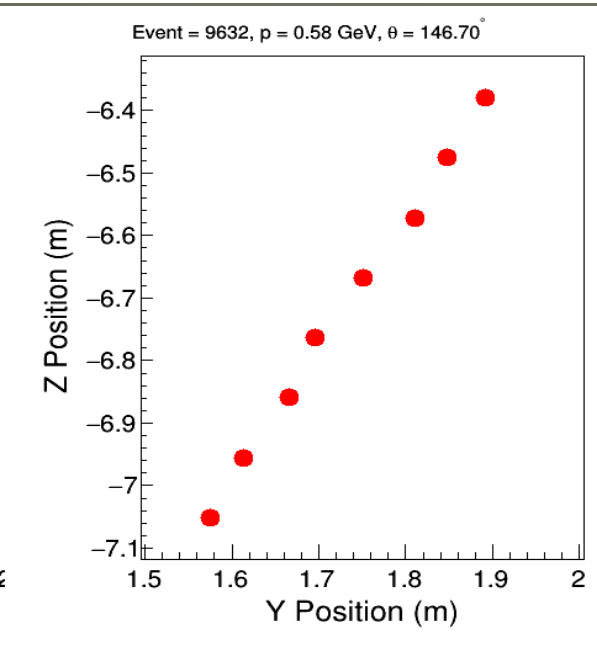
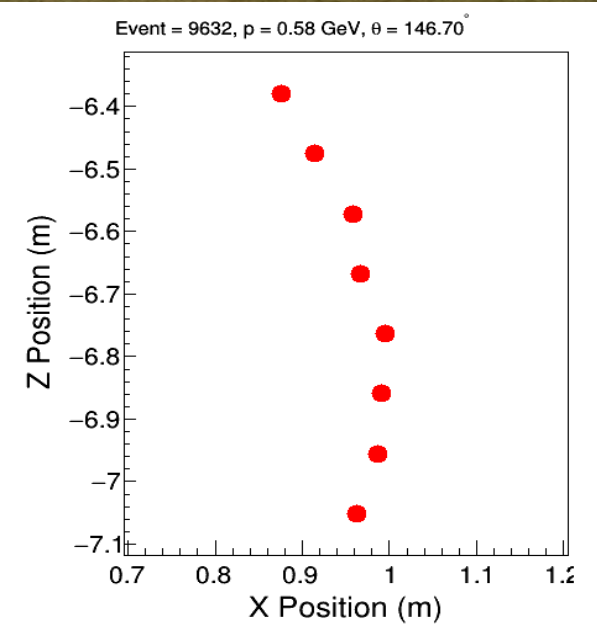


Integration of RPCs in ICAL

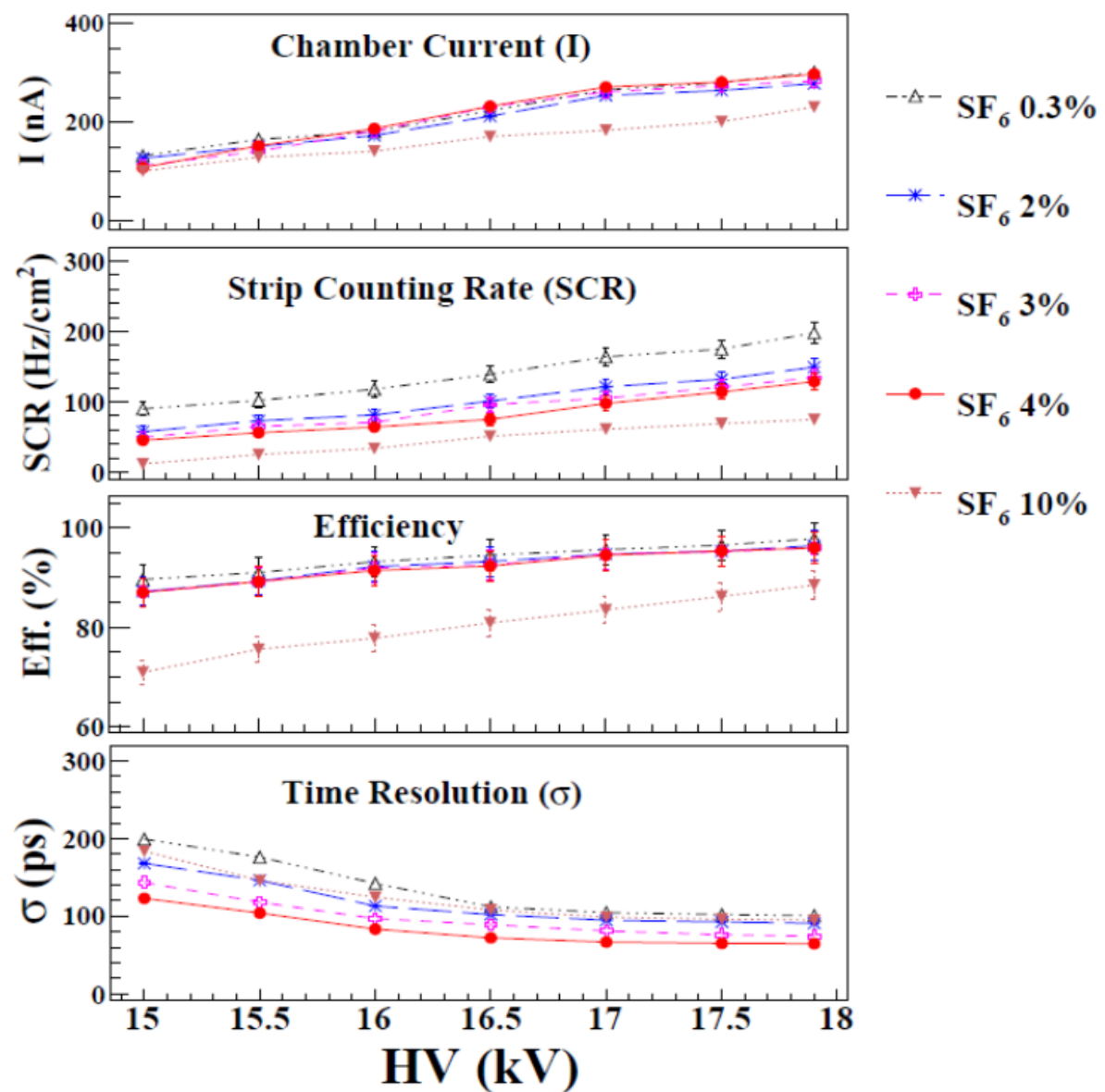
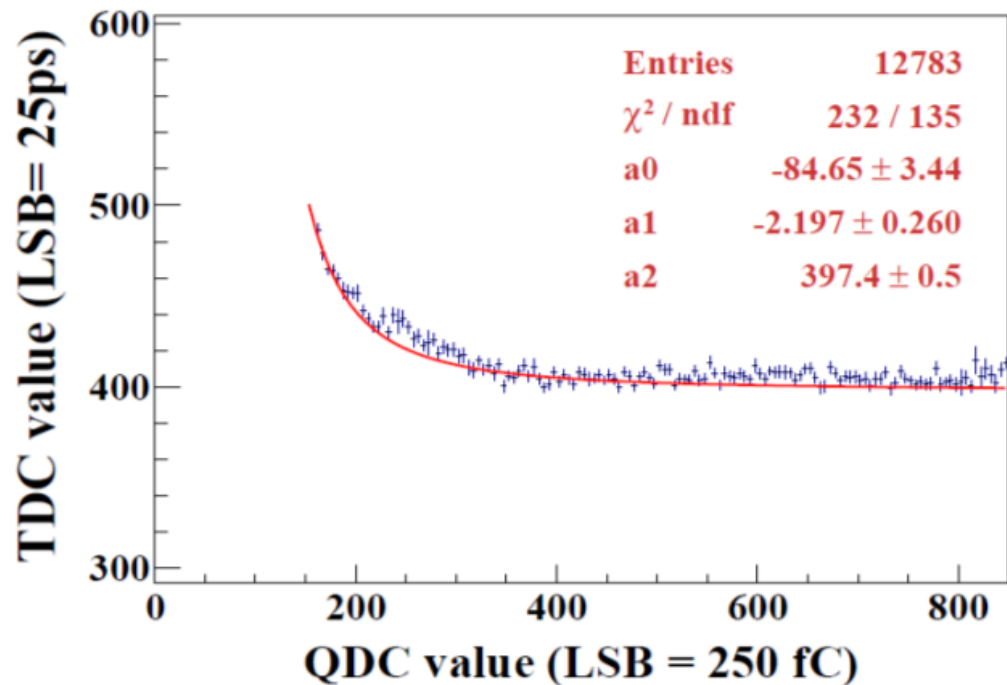
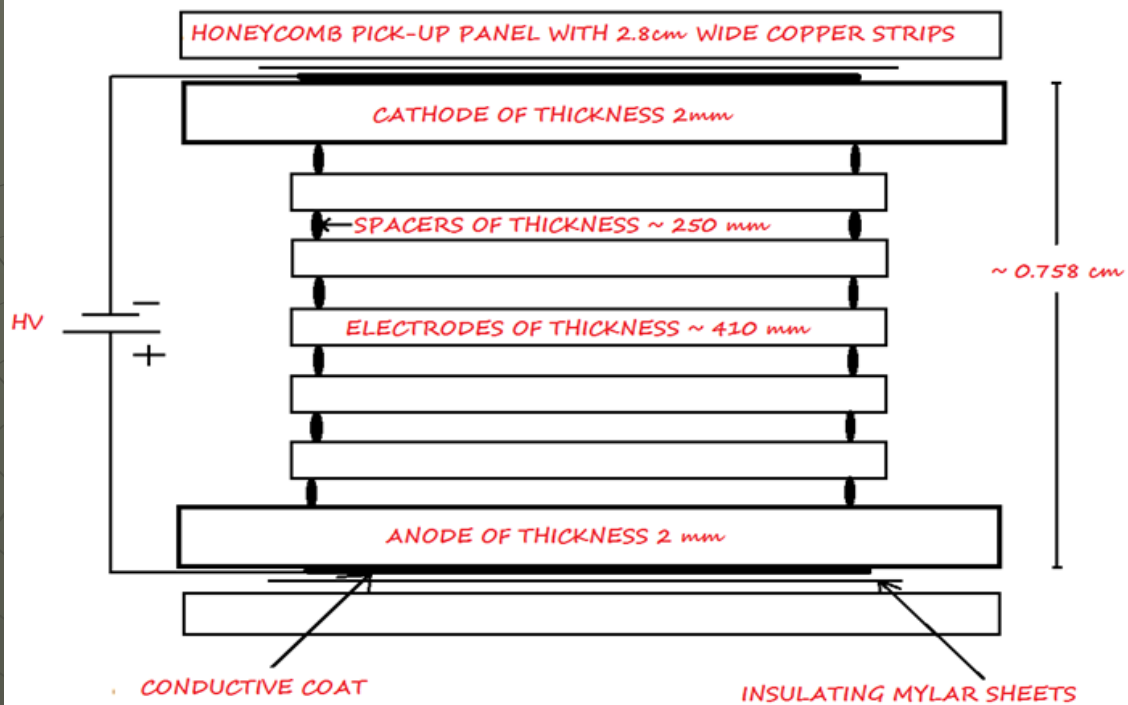


mini-ICAL detector taking data at IICHEP

85-ton, 4m×4m×11 layer magnet,
with 20, 2m×2m RPCs and ICAL
electronics operating for 3 years

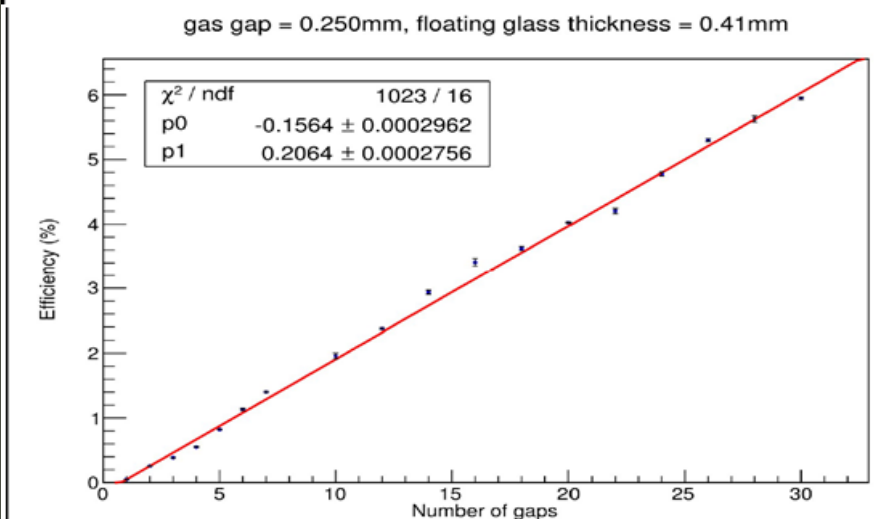
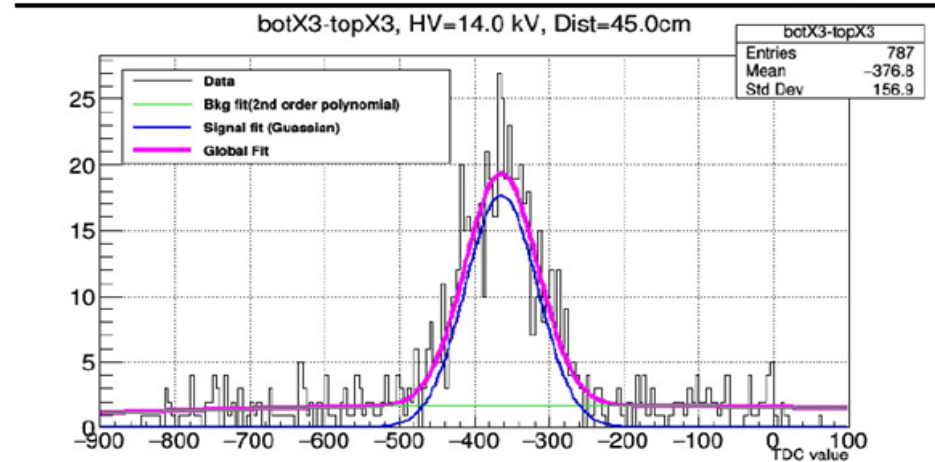
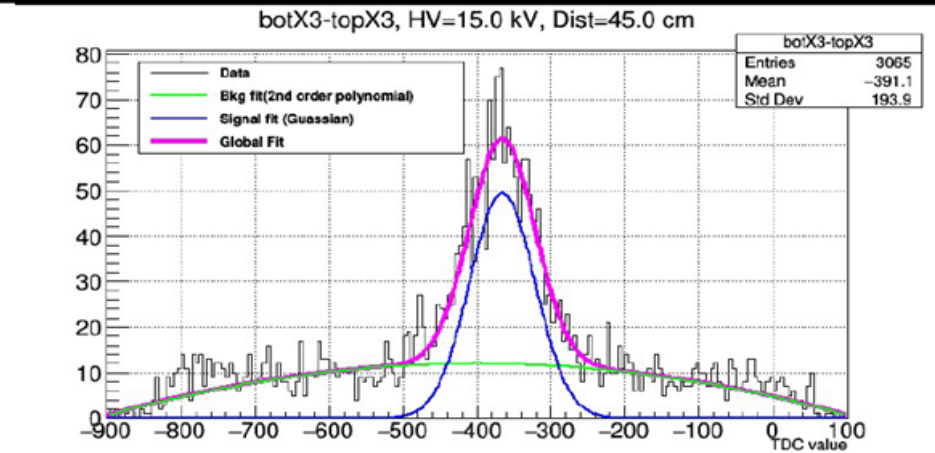
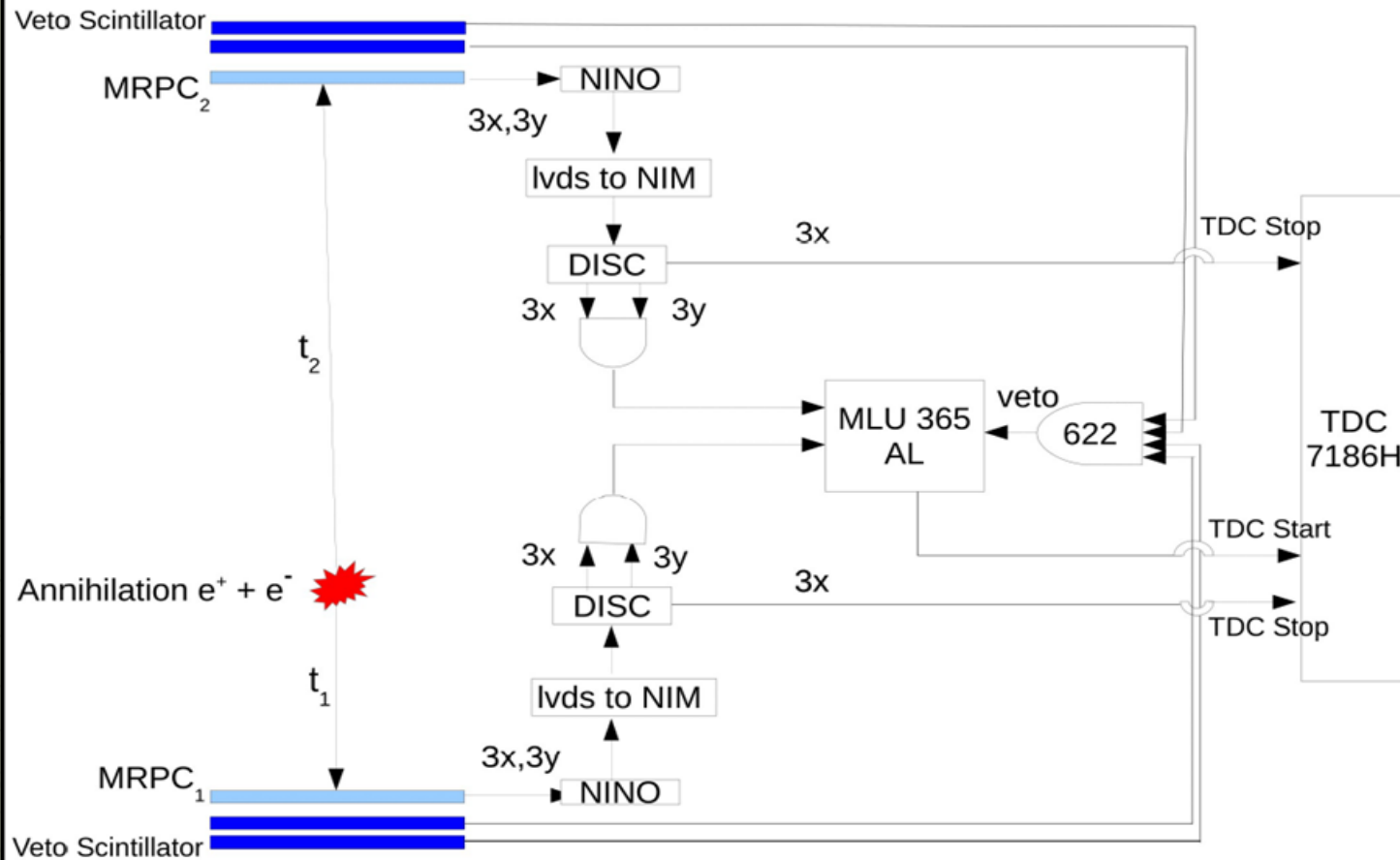


Multi-gap RPC



	Trigger	Eff.(%)	Time res.(ns)	Noise($\frac{\text{Hz}}{\text{cm}^2}$)	I(nA)
I	P1, P2	85	1.42	1.5	305
II	P1, P2, MRPC	85.9	0.87	2.85	312
III	P1, P2, MRPC	87.8	0.85	1.87	311

Feasibility of MRPC for PET



Distance b/w MRPCs	Source at bottom MRPC Δt_1	Source at top MRPC Δt_2	diff= $ \Delta t_1 - \Delta t_2 /2$	Time of flight(TOF) = diff x 25 ps	Actual TOF
30 cm	Mean= -335.8 \pm 2.1 Sigma= 54.76 \pm 2.4	Mean=-248.4 \pm 2.8 Sigma=82.13 \pm 3.5	43.7 \pm 2.4	1.09 \pm 0.06 ns	1.0 ns
45 cm	Mean= -369.4 \pm 2.3 Sigma= 61.57 \pm 2.7	Mean=-256.8 \pm 2.1 Sigma=59.56 \pm 2.1	56.3 \pm 2.2	1.41 \pm 0.05 ns	1.5 ns
60 cm	Mean=-385.8 \pm 2.8 Sigma=63.36 \pm 3.6	Mean=-223.5 \pm 2.4 Sigma= -53.2 \pm 2.4	81.2 \pm 2.6	2.03 \pm 0.07 ns	2.0 ns
75 cm	Mean=-404.9 \pm 3.0 Sigma=77.72 \pm 4.5	Mean=-204.0 \pm 2.7 Sigma=63.85 \pm 3.6	100.5 \pm 2.8	2.51 \pm 0.07 ns	2.5 ns

RPC development in India

Date:

NKM and self went to Md. Ali Road to get glass samples. We brought 2mm thick Modi and 25mm Saint Gobien samples.

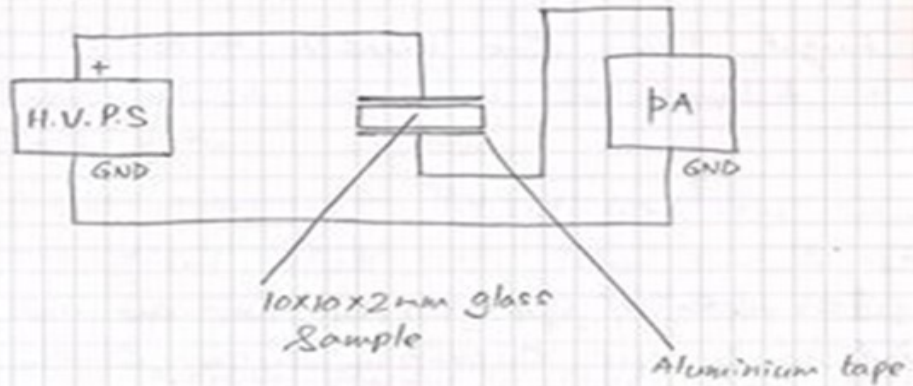
Date: 28/09/2001

Thickness measurements were done for the Modi glass (2mm thick) using ultra sound gauge.

Mean = 2.017 (mm) and RMS = 0.01267 (mm) (Entries = 27) obtained.

Date:

Resistivity measurement of modi glass (2mm) done as follows:



Typical resistivity measured was $10^{12} \Omega$

AMU	Aligarh
BARC	Mumbai
BHU	Varanasi
Bose Institute	Kolkata
CUK	Kalaburagi
DU	Delhi
IISER	Mohali
IITB	Mumbai
IITM	Chennai
KU	Kashmir
NISER	Bhubaneswar
PU	Chandigarh
SINP	Kolkata
TIFR	Mumbai
TKMCAS	Kollam
TU	Tezpur
VECC	Kolkata

The joy of building, together



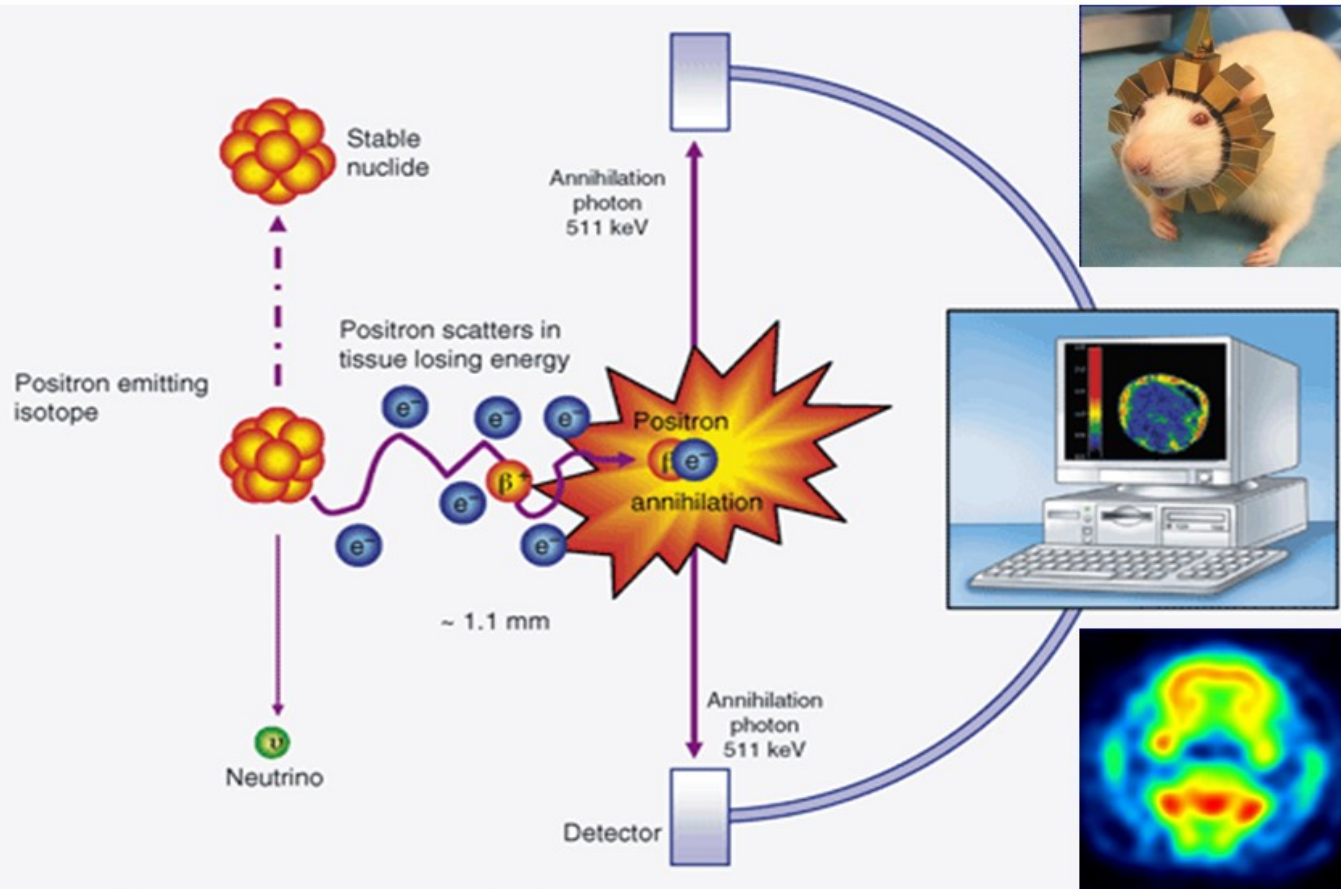
Stay tuned for ...

- ◆ High quality, but low cost RPC detector production by industries for e-ICAL and ICAL.
- ◆ Alternate gas mixtures for RPCs.
- ◆ 3D simulation of multi-component, viscous gas flow through RPC.
- ◆ Pixel readout techniques for RPCs.
- ◆ Neural networks and machine learning techniques for efficient track reconstruction.
- ◆ Muon tomography and cargo scanners.
- ◆ Prototypes of MRPC based PET devices.
- ◆ RPC detector technologies for contributing to accelerator and other futuristic experiments.

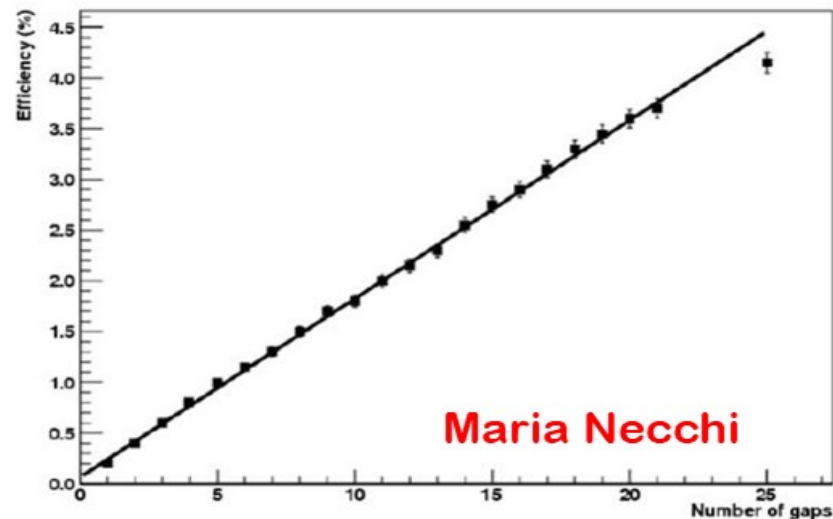
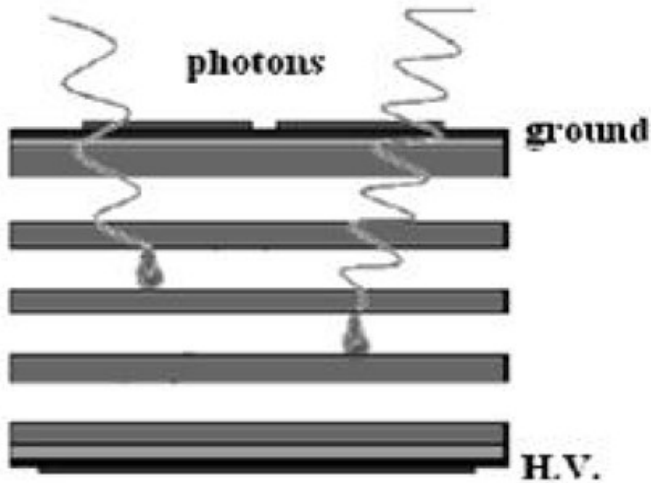


Backup slides

MRPC for PET imaging



- ◆ Detector with good efficiency, spatial, timing and energy resolutions.
- ◆ Low system dead time (lower dose)
- ◆ Rejection of scattered, random or multiple events.
- ◆ Scintillation crystals (Bismuth Germanium Oxide (BGO), Gadolinium Oxyorthosilicate (GSO), Lutetium Oxyorthosilicate (LSO), etc.) current choices.
- ◆ MRPC is a cheaper, works on direct detection, with higher FOV

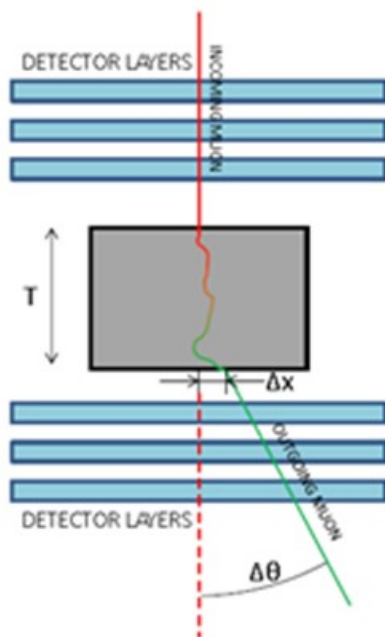


- ◆ Gamma sensitivity saturates at a thickness of 400 μ m for bakelite, 200 μ m common glass and 150 μ m for lead glass.
- ◆ Standard electrodes are coated with with high Z material acting as γ -e converter.

- Muons undergo multiple coulomb scattering within the detector volume.
- The angular distribution can be assumed to be Gaussian, with σ^2_0 depending on the radiation length X_0 (and ultimately on ρZ^2).
- Muon tracks scattering within the target volume provide information of its content.
- High sensitivity to high-Z, high-density materials.

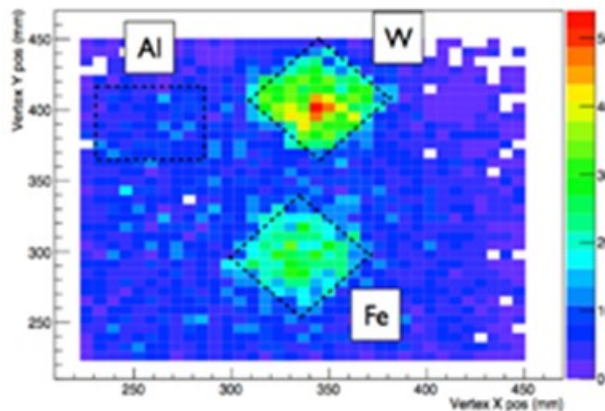
$$\sigma^2_0 \approx \left(\frac{15 \text{ MeV}}{pc\beta} \right)^2 \frac{T}{X_0}$$

$$X_0 \approx \frac{A \cdot 716.4}{\rho \cdot Z \cdot (Z + 1) \ln(287 / \sqrt{Z})} [\text{cm}]$$



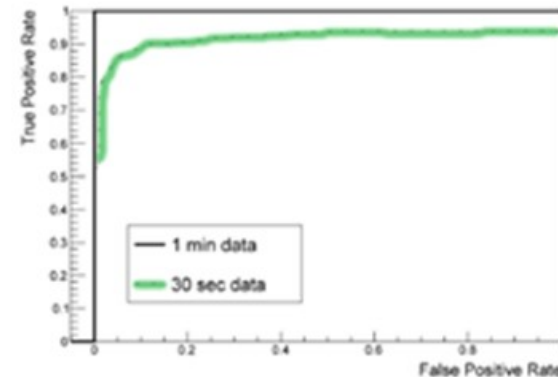
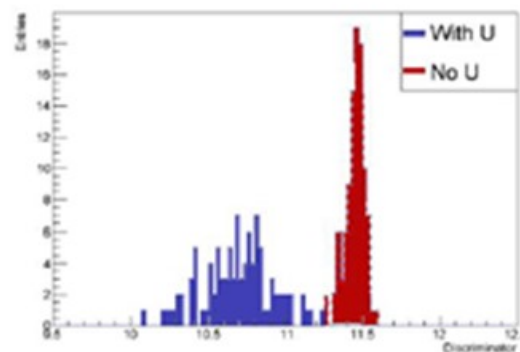
- Simple proof of principle:
 - Plot vertices with scatter angle above 0.03 rad
 - No momentum information
- Plot from prototype data:
 - Metal cubes 5 cm x 5 cm x 5 cm
 - Aluminium, iron, tungsten
- Clear separation between high and low Z materials.

Drift tubes and Scintillators are presently used.



28/02/2014

- Discriminator value is used as binary classifier, based on a pre-defined threshold.
- Evaluate classifier by comparing true positive and false positive rate on 100 sets of 1 minute simulated cosmics.
- Assuming perfect momentum information, 1 minute of data is enough to reliably identify the block of U in most scenarios.

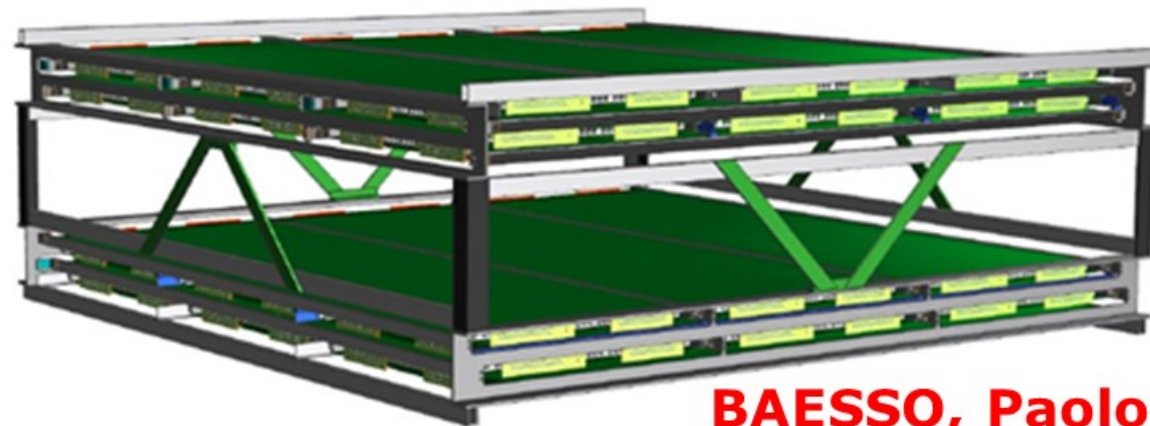


28/02/2014 Cargo container with stone

AWE is building a large size test setup in their facilities.

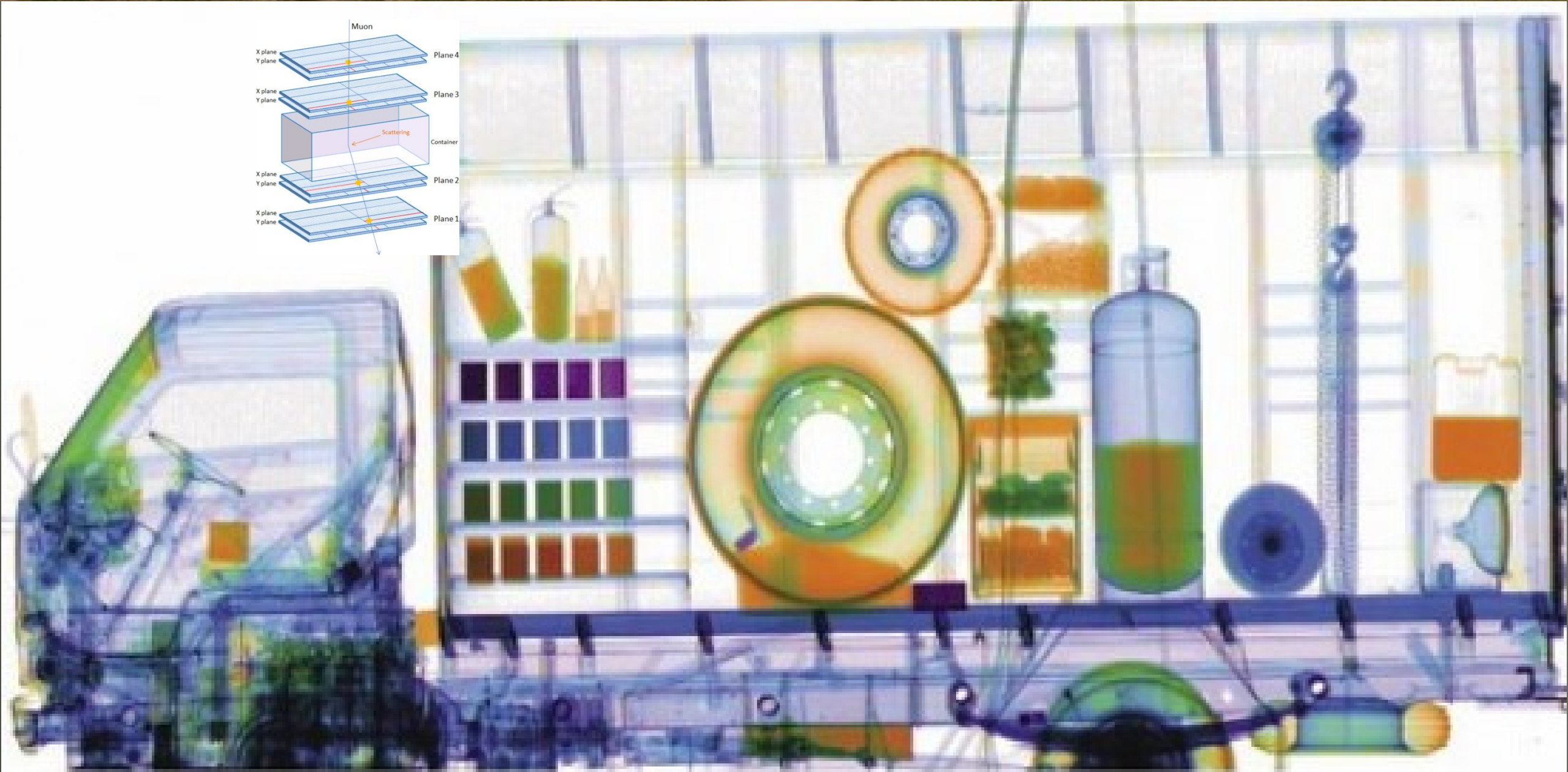
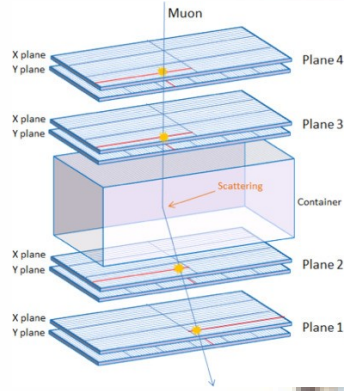
Large unit (1800 mm x 1800 mm) consisting of 6 RPC, in two orthogonal directions.

Modular construction to be used as a "detection tile".

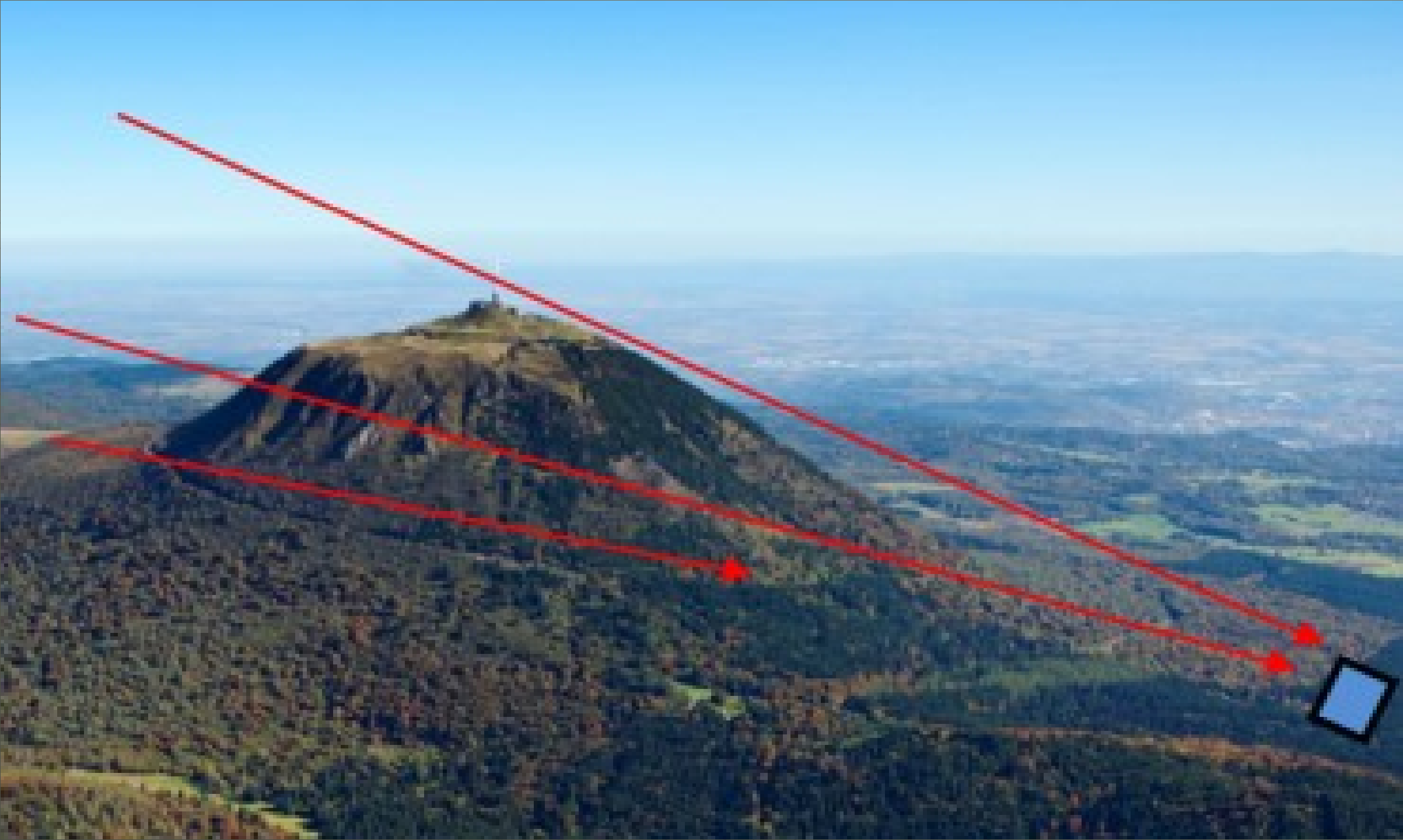


BAESSO, Paolo

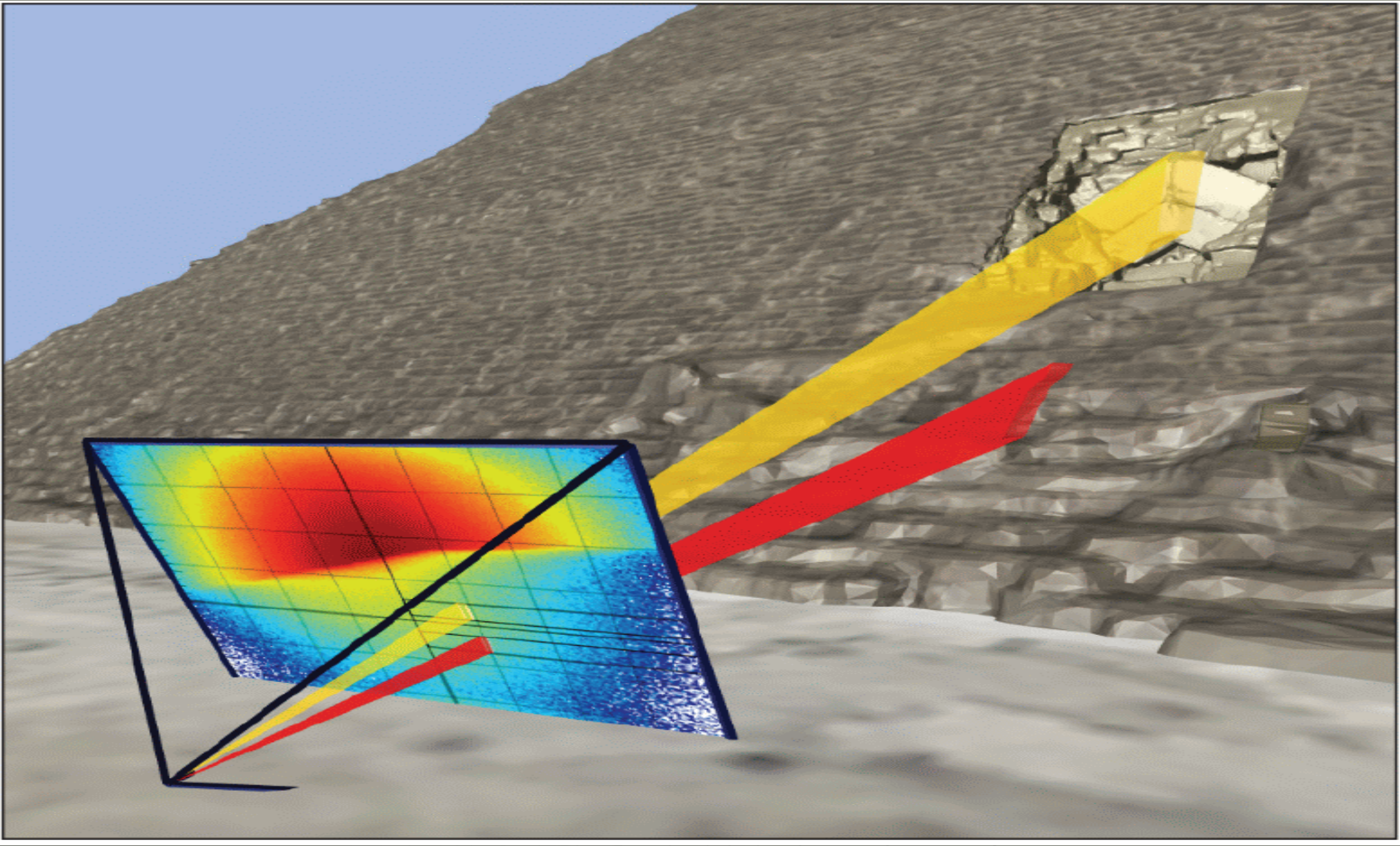
Cargo scanning with RPC detectors

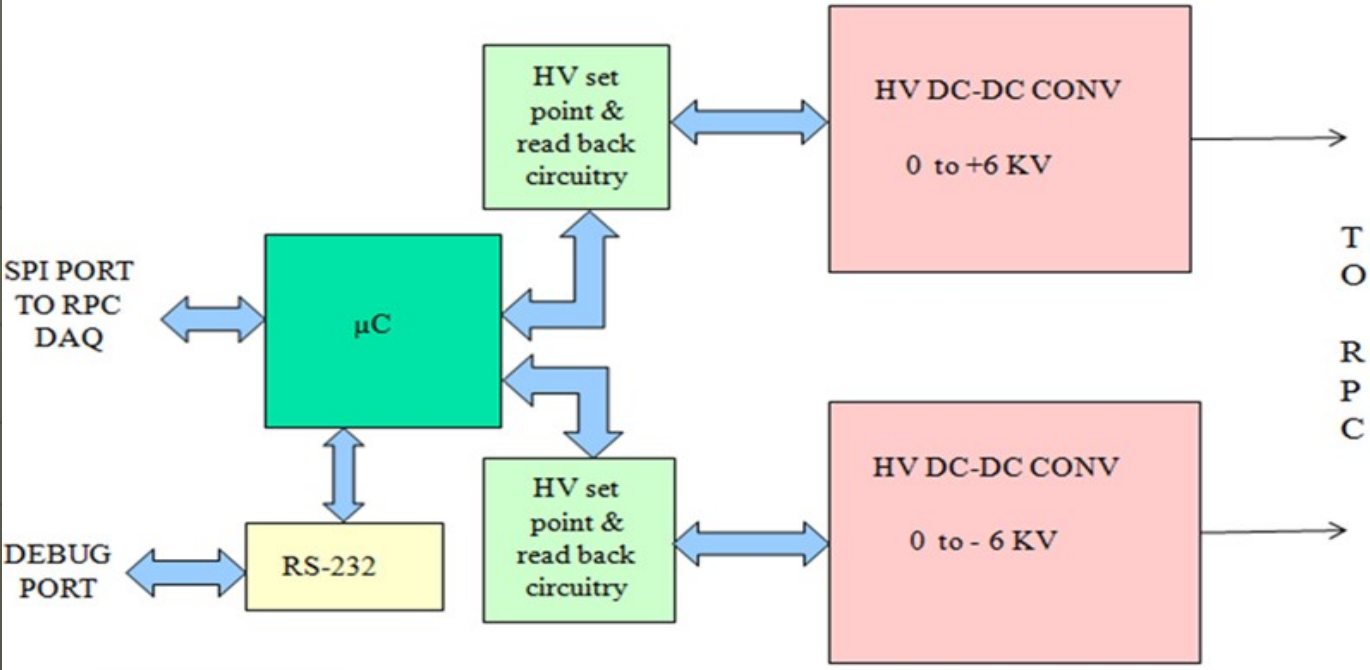


Monitoring of volcanoes using muons

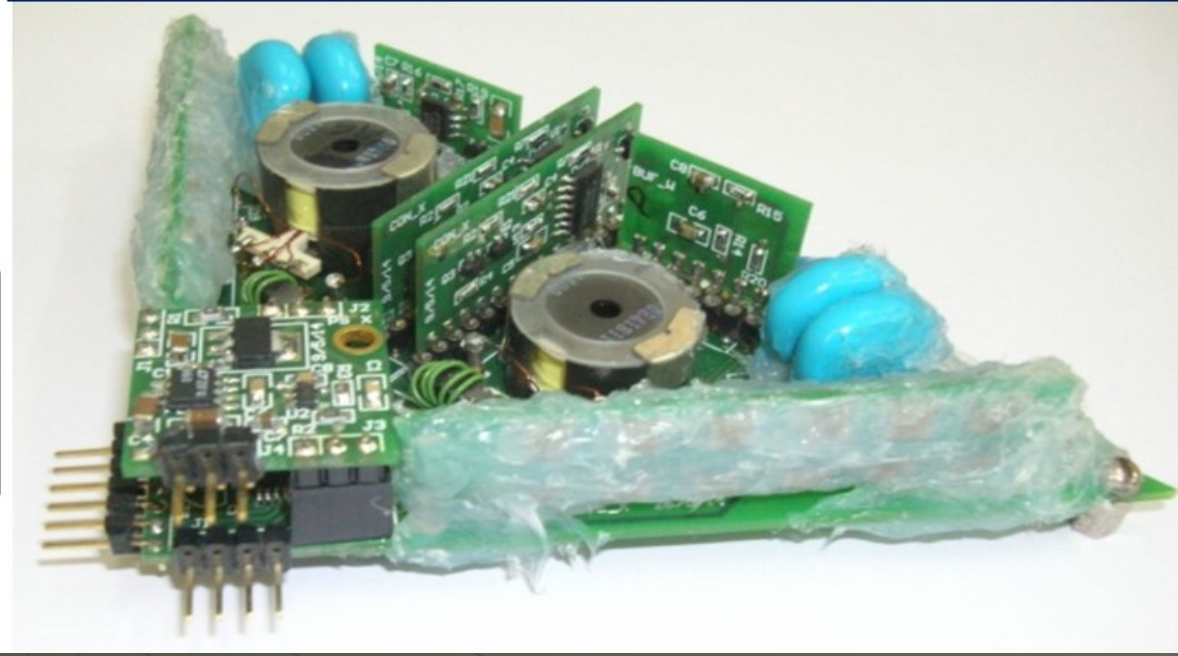
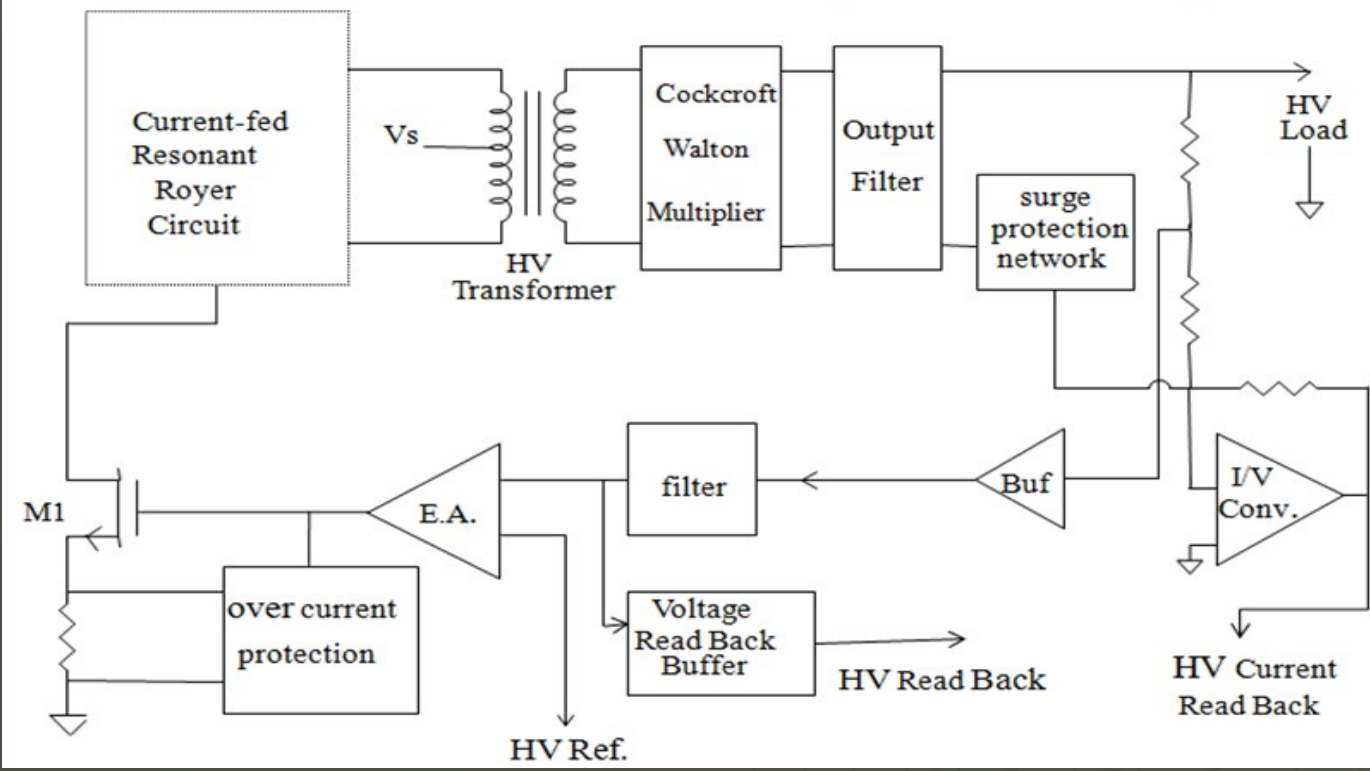


Muography for archaeology





- ◆ Output voltage adjustable in the range $\pm 0-6\text{KV}$ (to generate 0-12KV) with output current up to $2\mu\text{A}$.
- ◆ HV load regulation: better than 0.1% F.S
- ◆ Output ripple/noise voltage: within 200 mV (p-p).
- ◆ Adjustable HV Ramp rate 10-1000 Volts/sec, HV on/off control, HV output read back facility.
- ◆ HV load current read back facility with a resolution of 5 nA.
- ◆ Required LV Input supply: 12V @200mA
- ◆ Ambient fringe magnetic field: 500 gauss



The heart of a mass flow controller is a thermal sensor. It consists of a small bore tube with two resistance-thermometer elements wound around the outside of the tube. The sensor tube is heated by applying an electric current to the elements. A constant proportion of gas flows through the sensor tube, and the cooling effect creates a temperature differential between the two elements. The change in the resistance due to the temperature differential is measured as an electrical signal.

The temperature differential created between the elements is dependent on the mass flow of the gas and is a function of its density, specific heat, and flow rate. Mass flow is normally displayed in terms of volume of the gas either in standard cubic centimeters per minute (sccm) or in standard liters per minute (slm). The electronics of a mass flow controller convert mass flow into volume flow at standard conditions of 0°C (32°F) and 1 atmosphere. Because the volume of 1 mole of an ideal gas at 0° C (32°F) and 1 atmosphere occupies 22.4 liters, a set point of 22.4 slm will cause 1 mole of gas to flow during 1 minute.

The bypass forces a constant proportion of the incoming gas to be fed into the sensor. The gas flow through the sensor tube causes heat to be transferred from the upstream resistance-thermometer element to the downstream resistance-thermometer element. This temperature differential is linearized and amplified into a 0 to 5 V flow output signal by means of a bridge circuit. The output signal is compared with the external set point signal to the mass flow controller. The error signal that results from comparing the output signal with the set point signal directs the control valve to open or close to maintain a constant flow at the set point level.

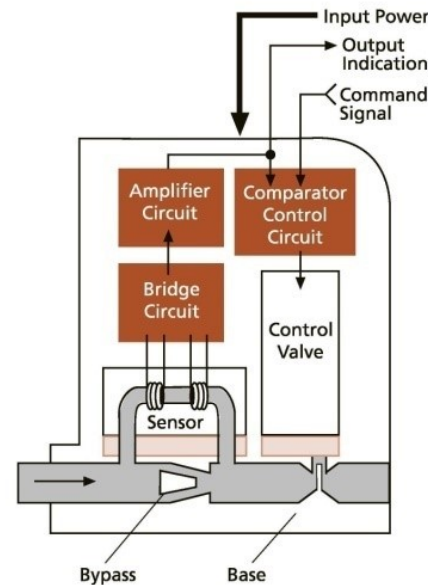


Figure 2. Operational diagram

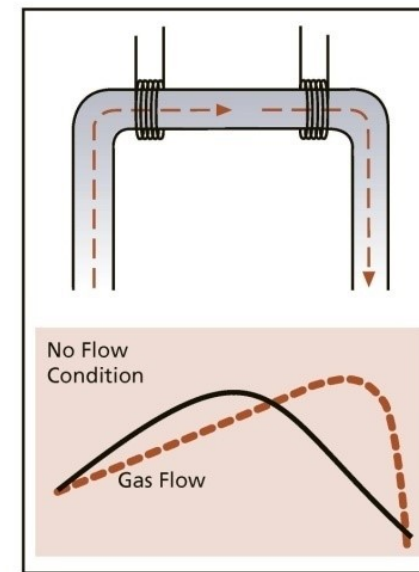


Figure 3. Sensor temperature profile

Operating principle of a gas MFC